

An introduction to Radio-Loud AGN

Paola Grandi (INAF-OAS Bologna)

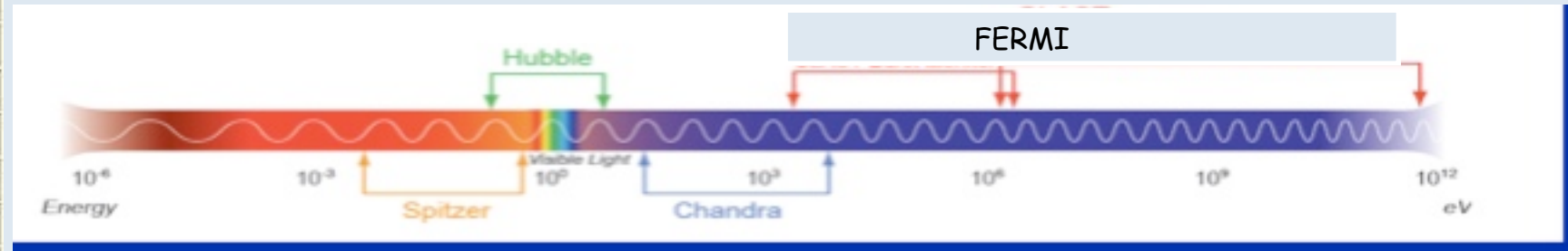


Laboratorio alte energie

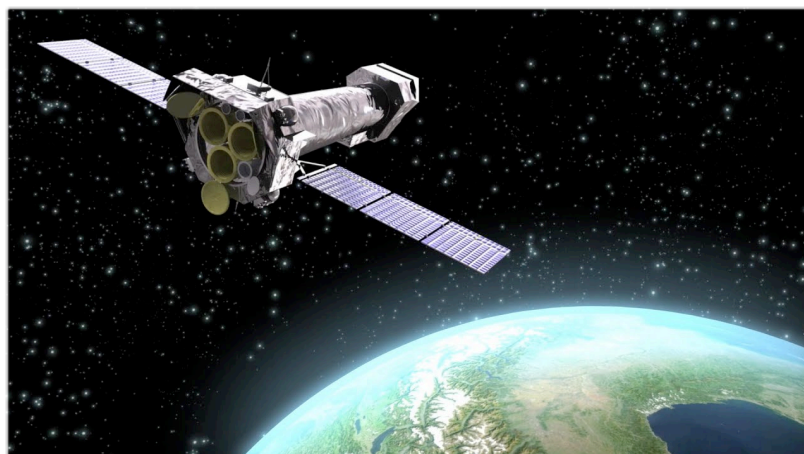
12.11.2019

High and very high energy observations

Spectrum of Electromagnetic Radiation			
Region	Wavelength (Angstroms)	Wavelength (centimeters)	Frequency (Hz)
Radio	$> 10^9$	> 10	$< 3 \times 10^9$
Microwave	$10^9 - 10^6$	$10 - 0.01$	$3 \times 10^9 - 3 \times 10^{12}$
Infrared	$10^6 - 7000$	$0.01 - 7 \times 10^{-5}$	$3 \times 10^{12} - 4.3 \times 10^{14}$
Visible	$7000 - 4000$	$7 \times 10^{-5} - 4 \times 10^{-5}$	$4.3 \times 10^{14} - 7.5 \times 10^{14}$
Ultraviolet	$4000 - 10$	$4 \times 10^{-5} - 10^{-7}$	$7.5 \times 10^{14} - 3 \times 10^{17}$
X-Rays	$10 - 0.1$	$10^{-7} - 10^{-9}$	$3 \times 10^{17} - 3 \times 10^{19}$
Gamma Rays	< 0.1	$< 10^{-9}$	$> 3 \times 10^{19}$



Chandra $\sim 0.5 - 7$ keV



FERMI -LAT ~ 100 MeV - 2 TeV

MAGIC ~ 30 GeV - 100 TeV



A detailed illustration of a black hole and its surrounding environment. At the center is a dark, circular event horizon. Surrounding it is a glowing, multi-layered accretion disk. The innermost part of the disk is bright yellow and orange, transitioning to pink and then purple as it moves further out. Two powerful jets of light blue and white energy are shown erupting from the poles of the black hole, extending into the dark, star-filled space. The background is a deep blue and purple, with faint, distant stars visible.

Non-thermal emission

Synchrotron

Inverse Compton

Thermal emission

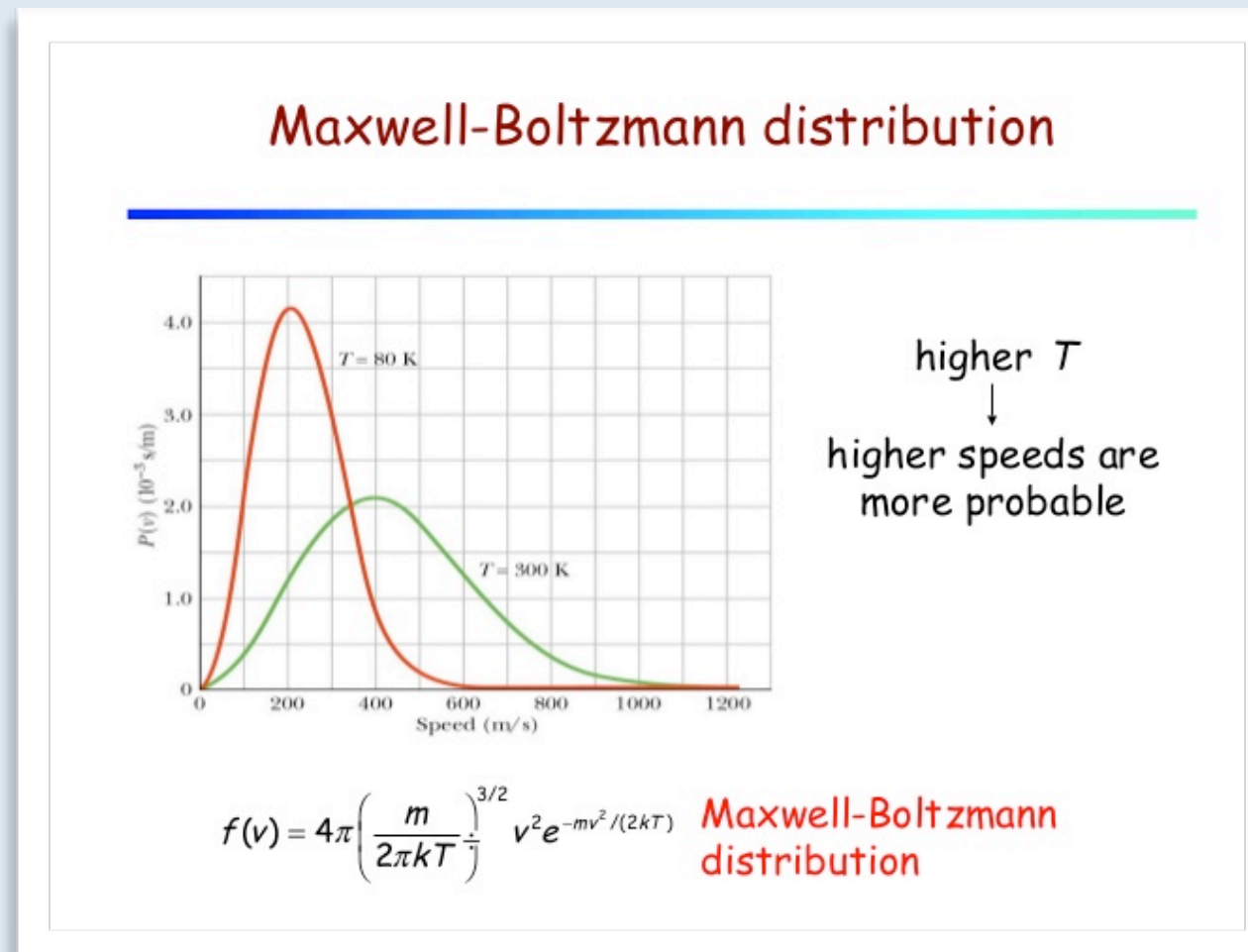
Accretion flow

Thermal Comptonization

Reprocessed features

Radiative processes

Thermal means that the radiation is dependent solely on the temperature of the emitter.



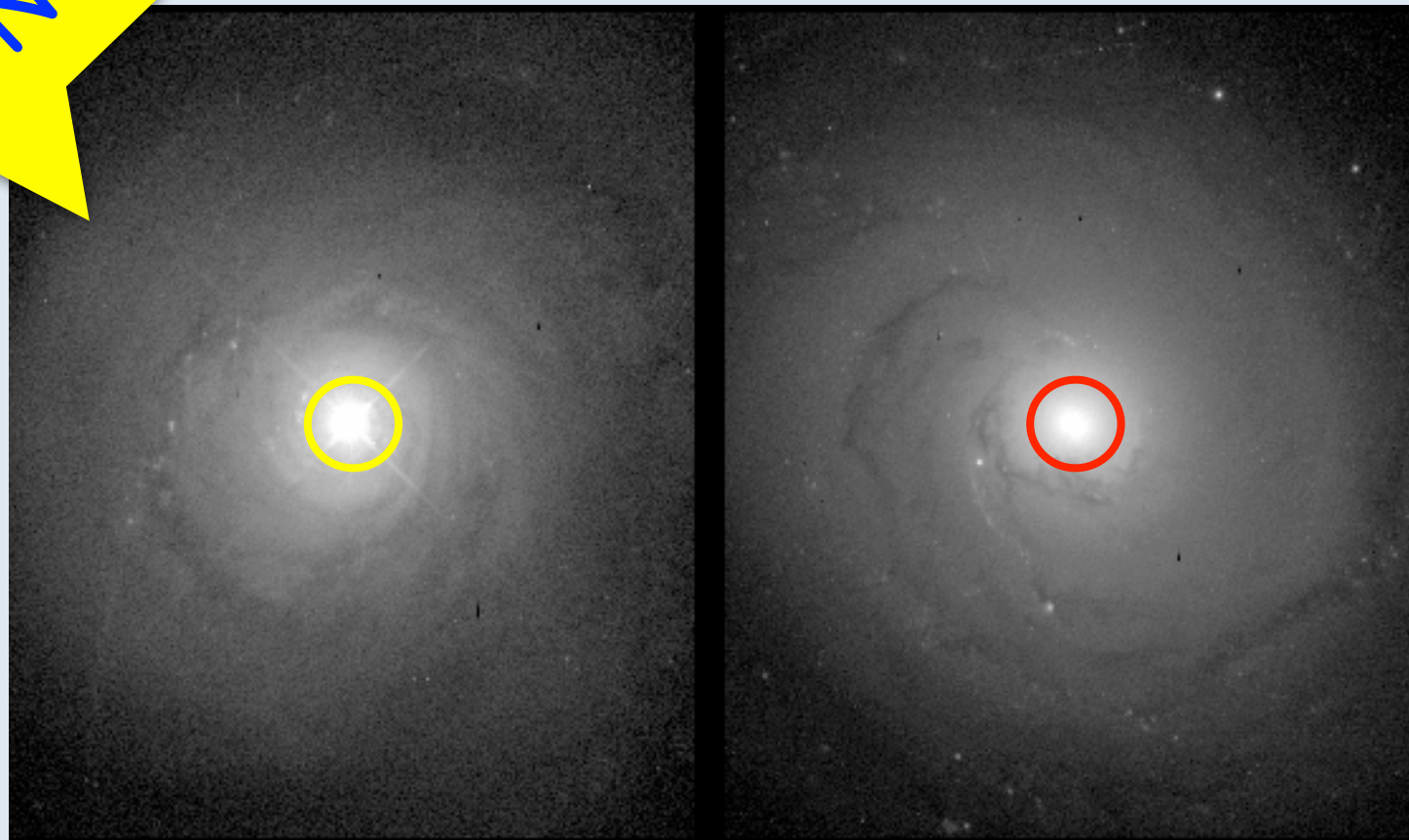
Non-thermal radiation involves other processes and generally requires accelerators

Almost every galaxy hosts a black hole
from millions to billions of solar masses

but...

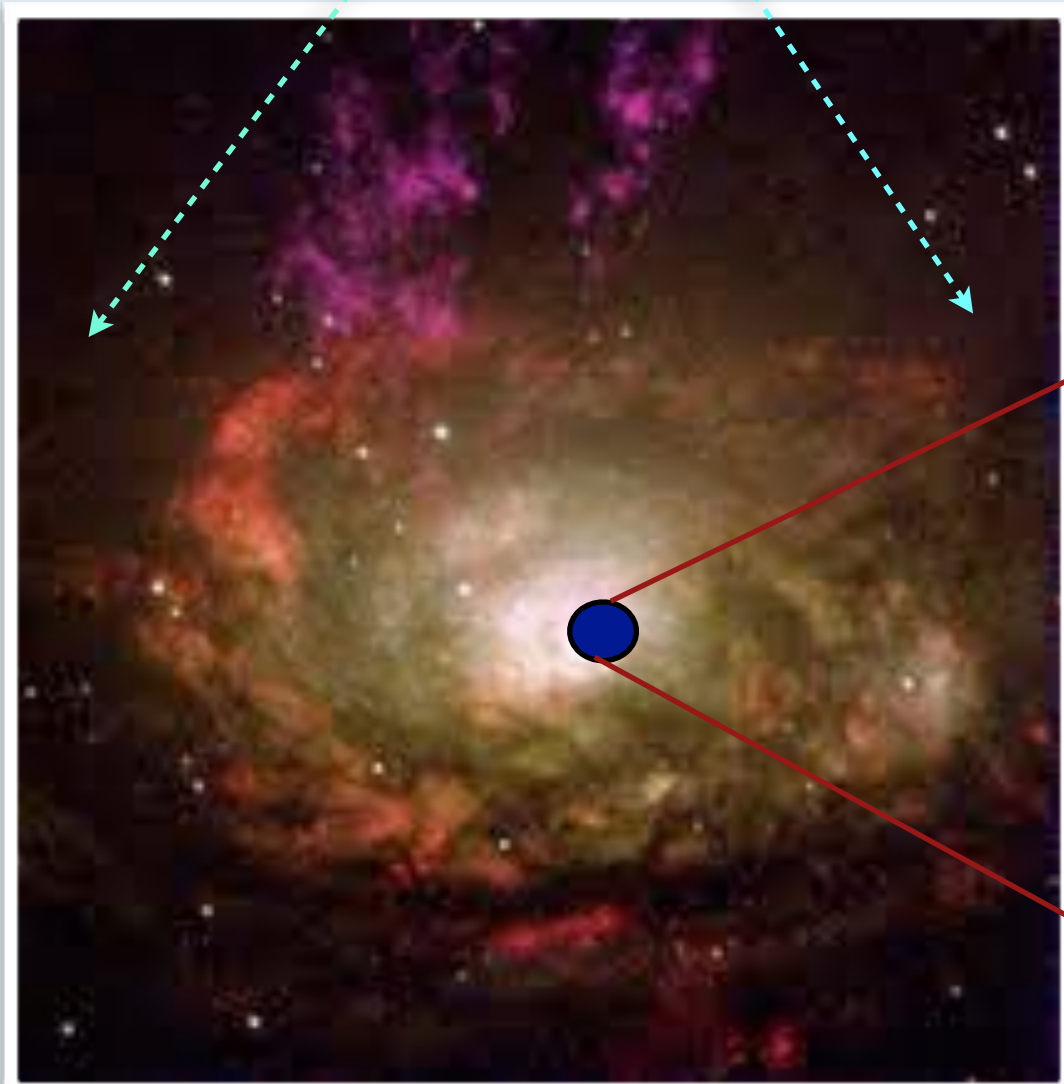
1% active

99% silent

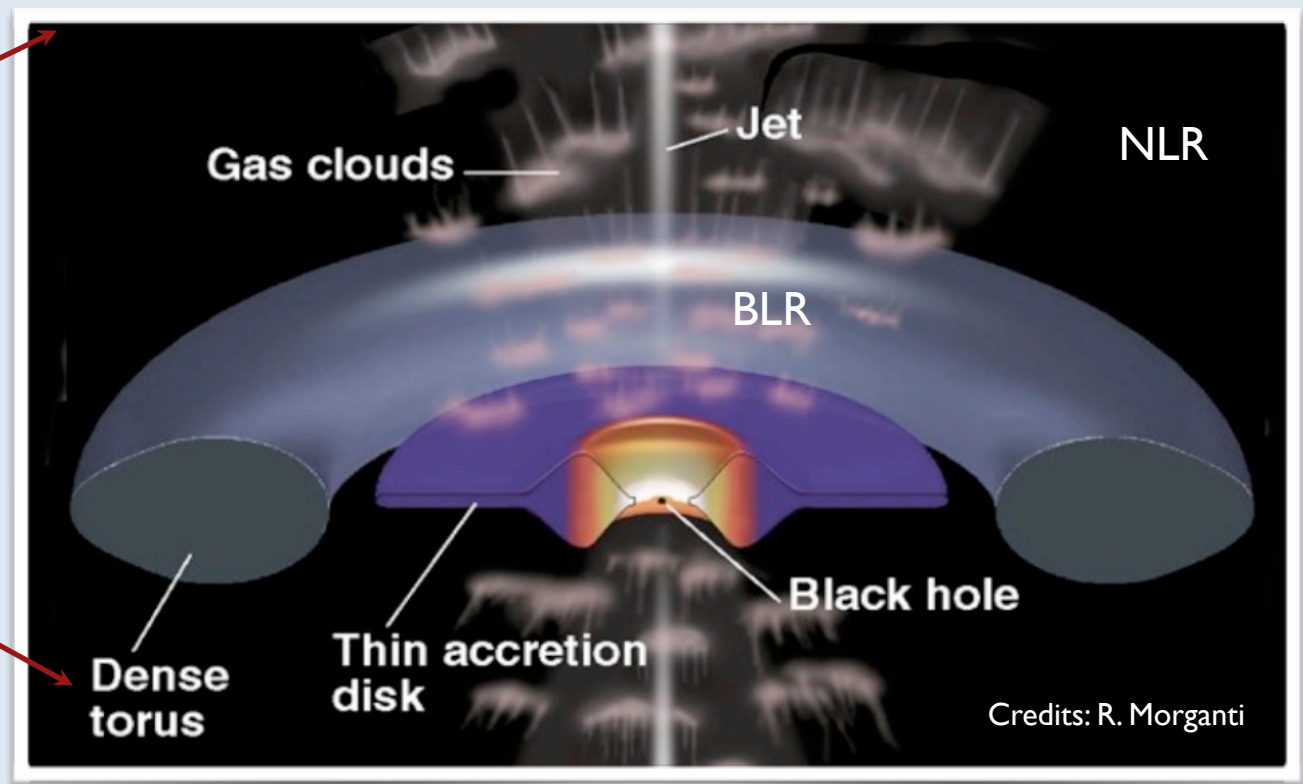


The engine occupies a tiny region in the center of the galaxy

30 kpc

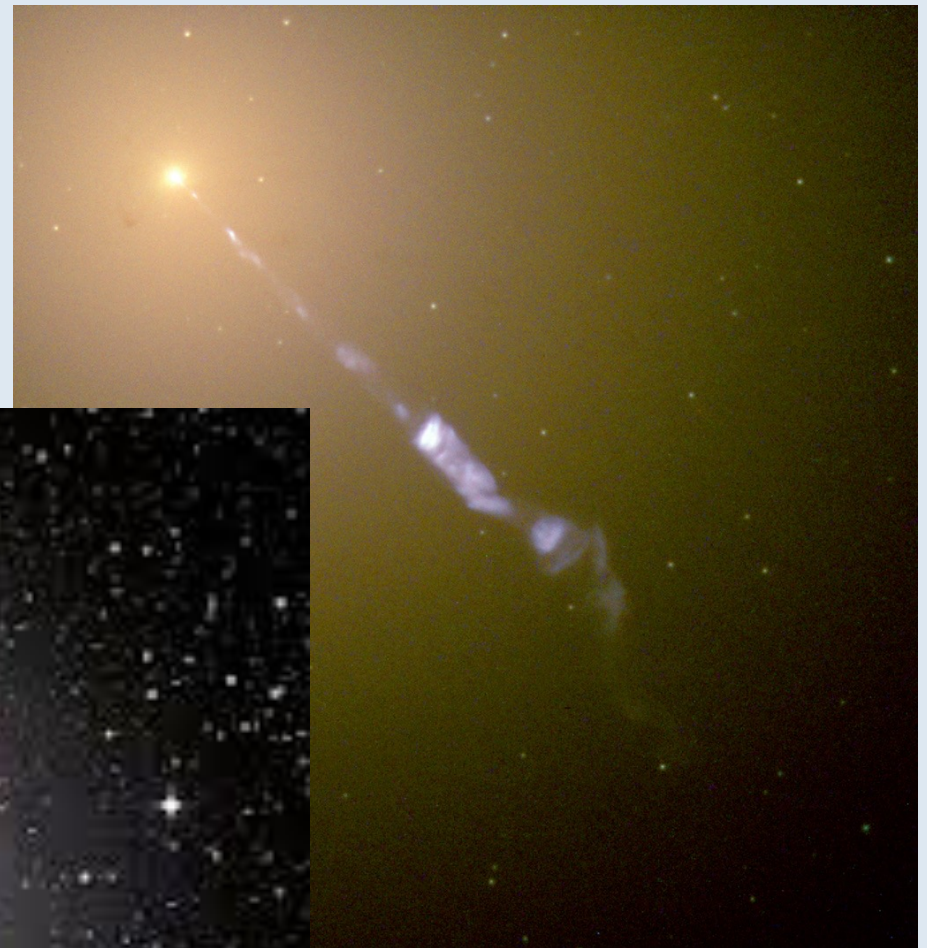


2-3 pc



The extraordinary amount of energy is produced through accretion of gas close to a SMBH

About 10% of AGNs are Radio-Loud,
i.e. these systems are able to launch relativistic jets



RL AGN lie in ellipticals

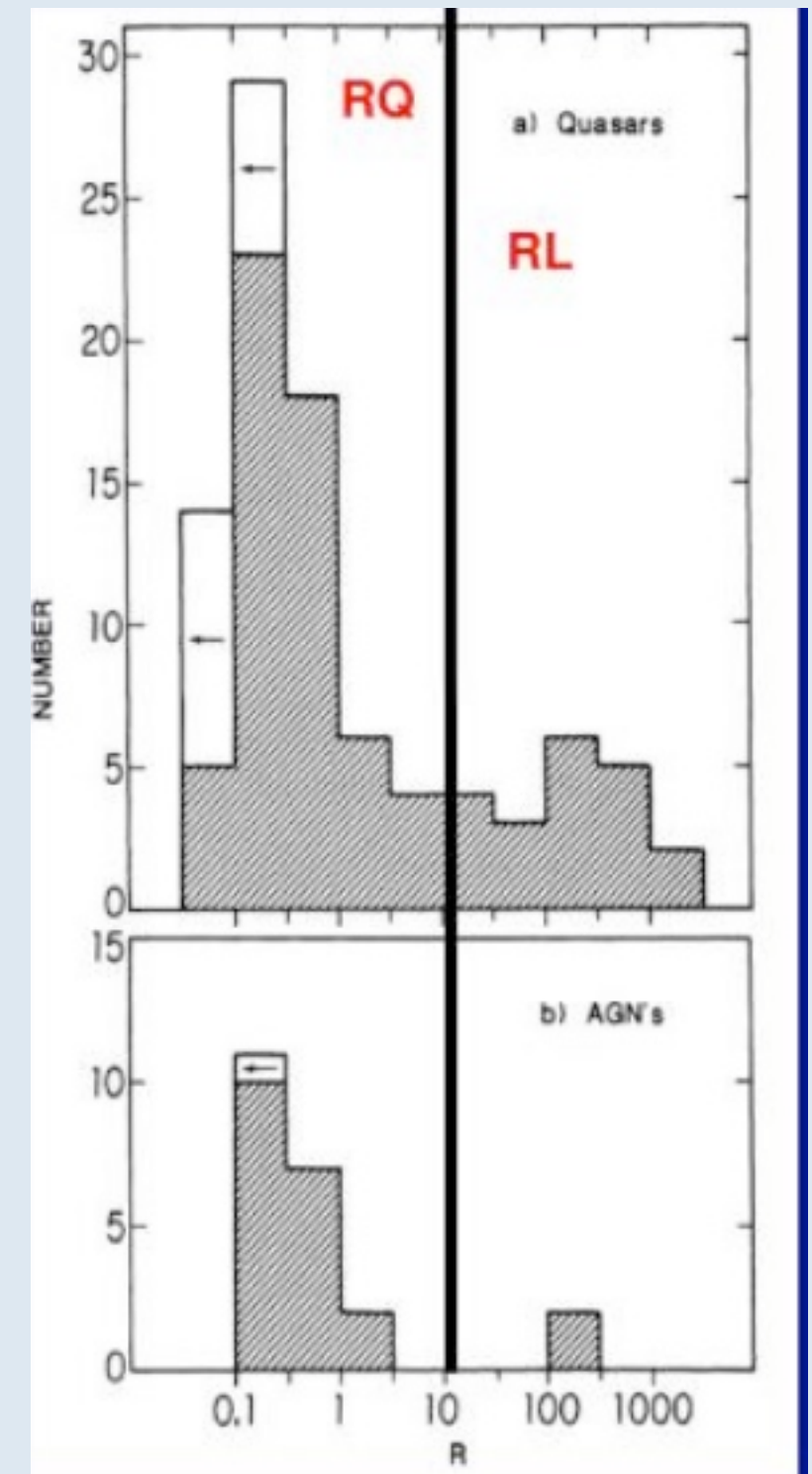
RQ AGN lie in spirals and ellipticals

RADIO LOUDNESS PARAMETER (R)

$$R = \frac{F_{GHz}}{F_B} \geq 10.$$

This definition is based on a study of 114 objects from the Palomar Bright Quasar Survey with VLA (Kellermann 1989)

Quasars have blue magnitude $M_B < -23$, while AGN have $M_b > -23$



Current Space Densities of Selected Objects

Type of objects	Space Density (Gpc ⁻³)
Radio Quiet	
Seyfert 2	$8 \times 10^5 h_0^3$
Seyfert 1	$3 \times 10^5 h_0^3$
QSO	$800 h_0^3$
Radio Loud	
FRI	$2 \times 10^4 h_0^3$
FRII	$80 h_0^3$

Some numbers for a typical AGN

Jets end at kpc/Mpc distances forming lobes

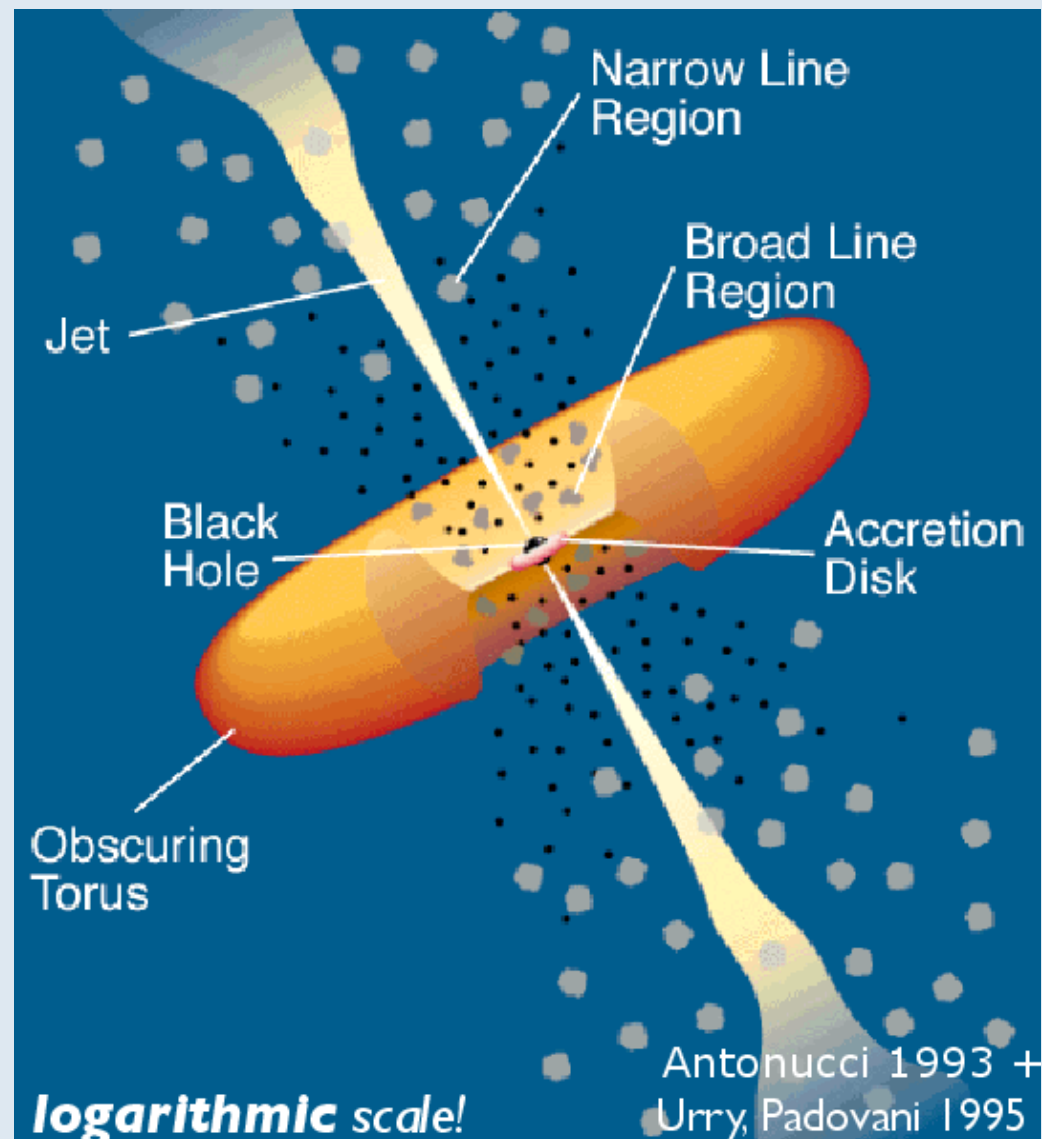
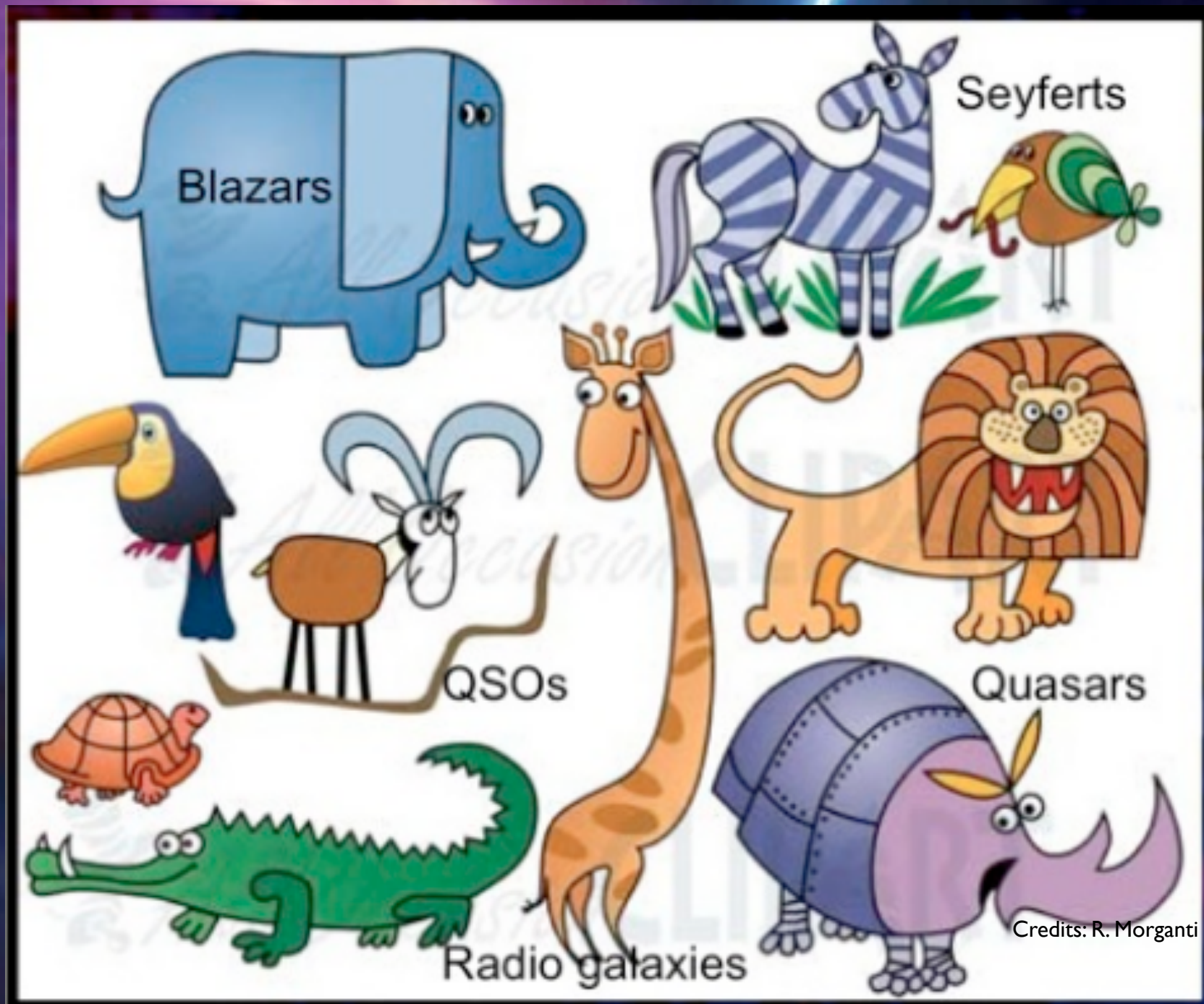


FIG. 1—A schematic diagram of the current paradigm for radio-loud AGN (not to scale). Surrounding the central black hole is a luminous accretion disk. Broad emission lines are produced in clouds orbiting above the disk and perhaps by the disk itself. A thick dusty torus (or warped disk) obscures the broad-line region from transverse lines of sight; some continuum and broad-line emission can be scattered into those lines of sight by hot electrons that pervade the region. A hot corona above the accretion disk may also play a role in producing the hard X-ray continuum. Narrow lines are produced in clouds much farther from the central source. Radio jets, shown here as the diffuse jets characteristic of low-luminosity, or FR I-type, radio sources, emanate from the region near the black hole, initially at relativistic speeds. For a $10^8 M_{\odot}$ black hole, the black hole radius is $\sim 3 \times 10^{13}$ cm, the accretion disk emits mostly from $\sim 1-30 \times 10^{14}$ cm, the broad-line clouds are located within $\sim 2-20 \times 10^{16}$ cm of the black hole, and the inner radius of the dusty torus is perhaps $\sim 10^{17}$ cm. The narrow-line region extends approximately from $10^{18}-10^{20}$ cm, and radio jets have been detected on scales from 10^{17} to several times 10^{24} cm, a factor of ten larger than the largest galaxies.

Urry & Padovani 1995

<http://articles.adsabs.harvard.edu/full/1995PASP..107..803U>

AGN classification

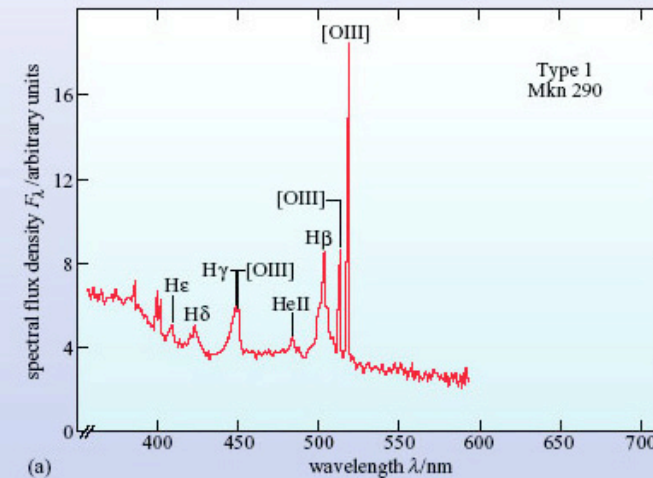


Optical Classification

[https://ned.ipac.caltech.edu/level5/Osterbrock3 Oster_contents.html](https://ned.ipac.caltech.edu/level5/Osterbrock3/Oster_contents.html)

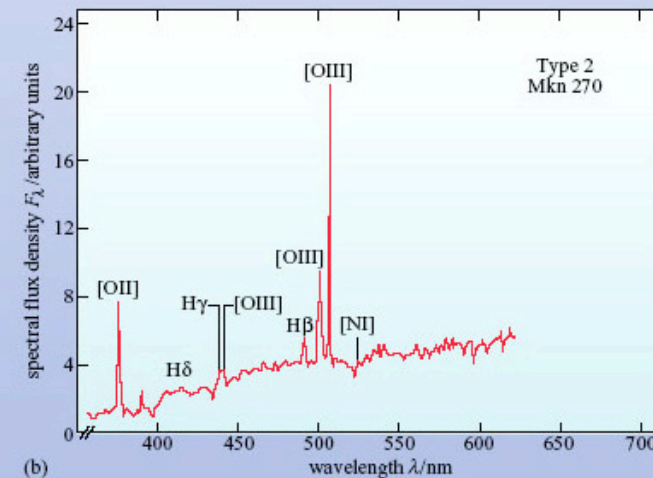
Type I

bright continuum and BROAD emission lines from hot high velocity gas (FWHM $\sim 10^3$ - 4 km s^{-1})



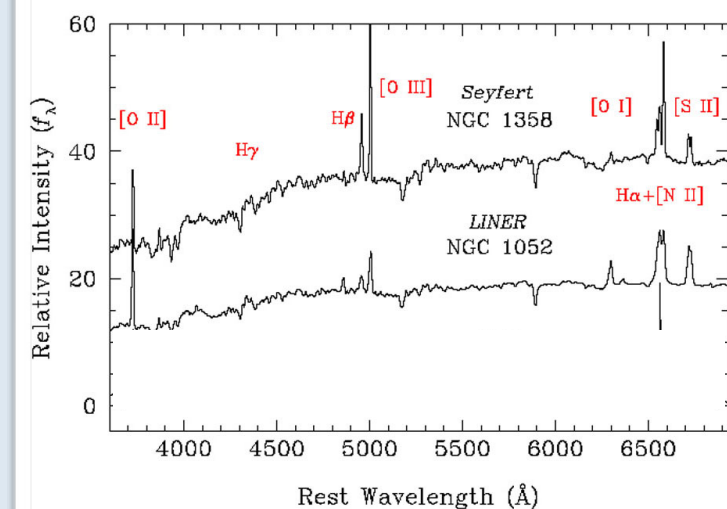
Type II

weak continuum and only NARROW emission lines (FWHM $\sim 10^2 \text{ km s}^{-1}$)



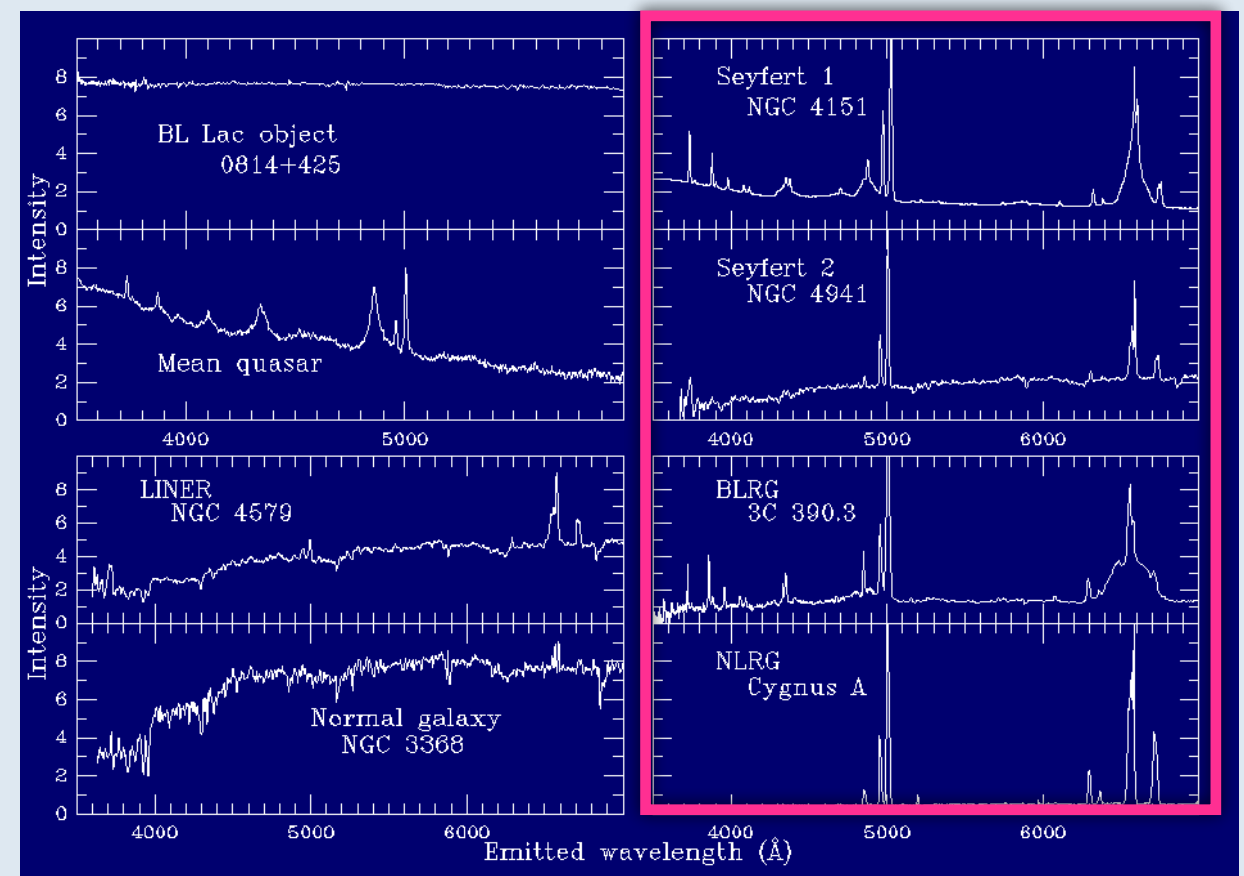
Liner

Low luminosity. Similar to Seyfert 2 galaxies, except that the low-ionization lines, e.g., [O I] 6300 and [N II] 6548, 6583, are relatively strong



RL AGN borrowed their optical classification from RQ AGN (old approach)

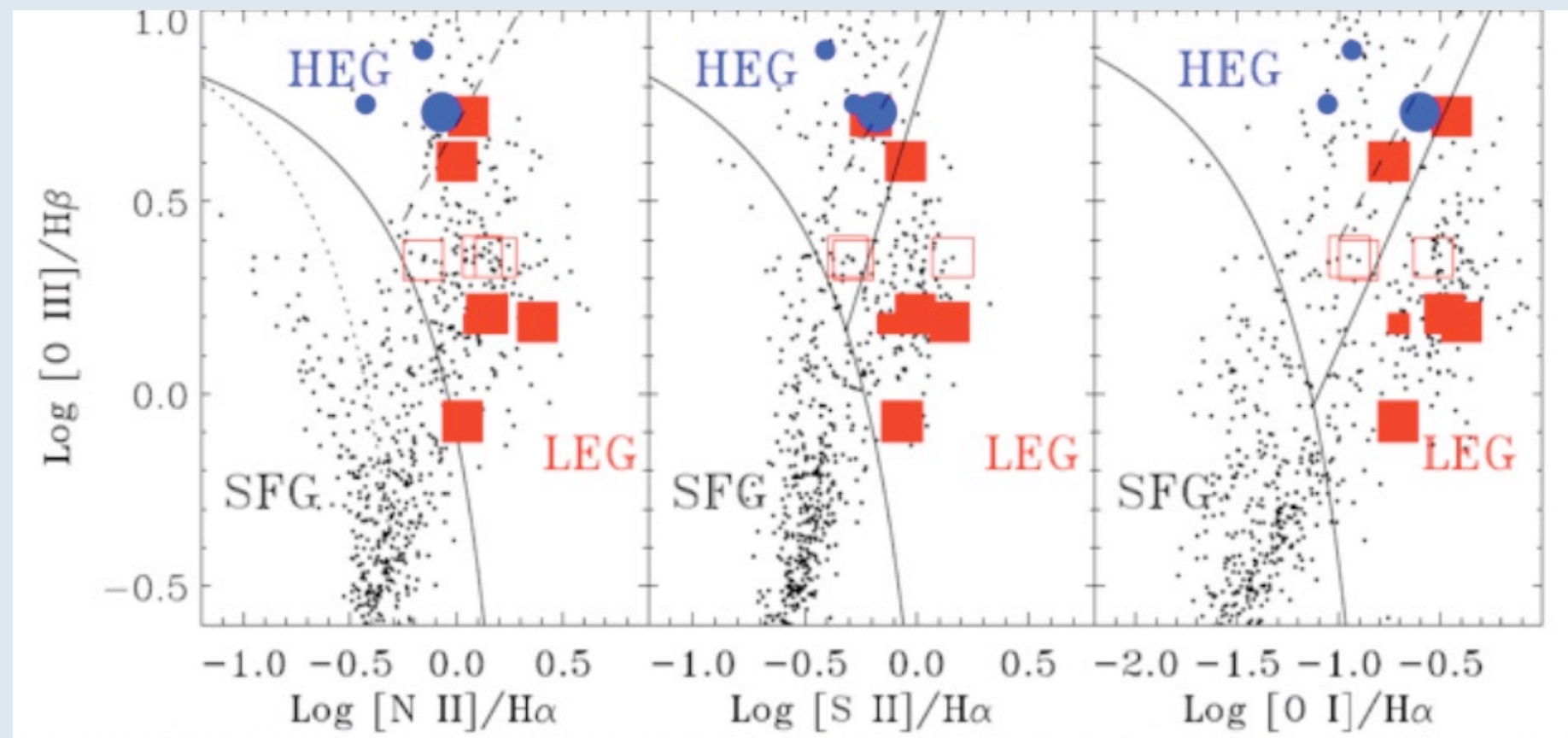
<p>Broad Line Radio Galaxy (BLRG)</p> <p>Quasars (large z)</p>	<p>bright continuum and broad emission lines from hot high velocity gas</p>	<p>TYPE I</p>
<p>Narrow line Radio Galaxy</p>	<p>weak continuum and only narrow emission lines</p>	<p>TYPE II</p>



New optical classification

High-excitation (HERG) low-excitation (LERG) Radio Galaxy

This classification is related to the excitation modes of the gas in the Narrow Line Regions: different excitation modes correspond to different accretion rates



Best & Heckmann

Buttiglione et al.

New optical Radio Loud classification

High-Excitation Radio Galaxy (HERG)

Efficient engine

Low-Excitation Radio Galaxy (LERG)

Inefficient engine

in converting gravitational power into radiation

FRI/FRII classification (Fanaroff & Riley 1974)

RADIO MORPHOLOGY

1974MNRAS...167P...31P

Mon. Not. R. astr. Soc. (1974) 167, Short Communication, 31P-35P.

THE MORPHOLOGY OF EXTRAGALACTIC RADIO SOURCES OF HIGH AND LOW LUMINOSITY

B. L. Fanaroff and J. M. Riley

(Received 1974 March 6)

SUMMARY

The relative positions of the high and low brightness regions in the extragalactic sources in the 3CR complete sample are found to be correlated with the luminosity of these sources.

It has become clear from recent observations of extended extragalactic radio sources that many consist of fairly compact regions of high brightness ('hot spots') embedded in more extensive regions of much lower brightness. It is of importance to the models of the origin of the radio emission and of the energy supply to understand the relationship between these regions and other parameters of the radio emission such as luminosity, spectral index and shape. In this note we suggest that there is a definite relationship between the relative positions of the high and low brightness regions of radio sources and their luminosity.

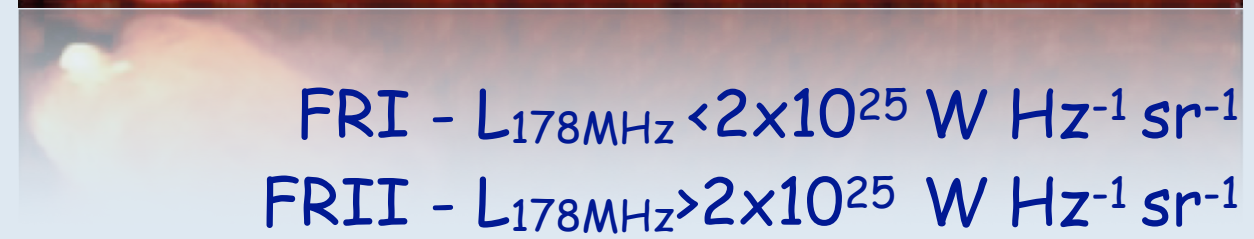
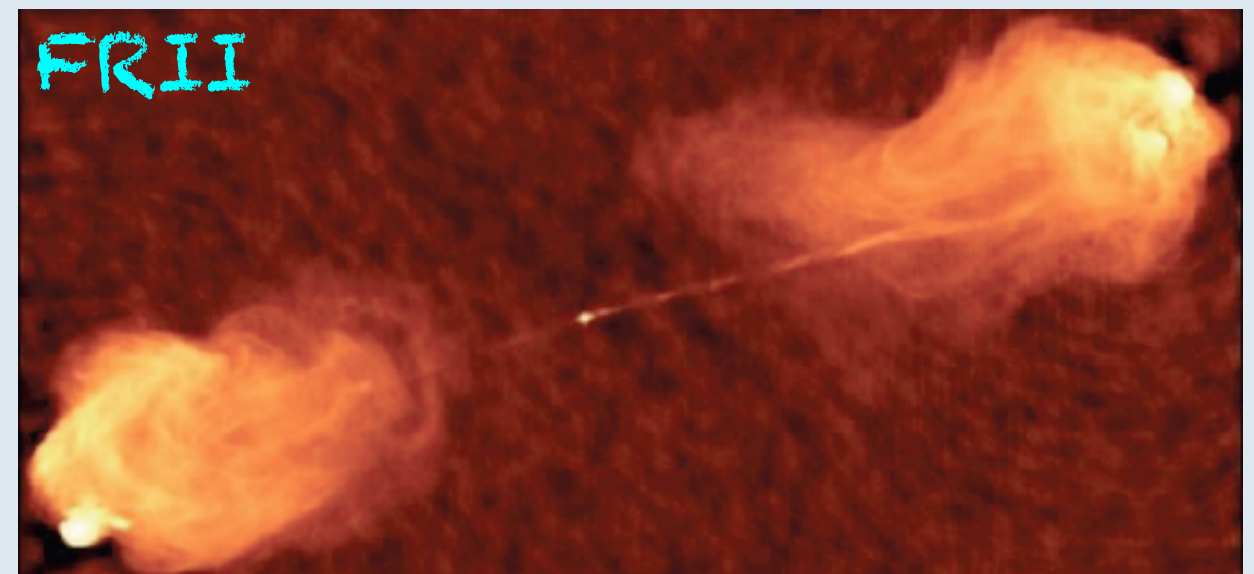
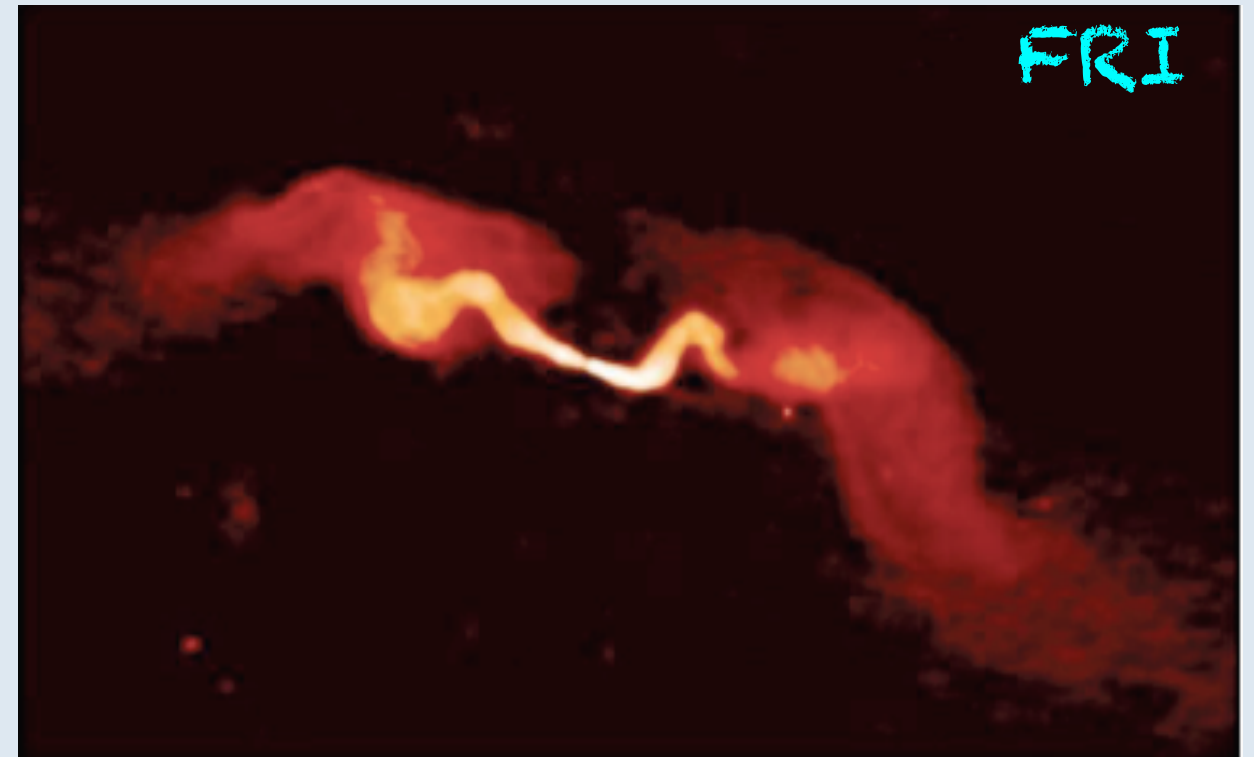
The 199 sources in the 3CR complete sample (Mackay 1971) have been studied with high resolution using the Cambridge One-Mile telescope. All 199 sources were mapped at 1.4 GHz with a resolution of $23''$ arc in RA and $23''$ cosec δ in Dec. (Macdonald, Kenderdine & Neville 1968; Mackay 1969; Elsmore & Mackay 1970), and 53 of them were observed at 5 GHz with a resolution of $6'' \times 6''$ cosec δ (Mitton 1970a, b, c; Graham 1970; Harris 1972, 1973; Branson *et al.* 1972; Riley 1972, 1973; Riley & Branson 1973; Northover 1973, 1974).

In the investigation described here we have used a sub-sample of the 3CR complete sample, consisting of all those sources which were clearly resolved into two or more components in any of the series of observations mentioned above. The sources were classified using the ratio of the distance between the regions of highest brightness on opposite sides of the central galaxy or quasar, to the total extent of the source measured from the lowest contour; any compact component situated on the central galaxy was not taken into account. Those sources for which this ratio is less than 0.5 were placed in class I; those for which it is greater than 0.5 were placed in class II. In sources for which we have maps of adequate resolution, this is equivalent to having the 'hot spots' nearer to (Class I) or further away from (Class II) the central bright galaxy or quasar than the regions of diffuse radio emission. The sensitivities of most maps were sufficient for brightness temperatures a few per cent of the peak brightness to have been detected. Those sources for which the sensitivities were not good enough to detect low brightness regions, and those of two or three beamwidths in extent for which classification is impossible, are listed in Table II and have not been included in the analysis.

The results are presented in Table I whose arrangement is as follows:

(i) The luminosity at 178 MHz in $\text{W Hz}^{-1} \text{sr}^{-1}$ (Hubble's constant = $50 \text{ km s}^{-1} \text{ Mpc}^{-1}$); the sources are arranged in order of their luminosity.

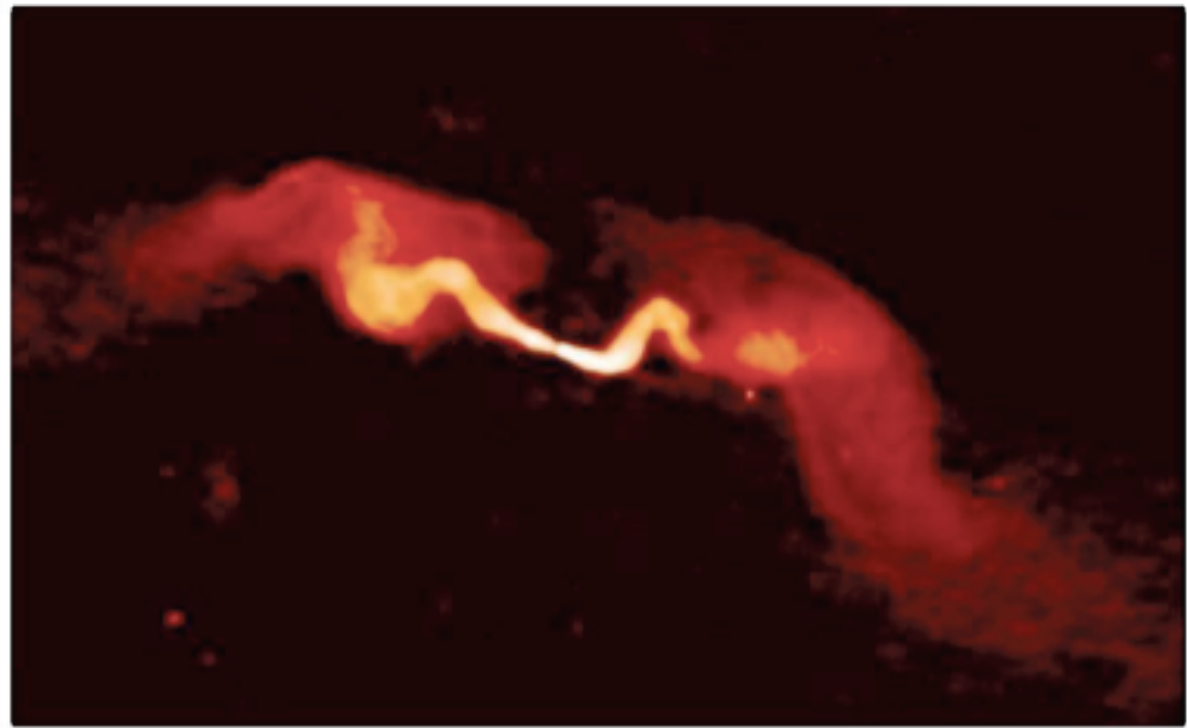
31P



FRI - $L_{178\text{MHz}} < 2 \times 10^{25} \text{ W Hz}^{-1} \text{sr}^{-1}$

FRII - $L_{178\text{MHz}} > 2 \times 10^{25} \text{ W Hz}^{-1} \text{sr}^{-1}$

FRI/jet dominated



Edge-darkened

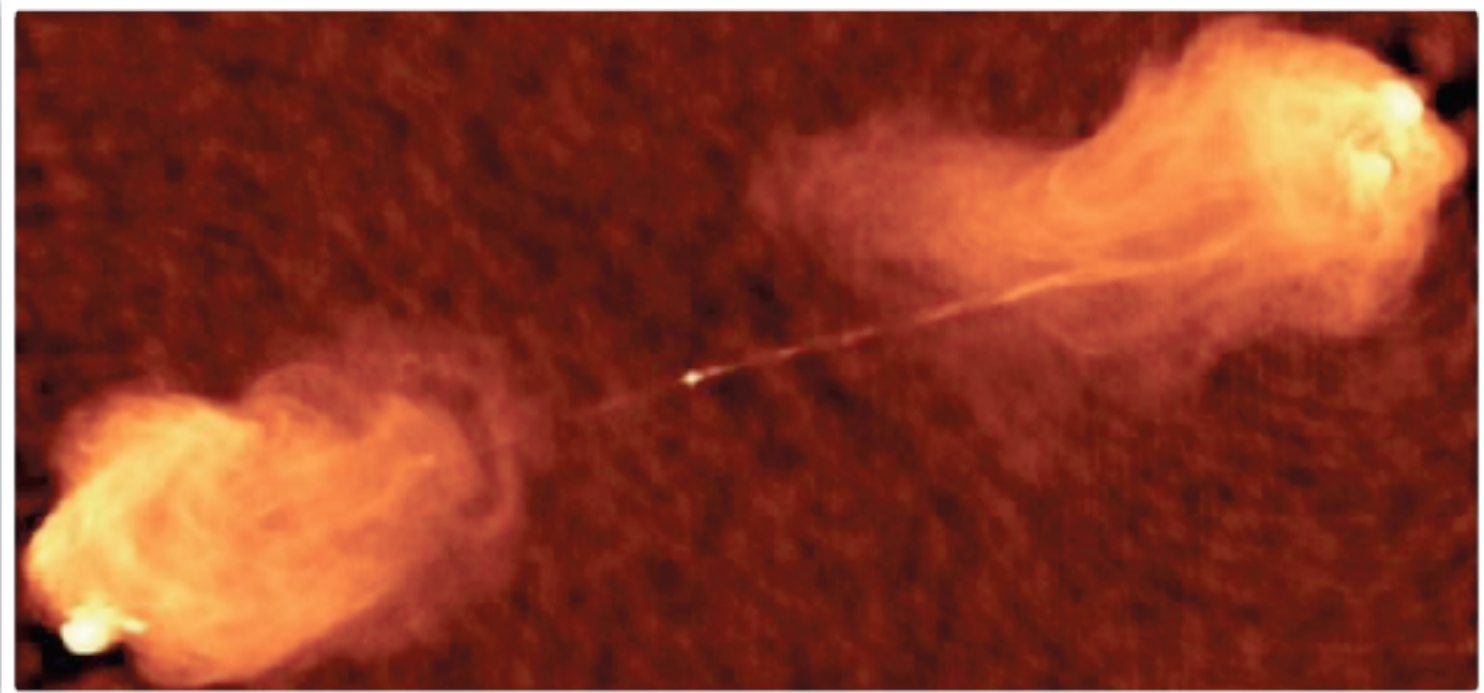
In FRI the jets are thought to decelerate and become sub-relativistic on scales of hundred of pc to kpc.

The nuclei of FRI are powered by inefficient engine

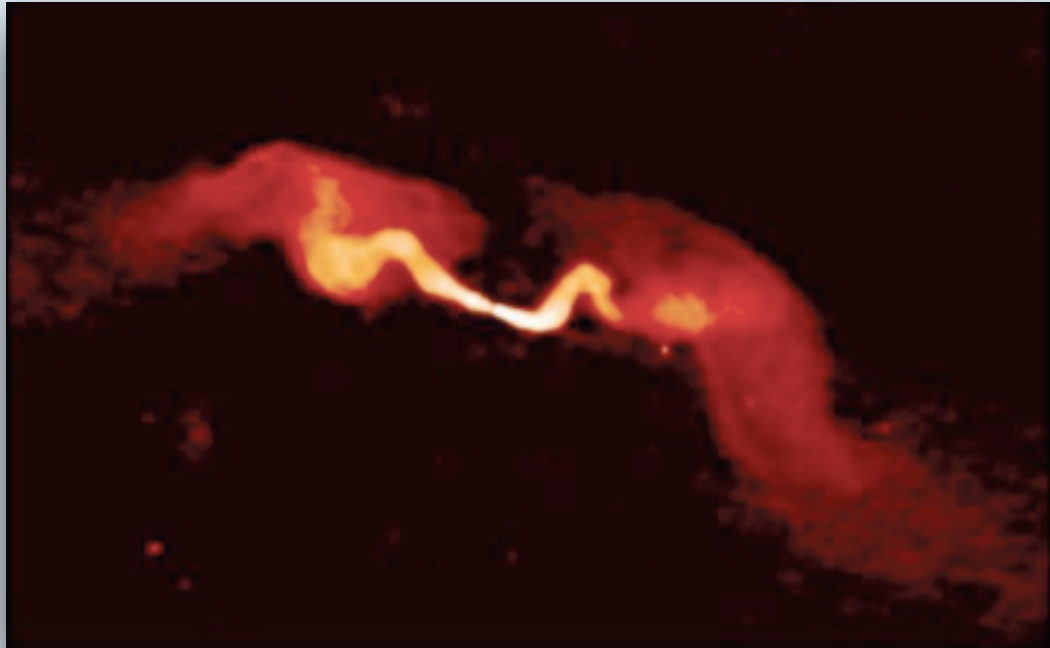
The jets in FRII are at least moderately relativistic and supersonic from the core to the hot spots.

Most FRII are **thought** to have an efficient engine

FRII/lobe dominated

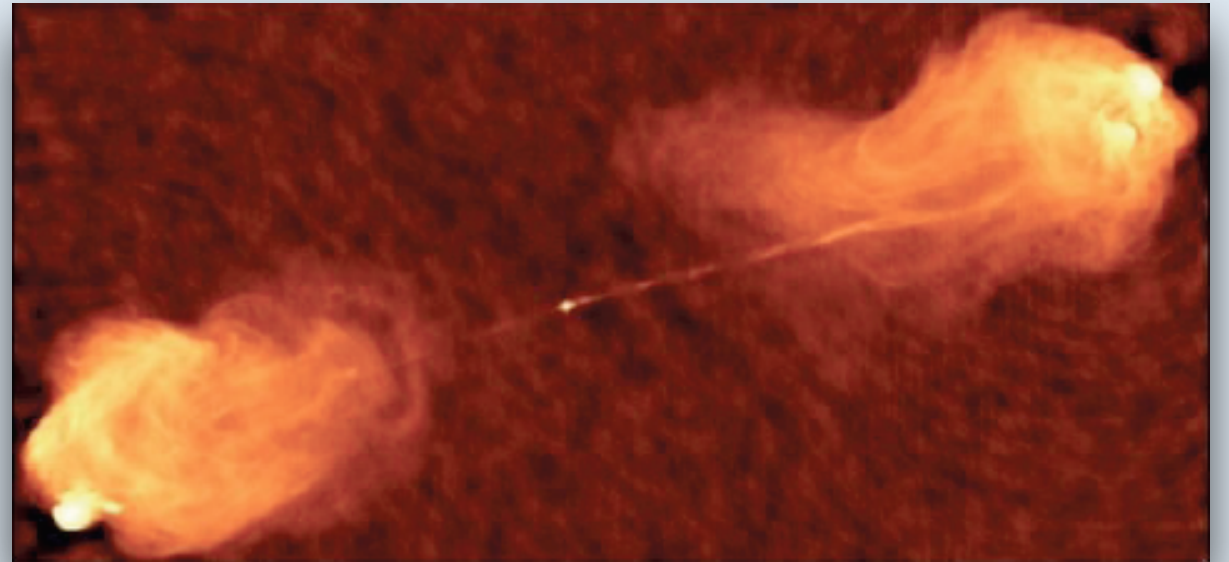


Edge-brightened



FRI/jet dominated

FRI -> LERG

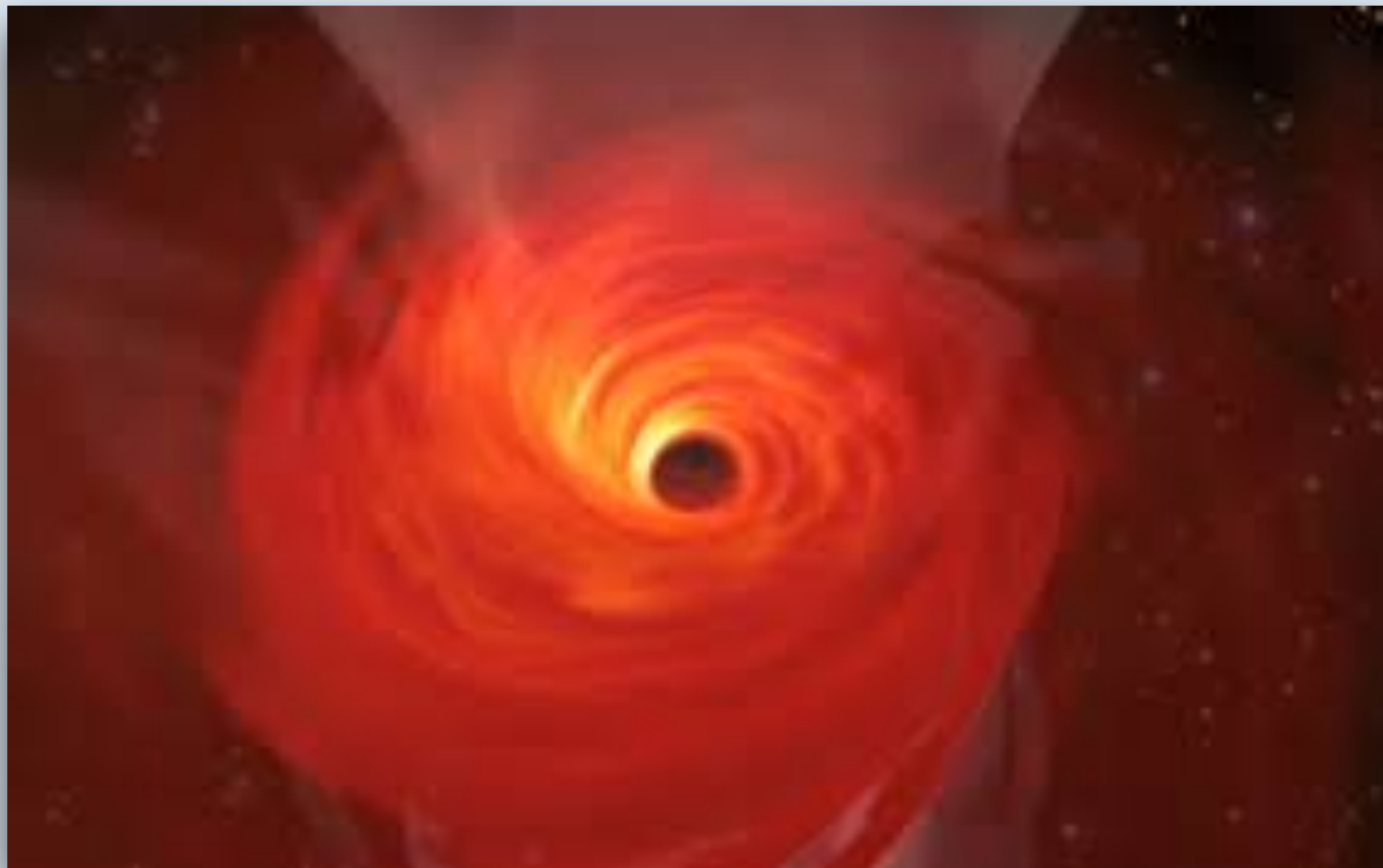


FR II/lobe dominated

FR II -> HERG

Different Engine

The inner AGN engine



Black Hole as engine of AGN

Accretion process is very efficient in producing energy

Assuming $M \sim M_{\text{sun}}$ and $R=10 \text{ Km}$

$$\Delta E_{acc} = \frac{GMm}{R} \sim 10^{20} \text{ erg/g}$$

NOTE that in case of nuclear energy generation, the greatest release of nuclear binding energy is:

$$\Delta E_{nuc} = 7 \times 10^{-2} mc^2 \sim 6 \times 10^{18} \text{ erg/g}$$

Black Hole as engine of AGN

If the rate at which mass is accreted onto M is \dot{M} the luminosity of the source is

$$L_{acc} = GM\dot{M}/R$$

Note: M/R is the compactness of the accretion. The more compact, the more energy can be released.

Eddington Luminosity L_E is a sort of “unit of measurement”. It is the luminosity at which the outward force of the radiation pressure is balanced by the inward gravitational force, i.e. it is the maximum luminosity a spherically symmetric source of mass M can emit in a steady state

$$L_{Edd} = \frac{4\pi GM_{pc}}{\sigma_T} \sim 1.3 \times 10^{38} \frac{M}{M_{\odot}} \text{erg/s}$$

$$L_{acc} = GM\dot{M}/R$$

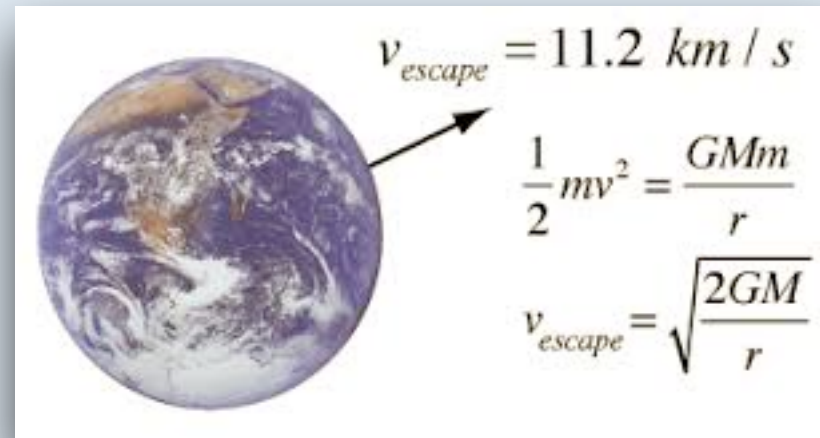
Introducing the Schwarzschild radius

$$R_S = \frac{2GM}{c^2}$$

L_{acc} can be written as:

$$L_{acc} = 2\eta GM\dot{M}/R = \eta\dot{M}c^2$$

Black hole radius can be derived by the escape velocity of the light



$$v_{\text{escape}} = c = \left(\frac{2GM}{R_S} \right)^{\frac{1}{2}}$$

Schwarzschild radius $R_S = \frac{2GM}{c^2}$

Accretion processes around black holes involve rotating gas flow. Therefore the accretion flow structure is determined by solving simultaneously four conservation equations:

conservation of vertical momentum
conservation of mass
conservation of energy
conservation of angular momentum

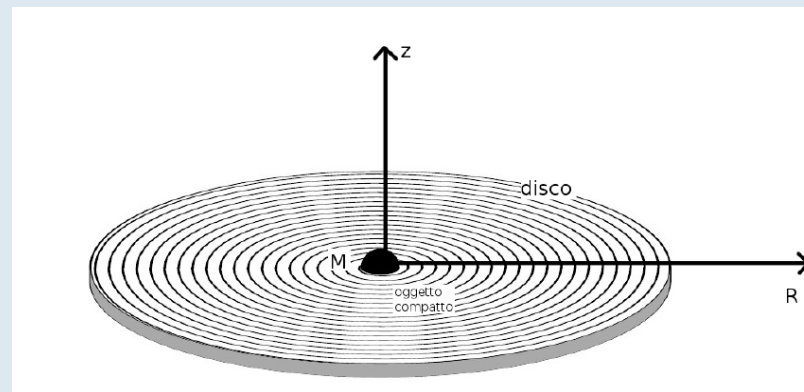
Four solutions are currently known. In these solutions viscosity transports angular momentum outward, allowing the accretion gas to spiral in toward the BH. Viscosity acts a source of heat that is radiated away.

The most famous solutions are:

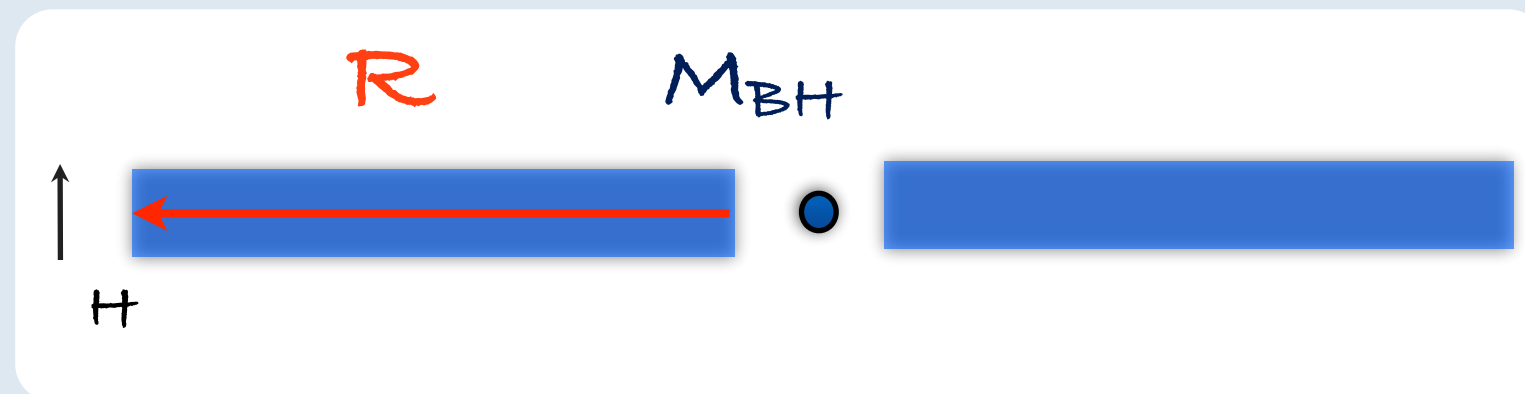
- i) Shakura & Sunyaev thin optically thick disk model (standard model)
- ii) Optically thick Advection-Dominated Accretion Flow (ADAF)

Efficient Engine

Shakura & Sunyaev thin optically thick disk model (standard model)



Thin $H/R \ll 1$



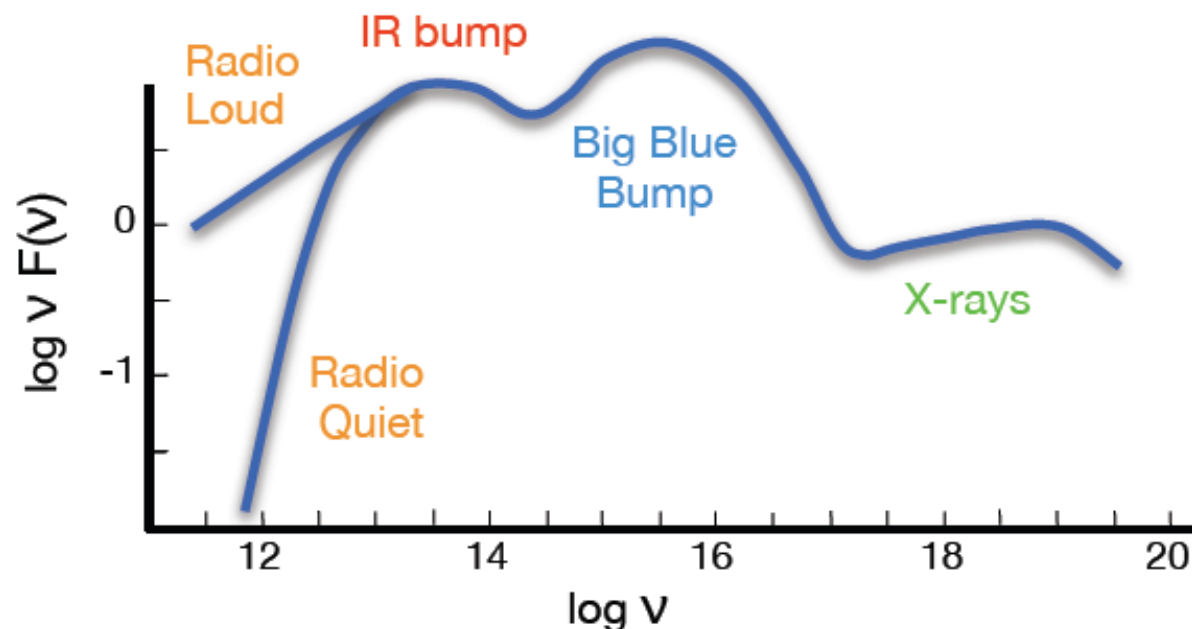
Thick, in the sense that each element of the disk radiates as a black body

If the the disk is optically thick, we can approximate the local emission as blackbody and the effective temperature of the photosphere

$$T(r) \sim 6.3 \times 10^5 \left(\frac{\dot{M}}{\dot{M}_E} \right)^{1/4} M_8^{-1/4} \left(\frac{r}{R_s} \right)^{-3/4} K$$

For AGN with $M_{BH} = 10_8 = 10^8 M_\odot$ $\dot{M} \sim \dot{M}_E = \frac{L_E}{\eta c^2}$

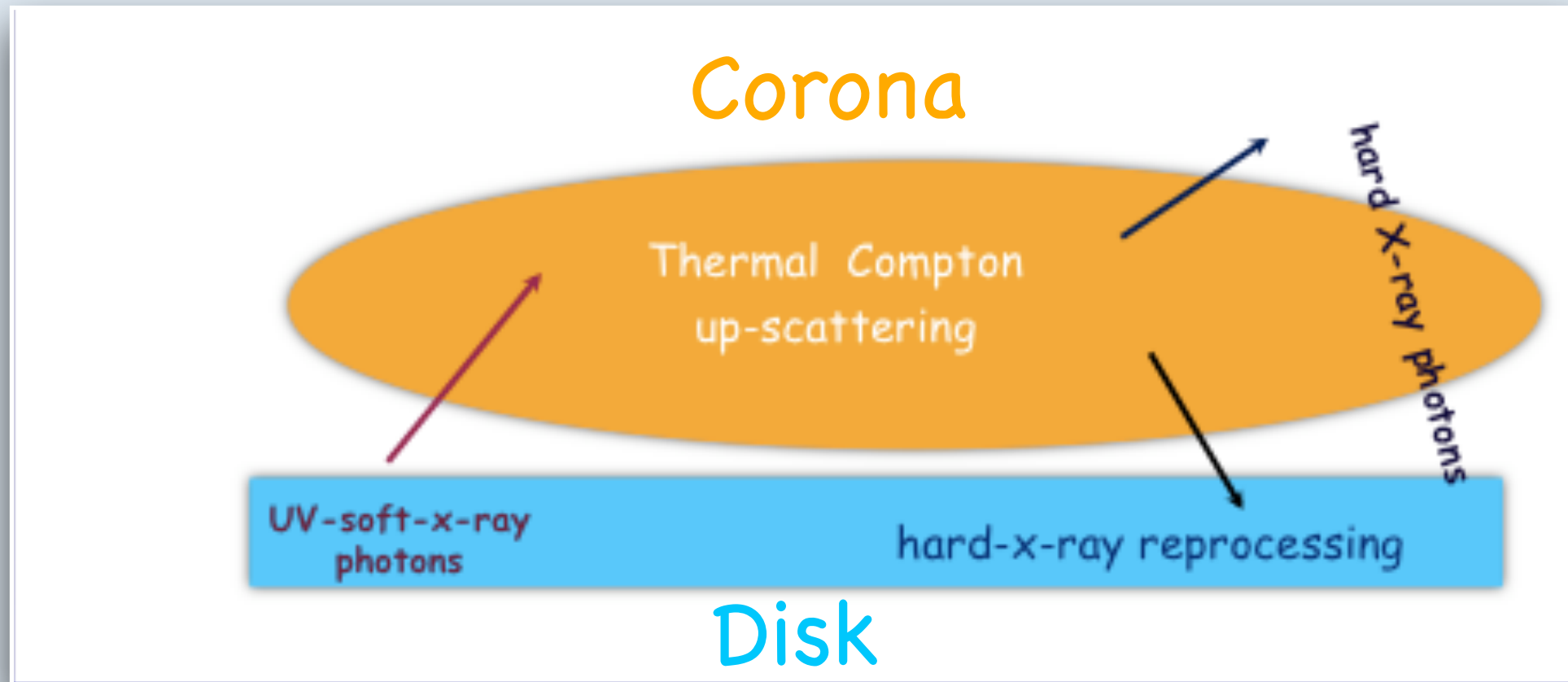
Spectral Energy Distribution (SED)



the peak occurs at UV-soft-X-ray region

$$\frac{\partial B}{\partial \nu} = 0 \quad B(\nu) \propto \nu^3 [e^{\frac{h\nu}{kT}} - 1]^{-1}$$

$$\nu_{max} = 2.8kT/h \sim 10^{16} Hz$$



Thermal Comptonization

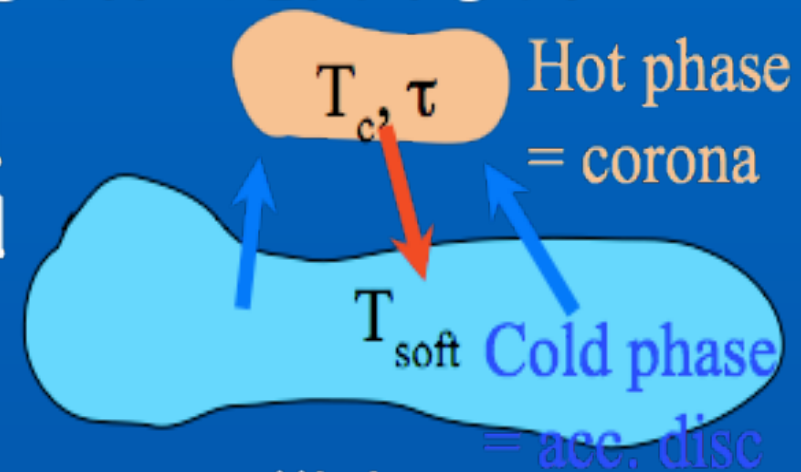
With this term we mean the process of multiple scattering of a photon due to a **thermal (Maxwellian)** distribution of electrons.

There is one fundamental parameter measuring the importance of the Inverse Compton process in general, and of multiple scatterings in particular: the Comptonization parameter, usually denoted with the letter y .

$$y = [\text{average \# of scatt.}] \times [\text{average fractional energy gain for scatt.}]$$

Thermal Comptonization

Comptonization on a thermal plasma of electrons characterized by a temp. T and optical depth τ



✓ mean relative energy gain per collision

$$\frac{\Delta E}{E} \simeq \left(\frac{4kT}{mc^2} \right) + 16 \left(\frac{kT}{mc^2} \right)^2 \quad \text{for } E \ll kT$$

$$\leq 0 \quad \text{for } E \gtrsim kT$$

✓ mean number of scatterings

$$N \simeq (\tau + \tau^2)$$

➡ Compton parameter $y = \frac{\Delta E}{E} N$

$$E_f = E_i e^y$$

Thermal Comptonization Spectrum: the Continuum

$$F_E \propto E^{-\Gamma(kT, \tau)} \exp \left(-\frac{E}{E_c(kT, \tau)} \right)$$

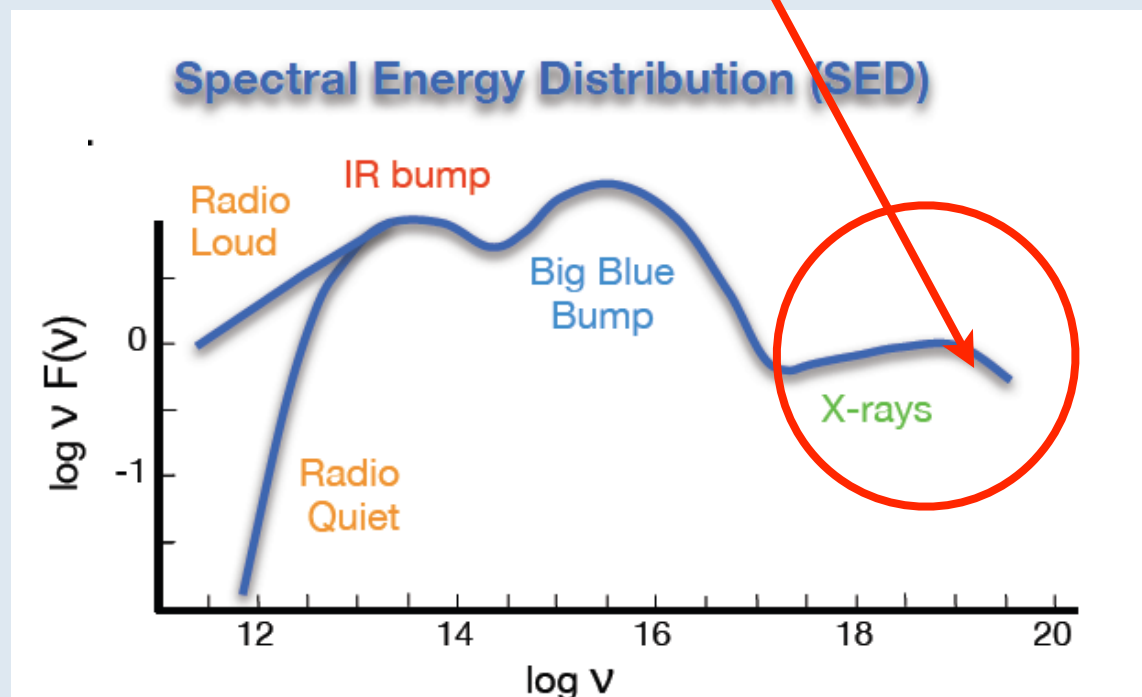
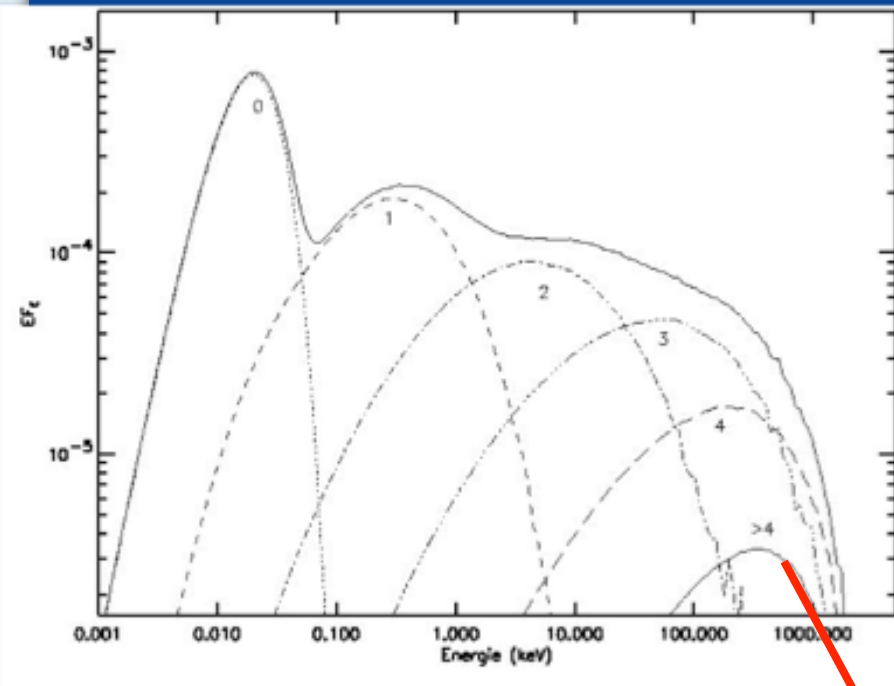
$$\Gamma(\tau, kT)$$

The exact relation between spectral index and optical depth depends on the geometry of the scattering region.

$$E_c \simeq kT$$

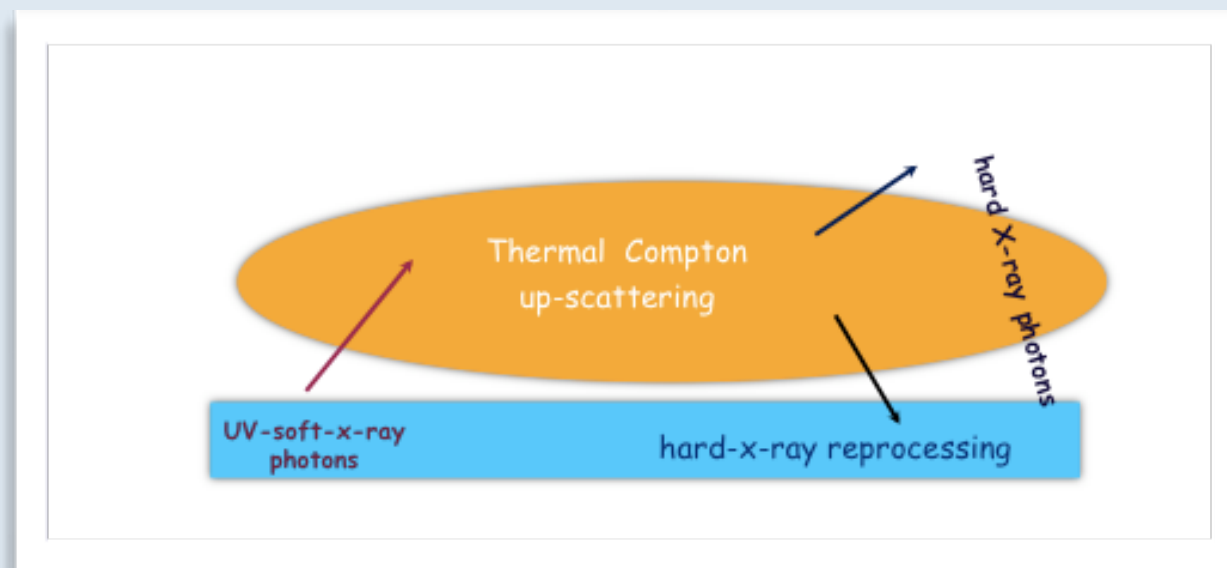
As photons approach the electron thermal energy, they no longer gain energy from scattering, and a sharp rollover is expected in the spectrum.

The observed high energy spectral cutoff yields information about the temperature of the underlying electron distribution.



Haardt & Maraschi 1991

Reprocessed features

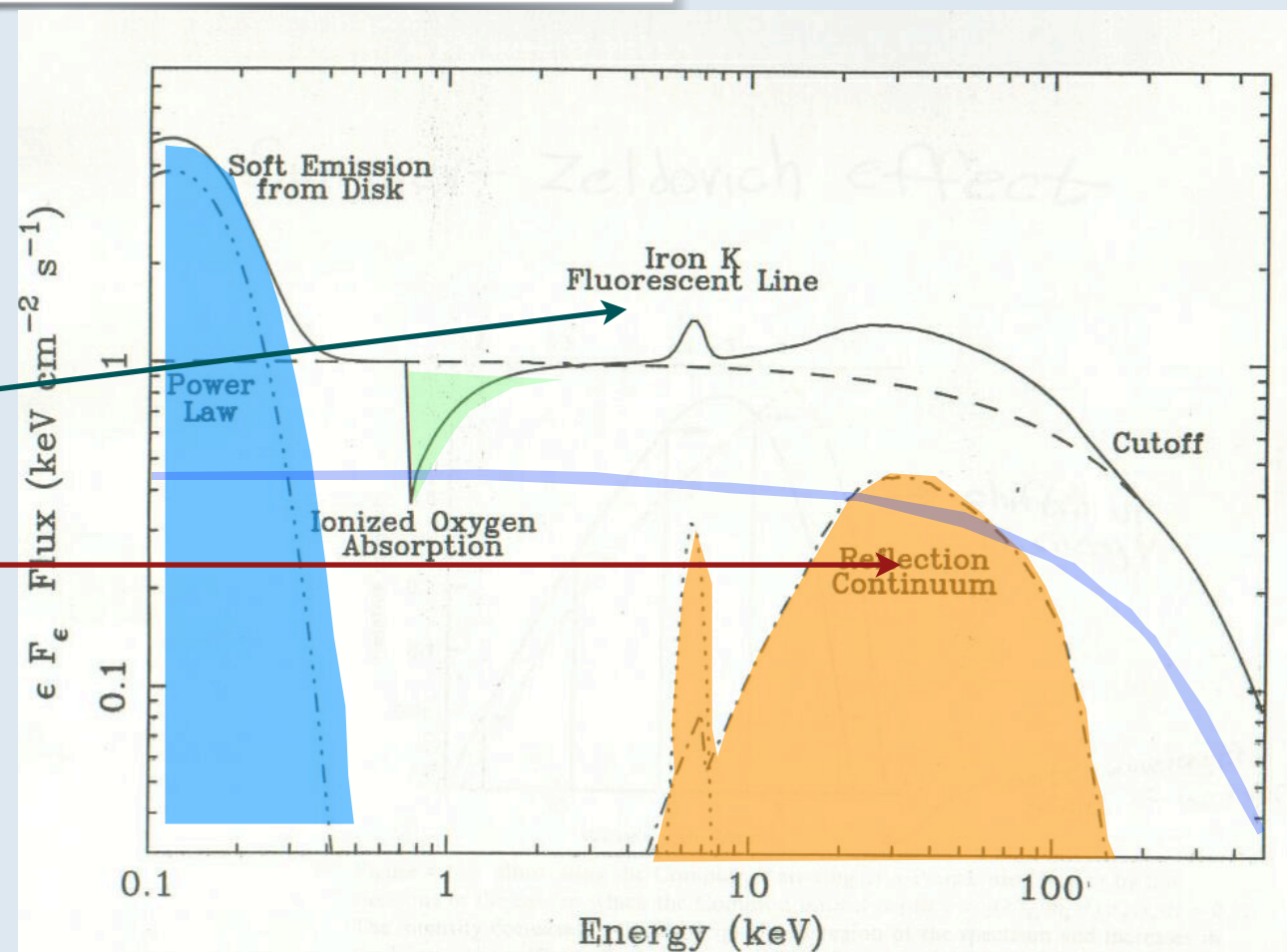


- Thermal Comptonization

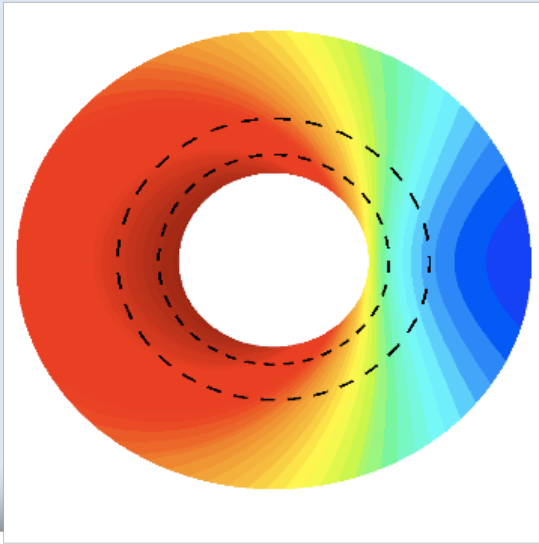
- Hard X-ray reprocessing

Iron line

Compton hump



IRON LINE



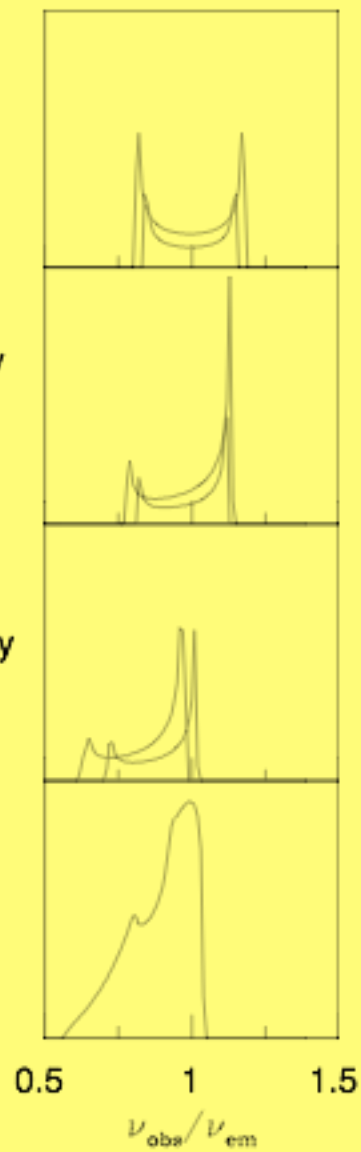
Schwarzschild

Newtonian

Special relativity

General relativity

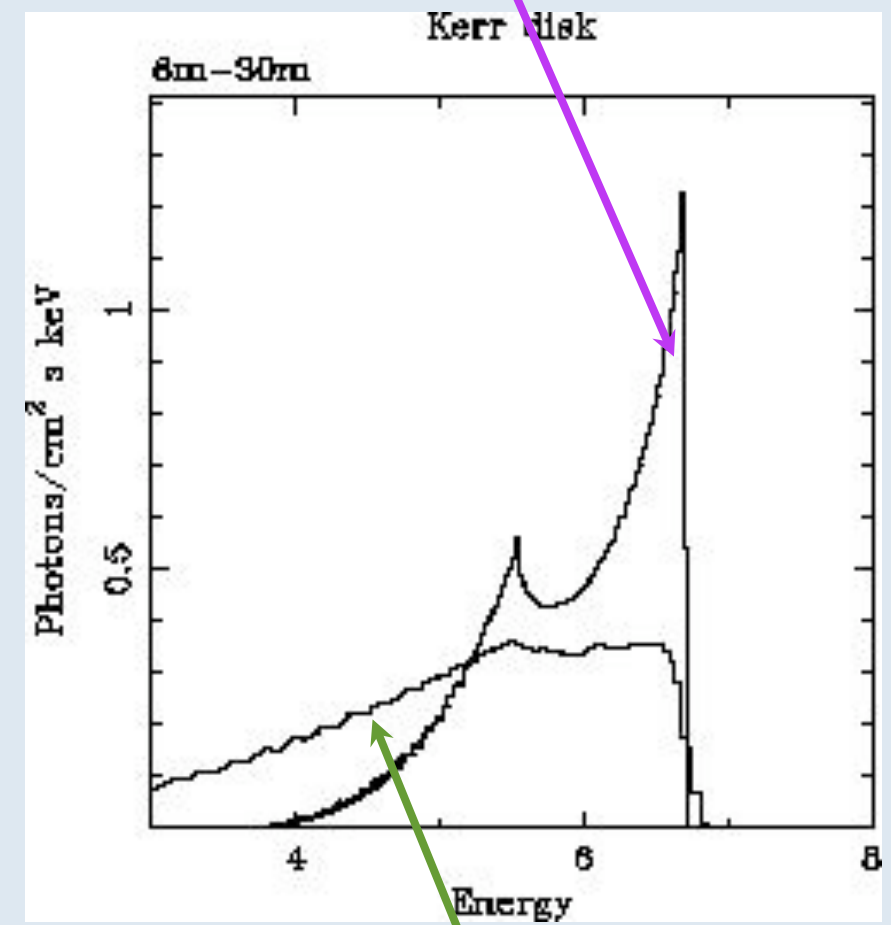
Line profile



Transverse Doppler shift

Beaming

Gravitational redshift

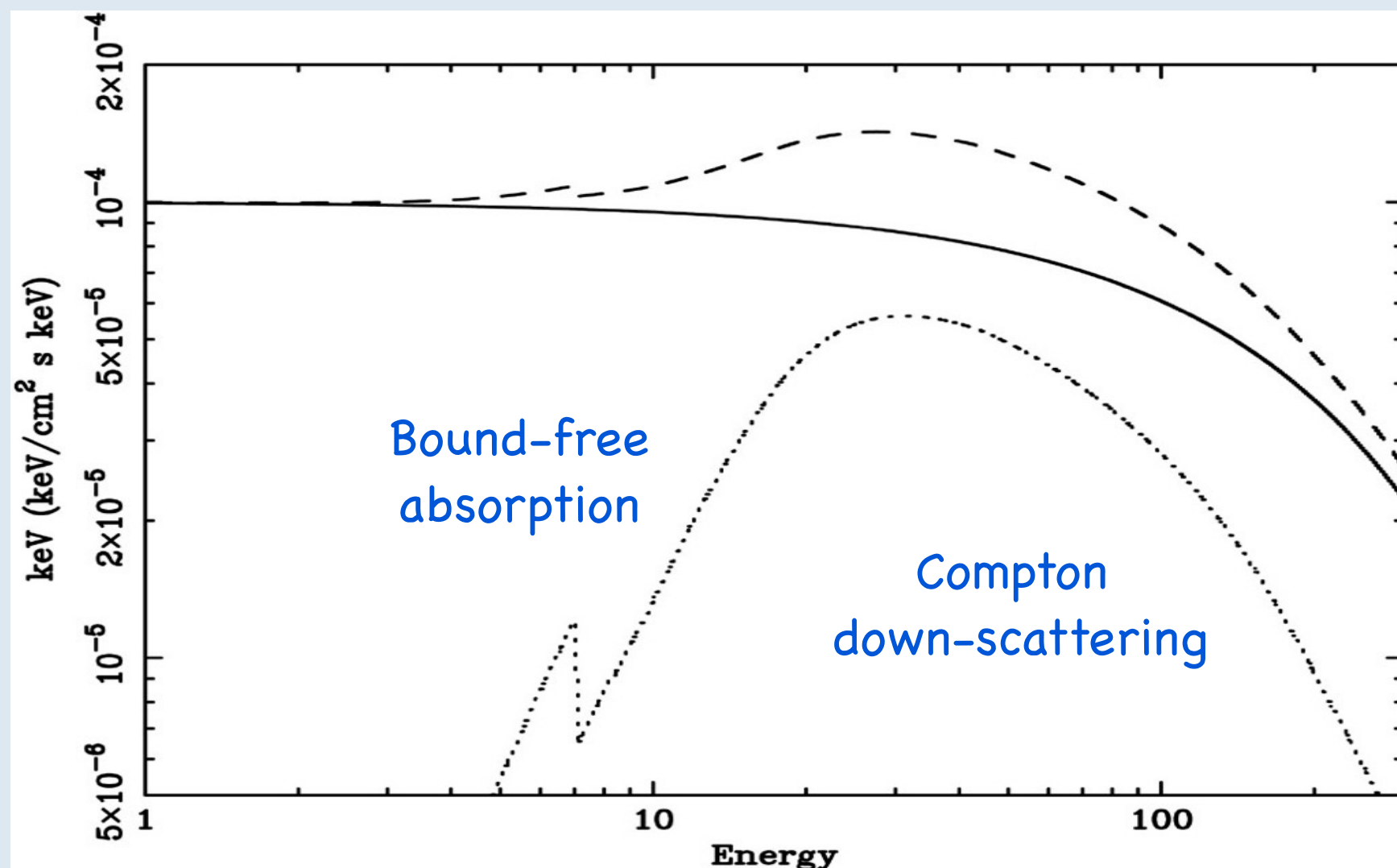


Kerr

Reflection

At low energies <10 keV the high-Z ions absorb the X-rays. A major part of the opacity above 7 keV is due to Fe K-edge opacity.

At high energies the Compton shift of the incident photons becomes important.



Inefficient Engine

Energy Equation

$$q^+ = q^- + q^{\text{adv}}$$

Thin Accretion Disk

(Shakura & Sunyaev 1973;
Novikov & Thorne 1973;...)

Most of the viscous heat
energy is radiated

$$q^- \approx q^+ \gg q^{\text{adv}}$$

$$L_{\text{rad}} : 0.1 \dot{M} c^2$$

Advection-Dominated Accretion Flow (ADAF)

(Ichimaru 1977; Narayan & Yi
1994, 1995; Abramowicz et al.
1995)

Most of the heat energy is
retained in the gas

$$q^- \ll q^+ \approx q^{\text{adv}}$$

$$L_{\text{rad}} \ll 0.1 \dot{M} c^2$$

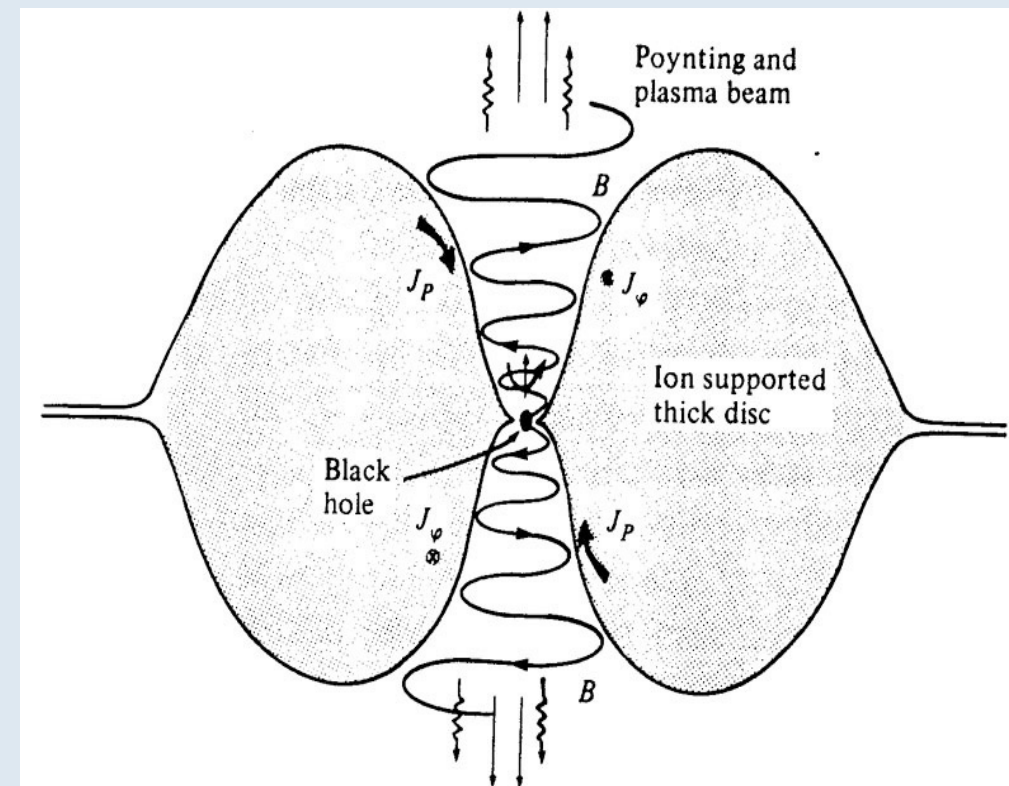
$$L_{\text{adv}} : 0.1 \dot{M} c^2$$

q^+ is the energy generated by viscosity per unit volume
 q^- is the radiative cooling per unit volume
 q^{adv} represents the advective transport of energy

ADAF

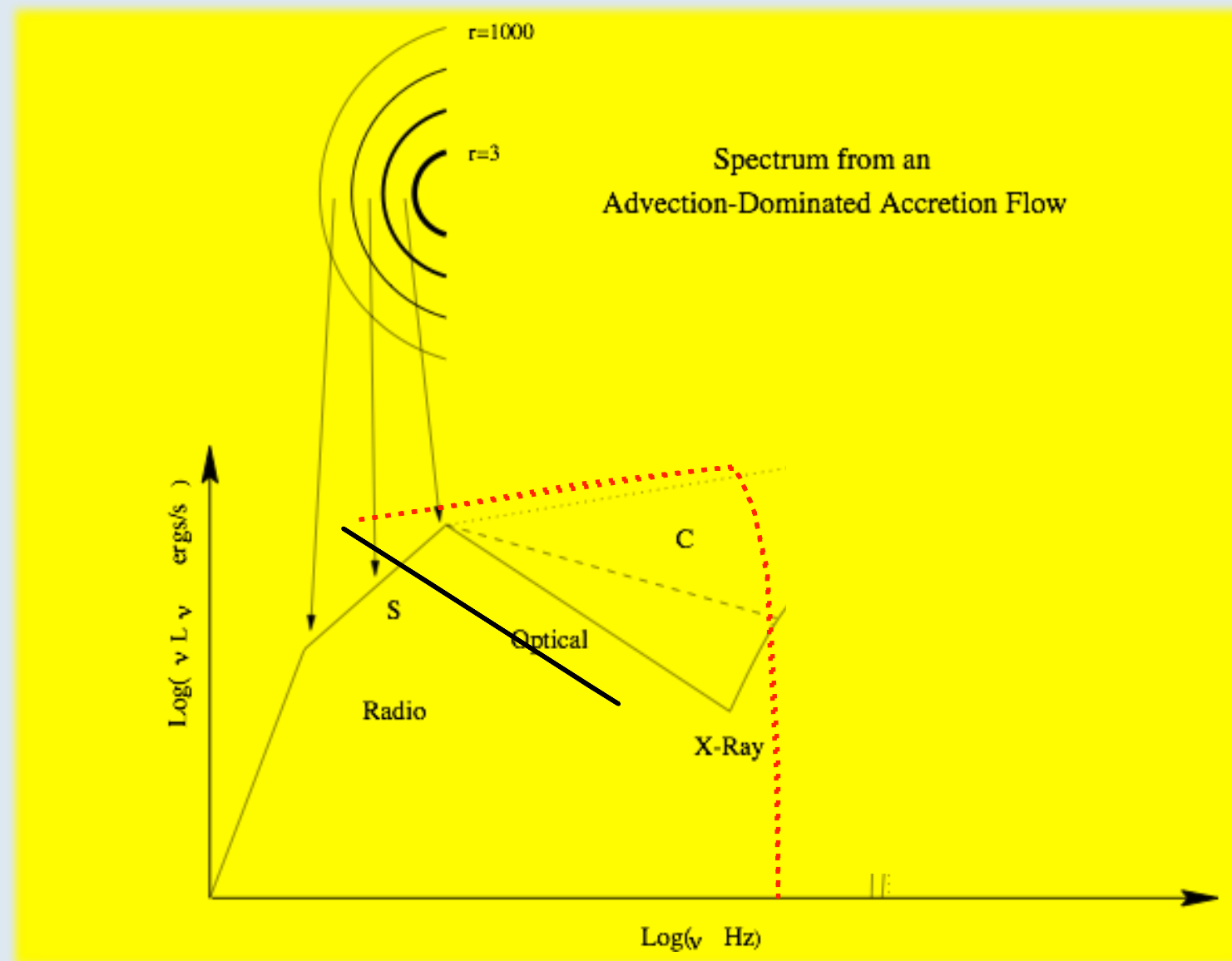
In this solution the accreting gas has a very low density and is unable to cool efficiently. The viscous energy is stored in the gas as thermal energy instead of being radiated and is advected onto the BH. Ions and electrons are thermally decoupled.

- Very Hot: $T_i \sim 10^{12} \text{K}$ (R_s/R), $T_e \sim 10^9\text{--}10^{11} \text{K}$ (since ADAF loses very little heat).
- Geometrically thick: $H \sim R$ (most of the viscosity generated energy is stored in the gas as internal energy rather than being radiated, the gas puffs up)
- Optically thin (because of low density)

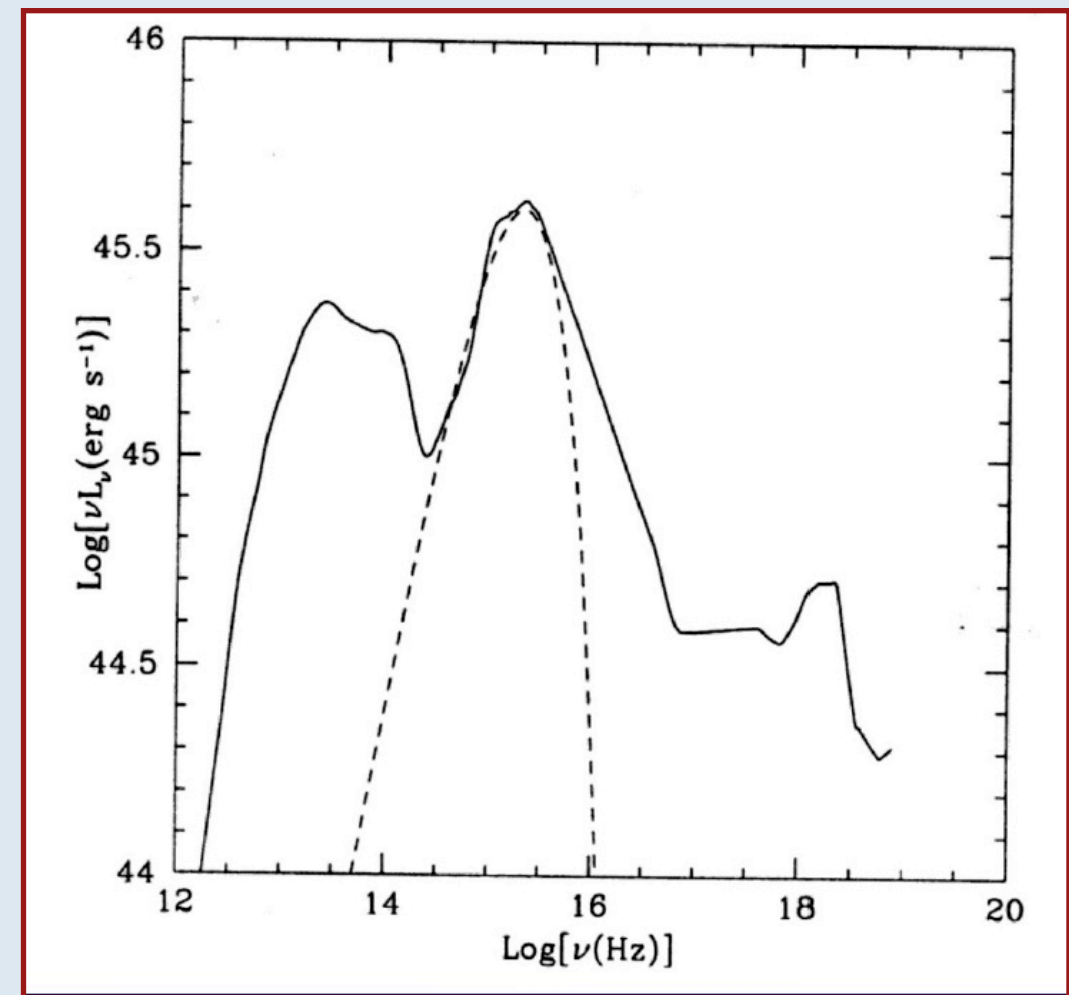
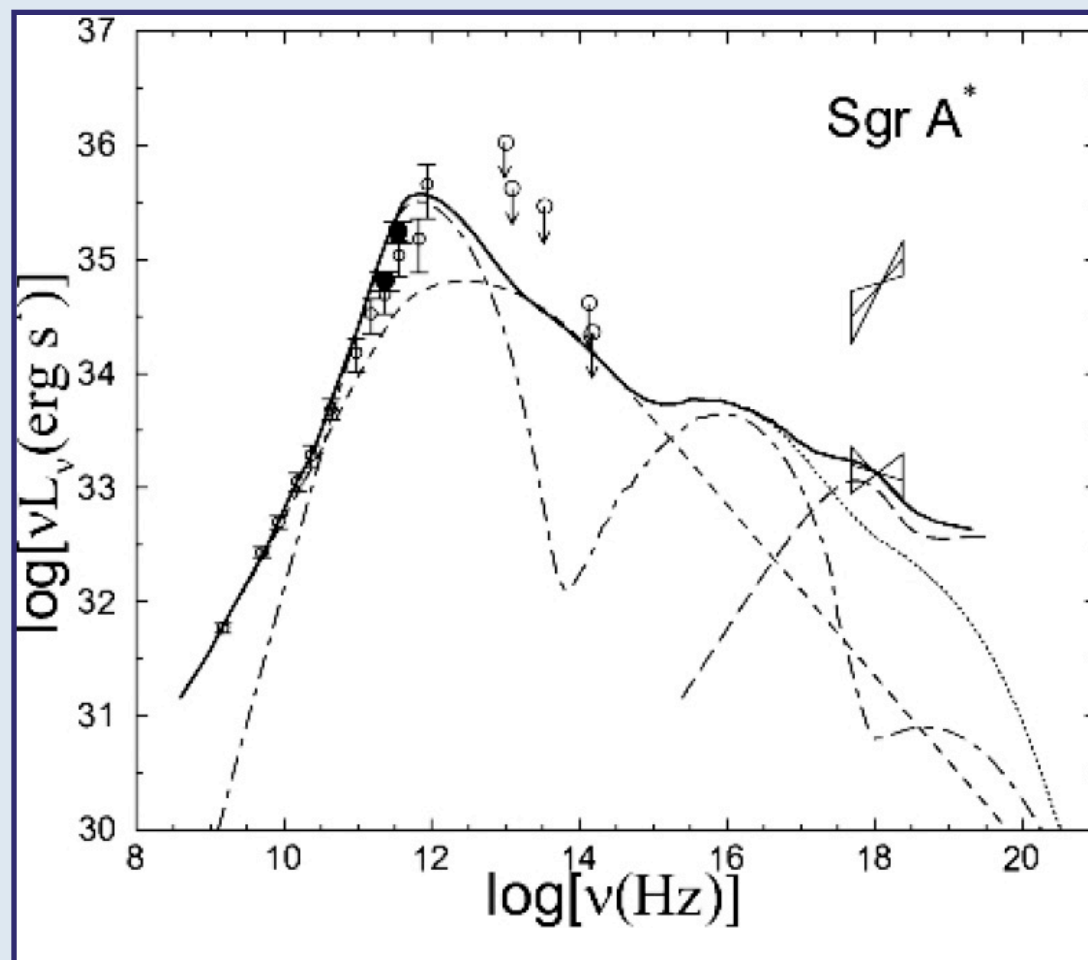


ADAF SED

Typical luminosities: $L < (0.01 - 0.1) L_{\text{Edd}}$

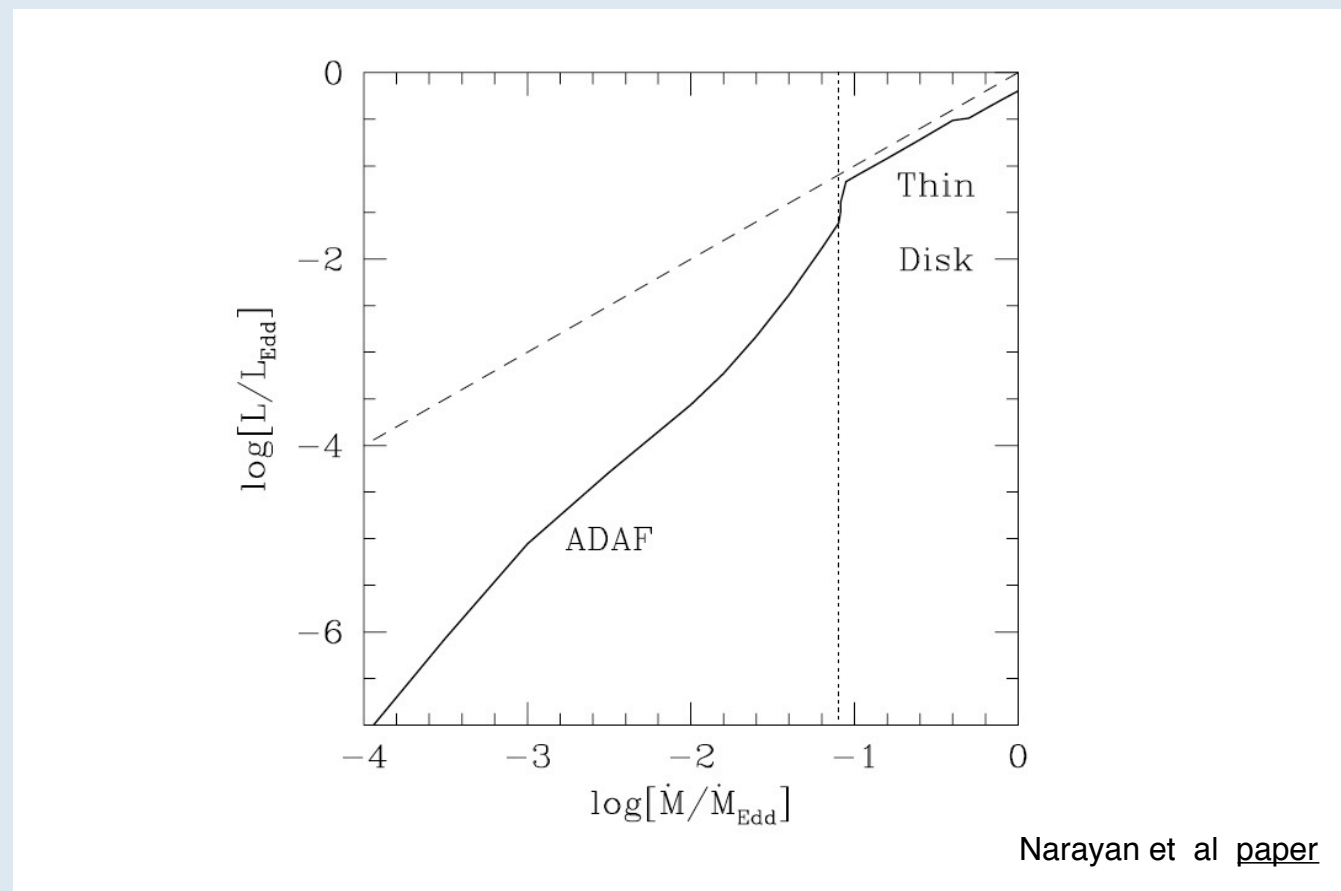


Schematic spectrum of an ADAF around a black hole. S, C, and B refer to electron emission by synchrotron radiation, inverse Compton scattering, and bremsstrahlung, respectively. The solid line corresponds to a low accretion, the dashed line to an intermediate accretion, and the dotted line to the highest (possible) accretion.




ADAF

Accretion disk



Narayan et al [paper](#)

An artistic rendering of an active galactic nucleus (AGN). At the center is a black hole, surrounded by a glowing accretion disk. A bright, narrow jet of light extends from the center towards the top right. The background is a deep purple and blue space with some distant stars.

AGN radio loud are more complex
than RQ:
They have another source of
anisotropy: the jet

Jet Scale

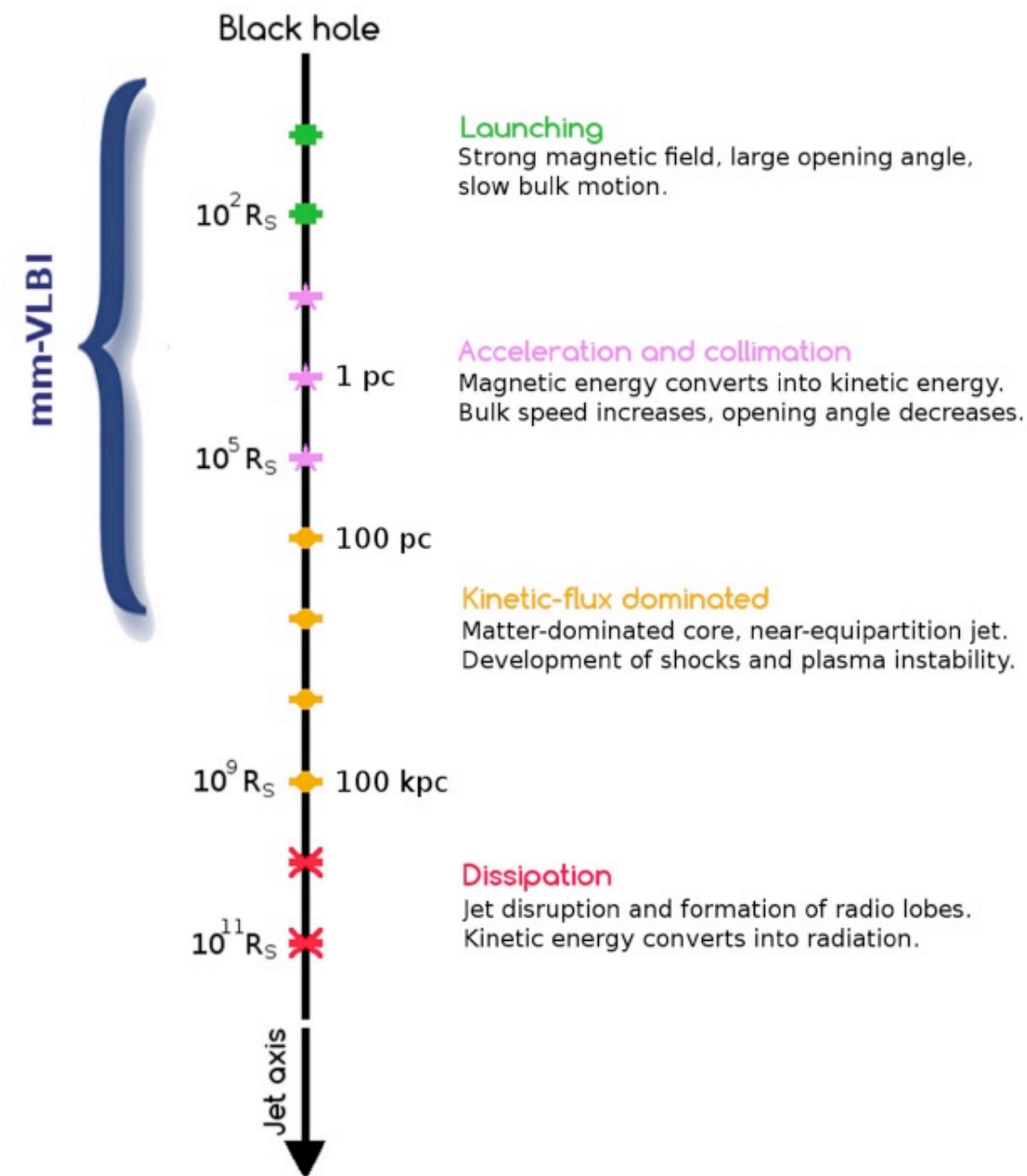


Fig. 5 Schematic view of the main regions of a relativistic jet, according to the current paradigm for magnetically-driven flows. The radial separation from the black hole is represented in a logarithmic scale, in units of Schwarzschild radii R_S . We also report the corresponding distance in units of parsecs (pc) for a black hole mass of $10^9 M_\odot$. The extension of each region is approximate, and may vary in different jets. VLBI observations at millimeter wavelengths are suited for probing the magnetically dominated jet base and the transition to the kinetic-flux dominated region.

The jet emission is strongly Doppler boosted

The key parameter is the Doppler Factor $\delta(\beta, \theta)$

$$\delta = [\gamma(1 - \beta \cos \theta)]^{-1}$$

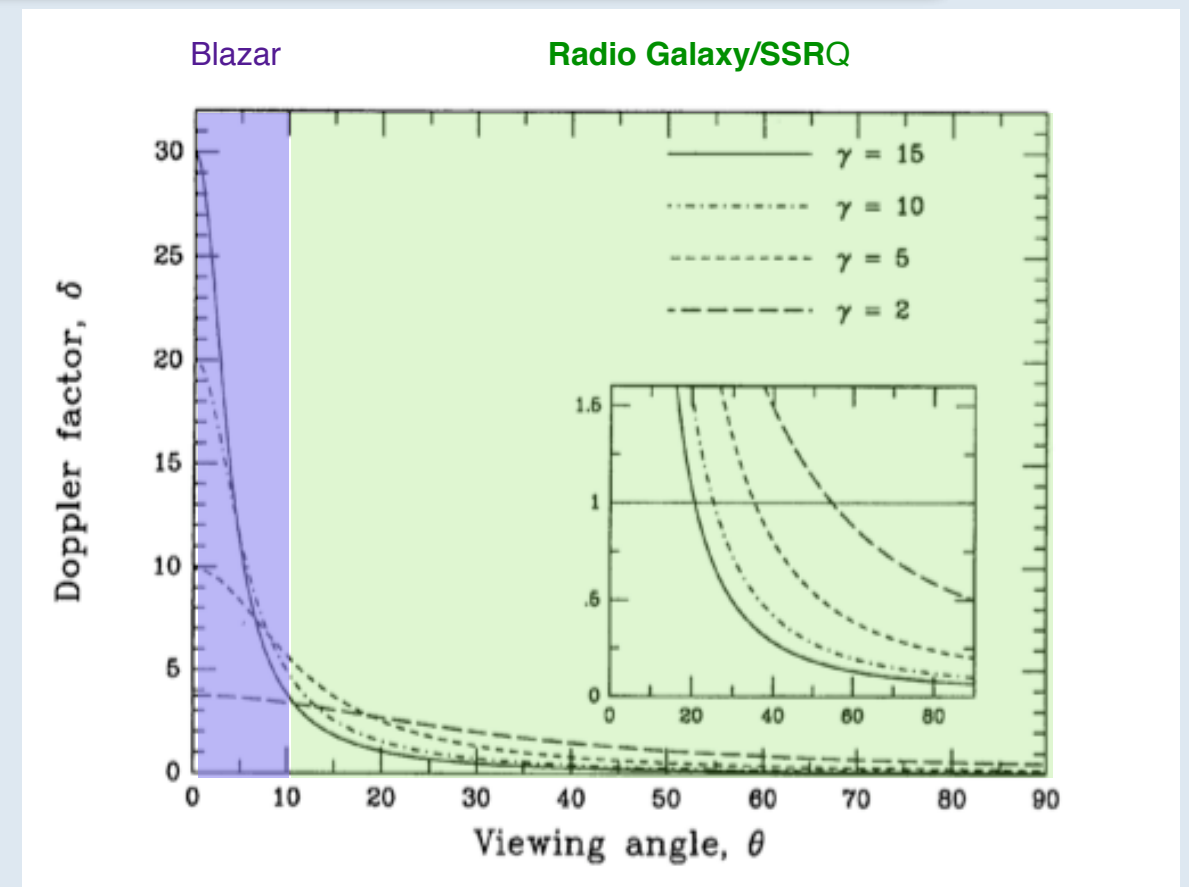
$\gamma = \frac{1}{\sqrt{1 - \beta^2}}$ Lorentz factor
 $\beta = v/c$ bulk velocity
 θ angle between the jet axis and the line of sight

The Doppler factor relates intrinsic and observed flux for a moving source at relativistic speed $v = \beta c$.

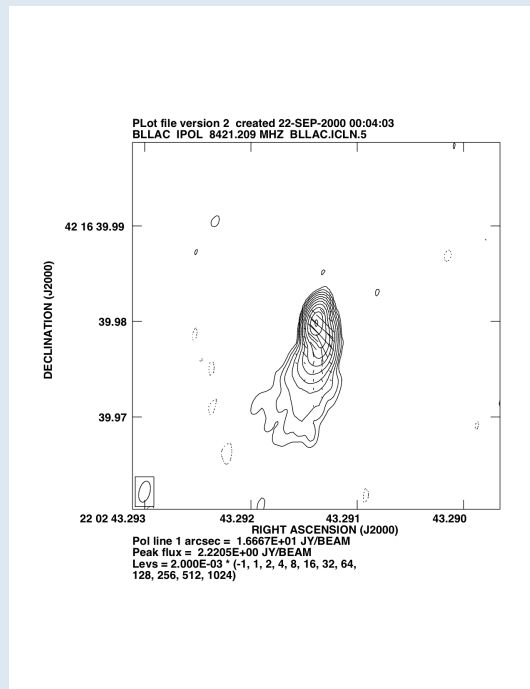
For an **intrinsic** power law spectrum: $F'(v') = K (v')^{-\alpha}$
 the **observed** flux density is

$$F_v(v) = \delta^{3+\alpha} F'_{v'}(v)$$

$$\Delta t = \Delta t' / \delta$$

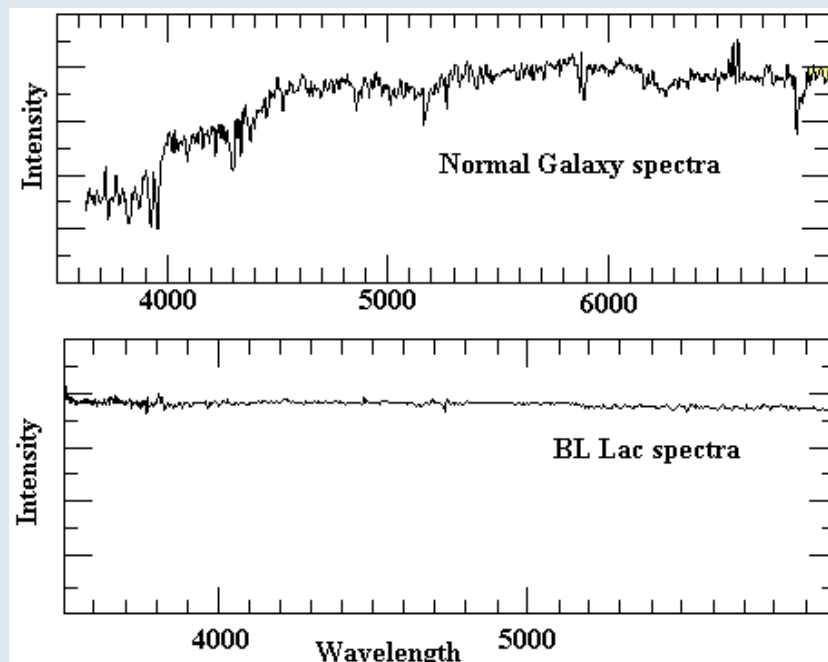


Blazars are divided into two classes: BL Lacs (BL) and Flat Spectrum Radio Quasar (FSRQ)

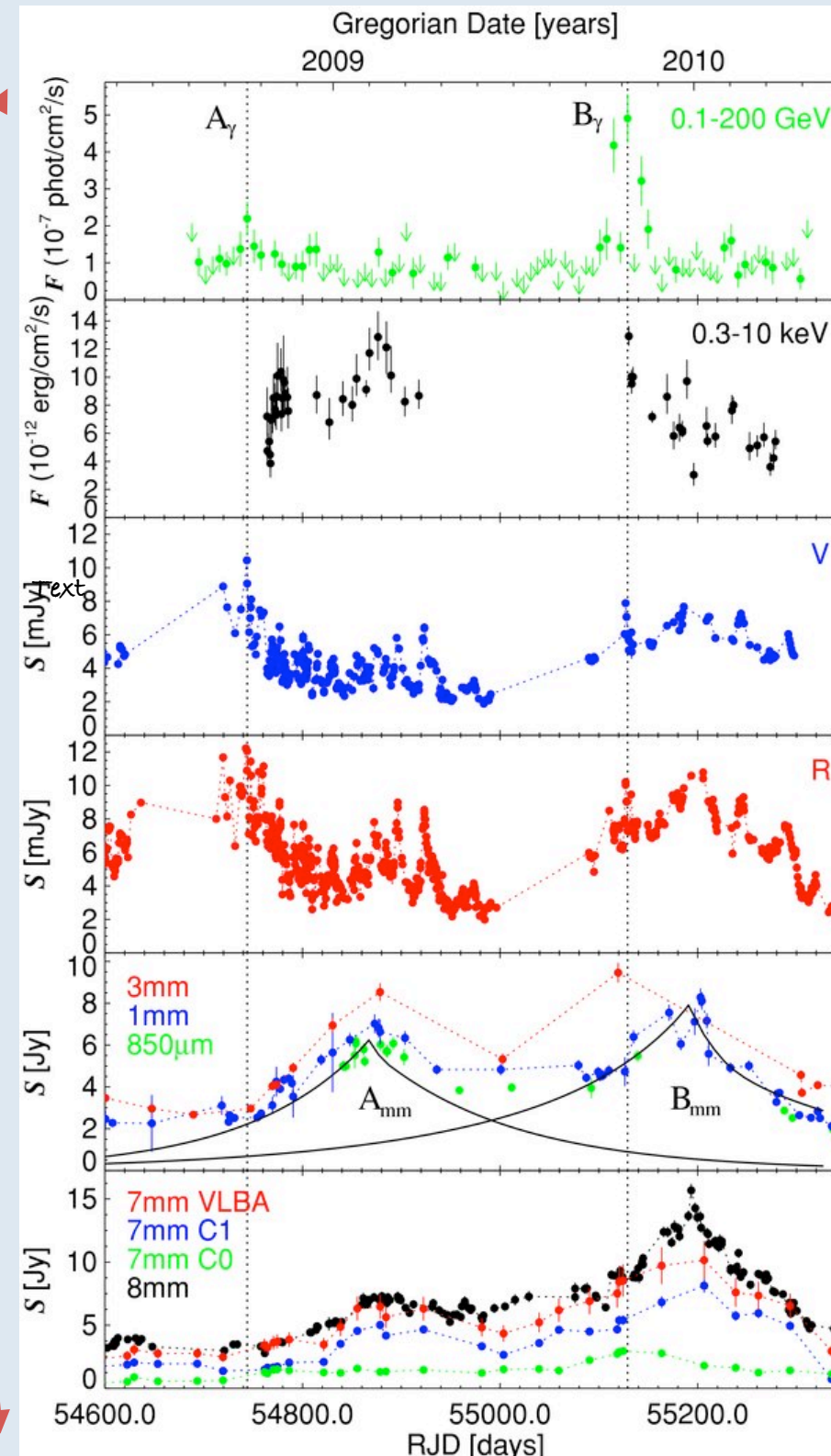


Both are compact in
radio maps and
extremely variable
at all frequencies

BL are almost featureless in the optical
band (FSRQ can show emission lines
overimposed on a strong continuum)

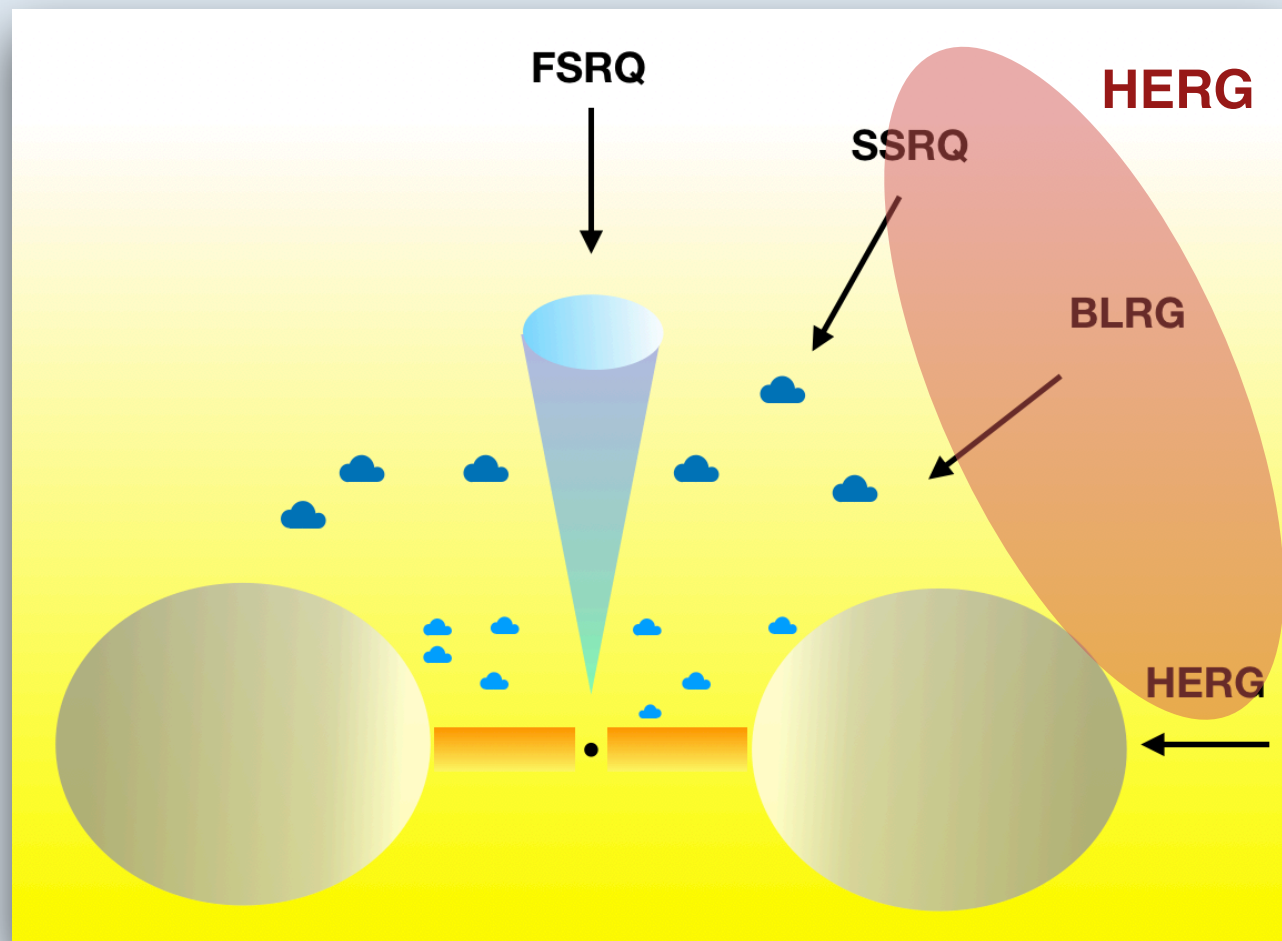


Extremely variable

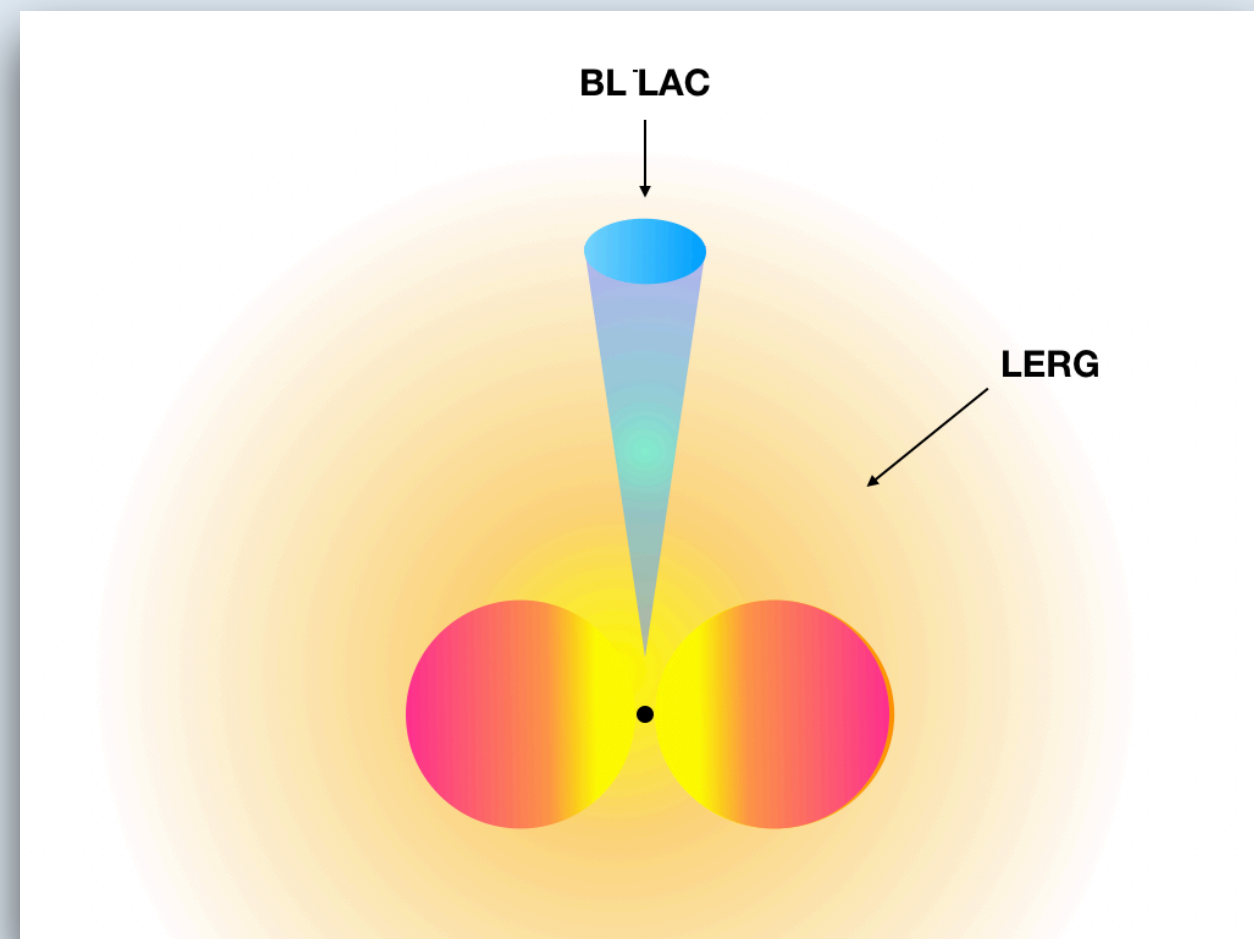


OJ 287 light curves
from radio to gamma
Agudo et al. 2011ApJL
726, L13

Revised AGN Unified Model



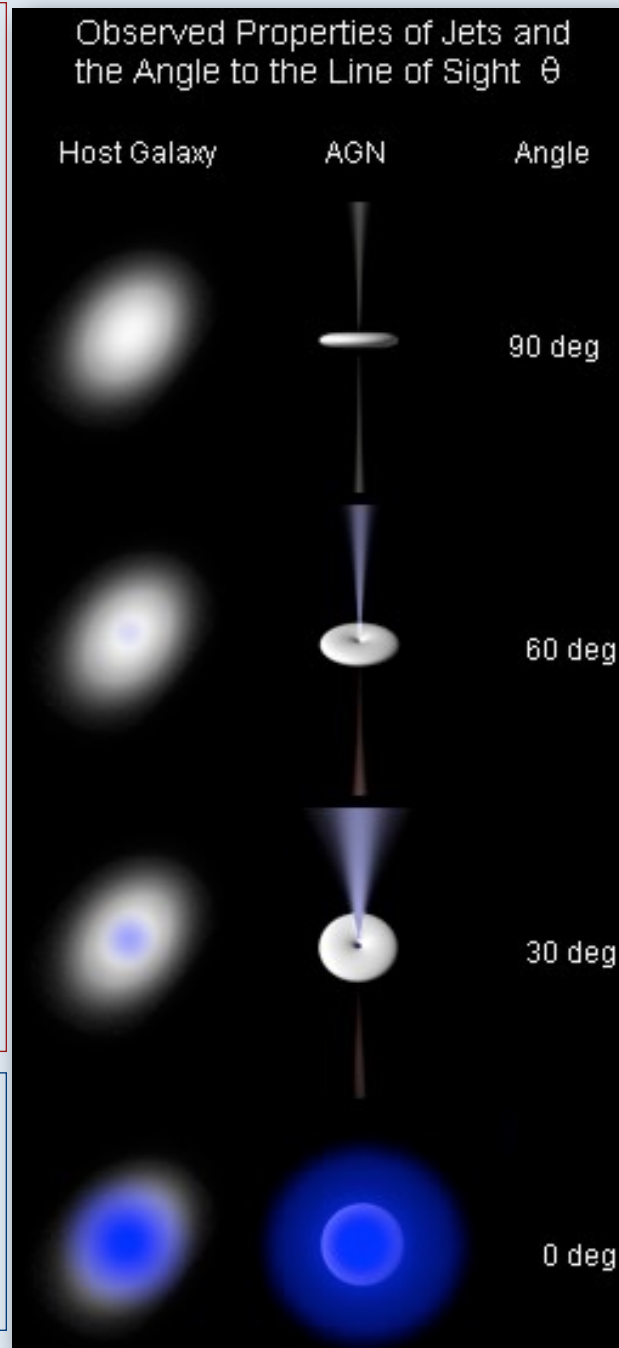
Efficient Accretion
DISK



Inefficient flow
ADAF

Radio Galaxies HERG

Blazar



HERG: Thermal radiation dominates the spectrum in the IR-optical-UV-X-ray band

HERG (BLRG): Thermal and non thermal radiation are in competition

Blazar: Non-Thermal radiation dominates all the spectrum

LERG: Non-Thermal radiation dominates the spectrum having an efficient accretion flow

Core Emission

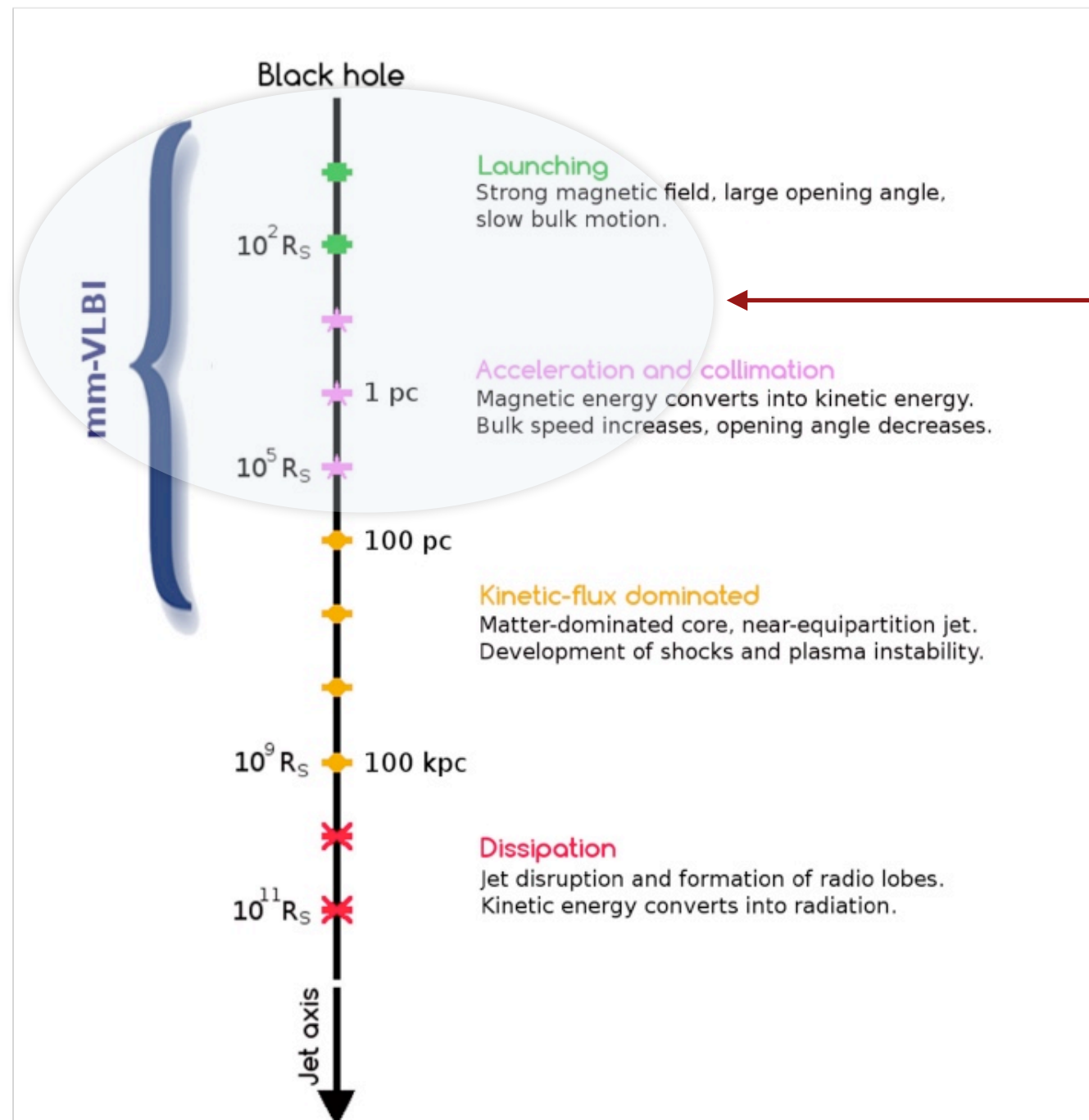
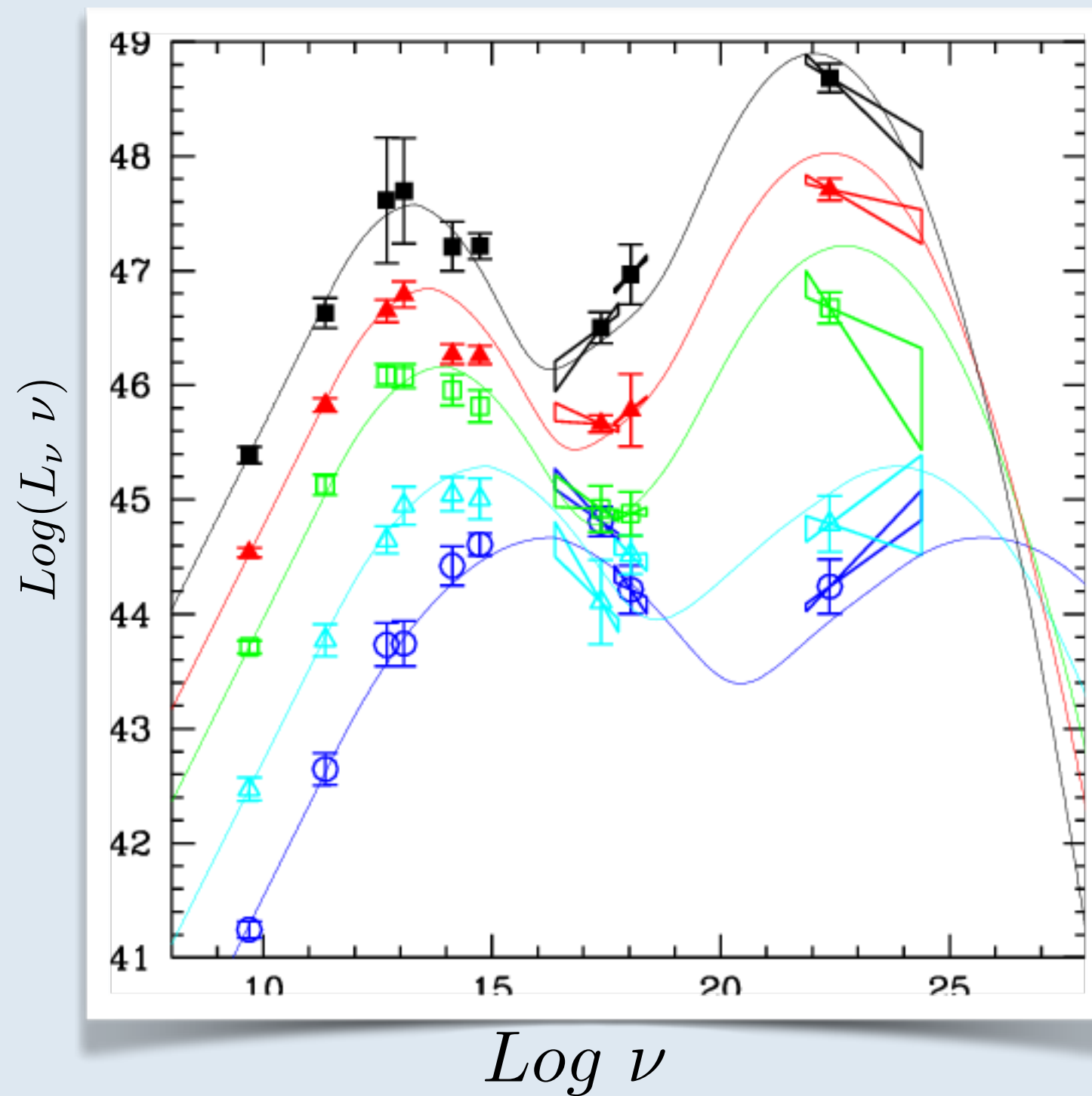


Fig. 5 Schematic view of the main regions of a relativistic jet, according to the current paradigm for magnetically-driven flows. The radial separation from the black hole is represented in a logarithmic scale, in units of Schwarzschild radii R_S . We also report the corresponding distance in units of parsecs (pc) for a black hole mass of $10^9 M_\odot$. The extension of each region is approximate, and may vary in different jets. VLBI observations at millimeter wavelengths are suited for probing the magnetically dominated jet base and the transition to the kinetic-flux dominated region.

Non-thermal radiation coming from the core region dominates the SED if the jet intercepts the line of sight of the observer (BLAZAR) and/or the accretion is inefficient (LERG). The Observed Spectral Energy Distribution consists of two peaks of emission

Double peaked Spectral Energy Distribution



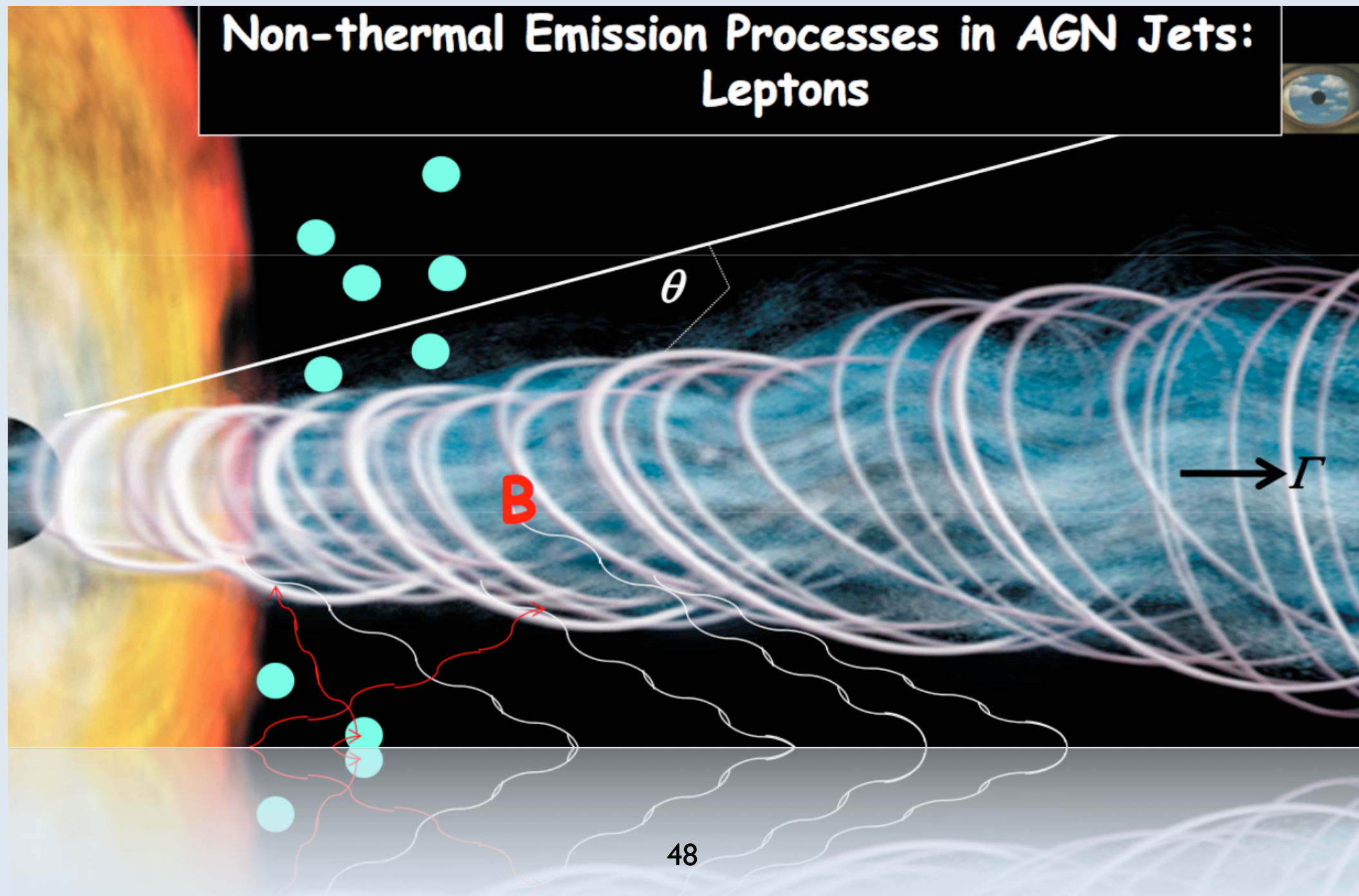
Fossati 's sequence --->paper

Non thermal emission:

Synchrotron: Magnetic Field + Leptons

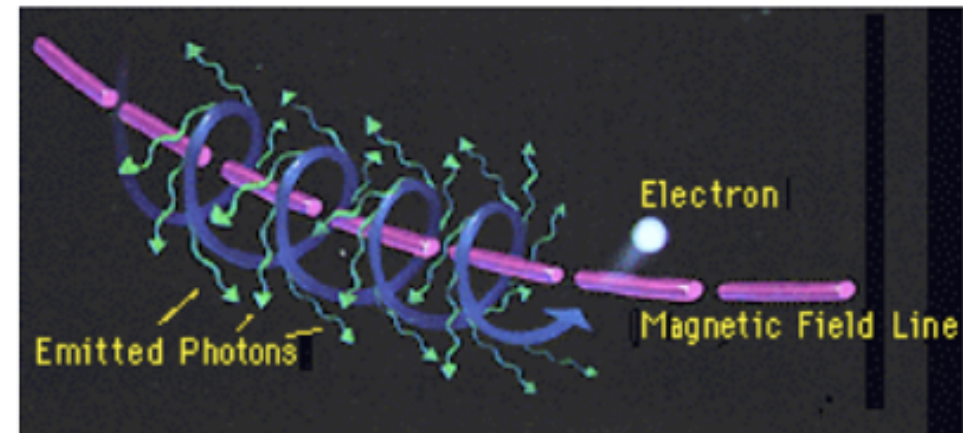
Inverse Compton: Photons + Leptons

Non-thermal Emission Processes in AGN Jets: Leptons

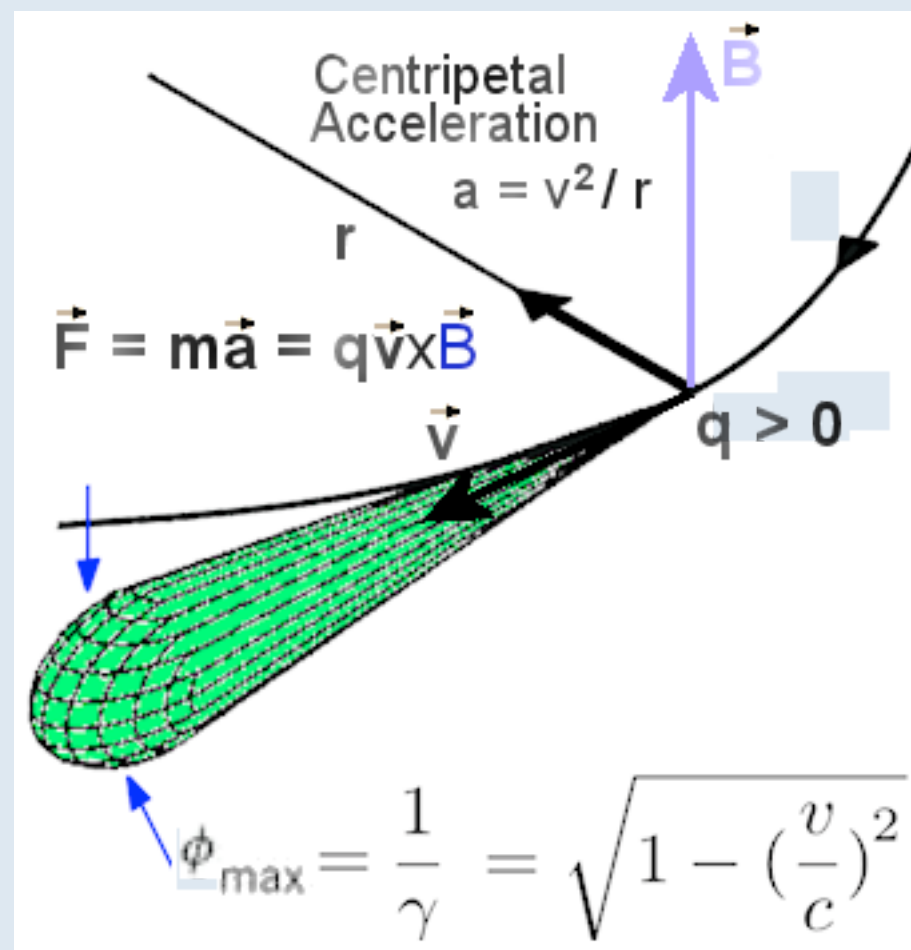


Synchrotron Radiation

Synchrotron radiation is due to the movement of an electron charge in a magnetic field. As a particle gyrates around a magnetic field, it will emit radiation at a frequency proportional to the strength of the magnetic field and its velocity.



Synchrotron radiation is highly polarized and is seen at all wavelengths. At relativistic speeds, the radiation can also be beamed. It is very common in radio spectrum, but can be seen in x-rays. It is usually fit as a power law. For full details, see the review by Ginzburg & Syrovatskii (1969)



A moving charged particle in a magnetic field would be reflected by the Lorentz force $\vec{F} = q (\vec{v} \times \vec{B})$, where q is the charge, \vec{v} is the velocity, and \vec{B} is the magnetic field.

In a region with uniform magnetic field, the curvilinear path of the charged particle becomes a circle and if the velocity has a component in the direction of the magnetic field then the trajectory will be a helix

The synchrotron radiation of a power law distribution of electron energies

Synchrotron

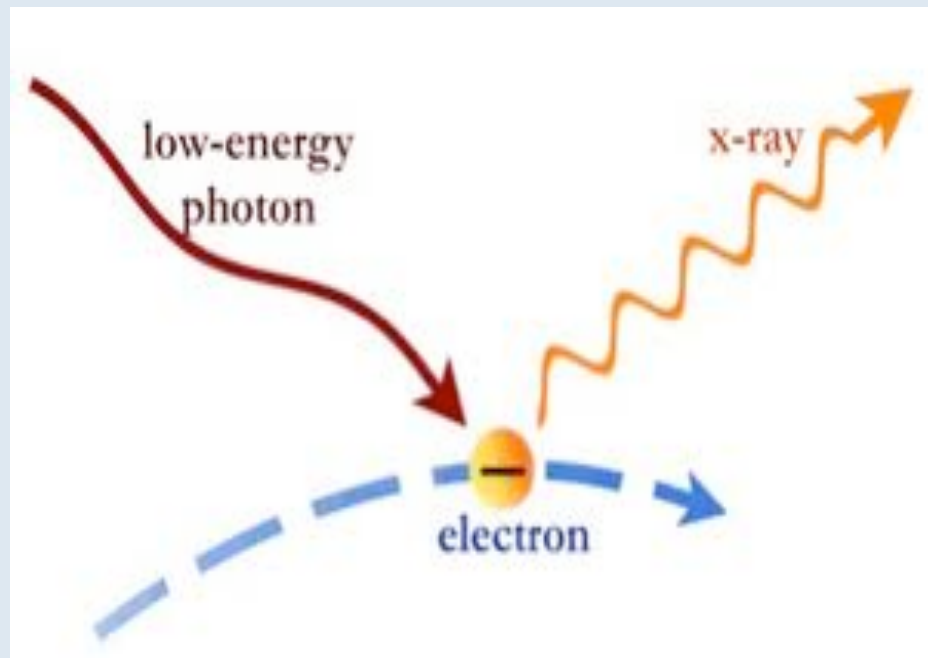
$$N(\gamma_e) = K \gamma_e^{-p}, \quad \gamma_{min} < \gamma_e < \gamma_{max}, \quad p = 1 + 2\alpha$$

$$\epsilon_{sin}(\nu) \propto K B^{\alpha+1} \nu^{-\alpha} \quad \text{erg cm}^{-3} \text{s}^{-1} \text{sr}^{-1}$$

$$\epsilon_{sin}(\nu) \propto K B^{\alpha+1} \nu^{-\alpha} \quad \text{erg cm}^{-3} \text{s}^{-1} \text{sr}^{-1}$$

Inverse Compton scattering

When the electron is not at rest, but has an energy greater than the typical photon energy, there can be a transfer of energy from the electron to the photon. This process is called Inverse Compton to distinguish it from the direct Compton scattering, in which the electron is at rest, and it is the photon to give part of its energy to the electron.



$$\langle \nu \rangle = \frac{4}{3} \gamma^2 \nu$$

Inverse Compton Radiation

The general result that the frequency of the scattered photons is $\nu \approx \gamma^2 \nu_0$ is of profound importance in high energy astrophysics. We know that there are electrons with Lorentz factors $\gamma \sim 100 - 1000$ in various types of astronomical source and consequently they scatter any low energy photons to very much higher energies. Consider the scattering of radio, infrared and optical photons scattered by electrons with $\gamma = 1000$.

<i>Waveband</i>	<i>Frequency (Hz)</i> ν_0	<i>Scattered Frequency (Hz)</i> <i>and Waveband</i>
Radio	10^9	$10^{15} = \text{UV}$
Far-infrared	3×10^{12}	$3 \times 10^{18} = \text{X-rays}$
Optical	4×10^{14}	$4 \times 10^{21} \equiv 1.6\text{MeV} = \gamma\text{-rays}$

Thus, inverse Compton scattering is a means of creating very high energy photons indeed. It also becomes an inevitable drain of energy for high energy electrons whenever they pass through a region in which there is a large energy density of photons.

Inverse Compton

For a power law distribution of electrons:

$$N(\gamma_e) = K\gamma_e^{-p}, \quad \gamma_{min} < \gamma_e < \gamma_{max}, \quad p = 1 + 2\alpha$$

Inverse Compton

$$\epsilon_c(\nu_c) \propto K\nu_c^{-\alpha} \int \frac{U_r(\nu)\nu^\alpha}{\nu} d\nu \quad \text{erg cm}^{-3} \text{ s}^{-1} \text{ sr}^{-1}$$

U_r is the radiation energy density

$$U_r = \int n(\epsilon)\epsilon d\epsilon$$

- Synchrotron photons in the jet
- Environment photons from Accretion Flow, BLR, NLR, Torus
- Cosmic Microwave Background (CMB) photons

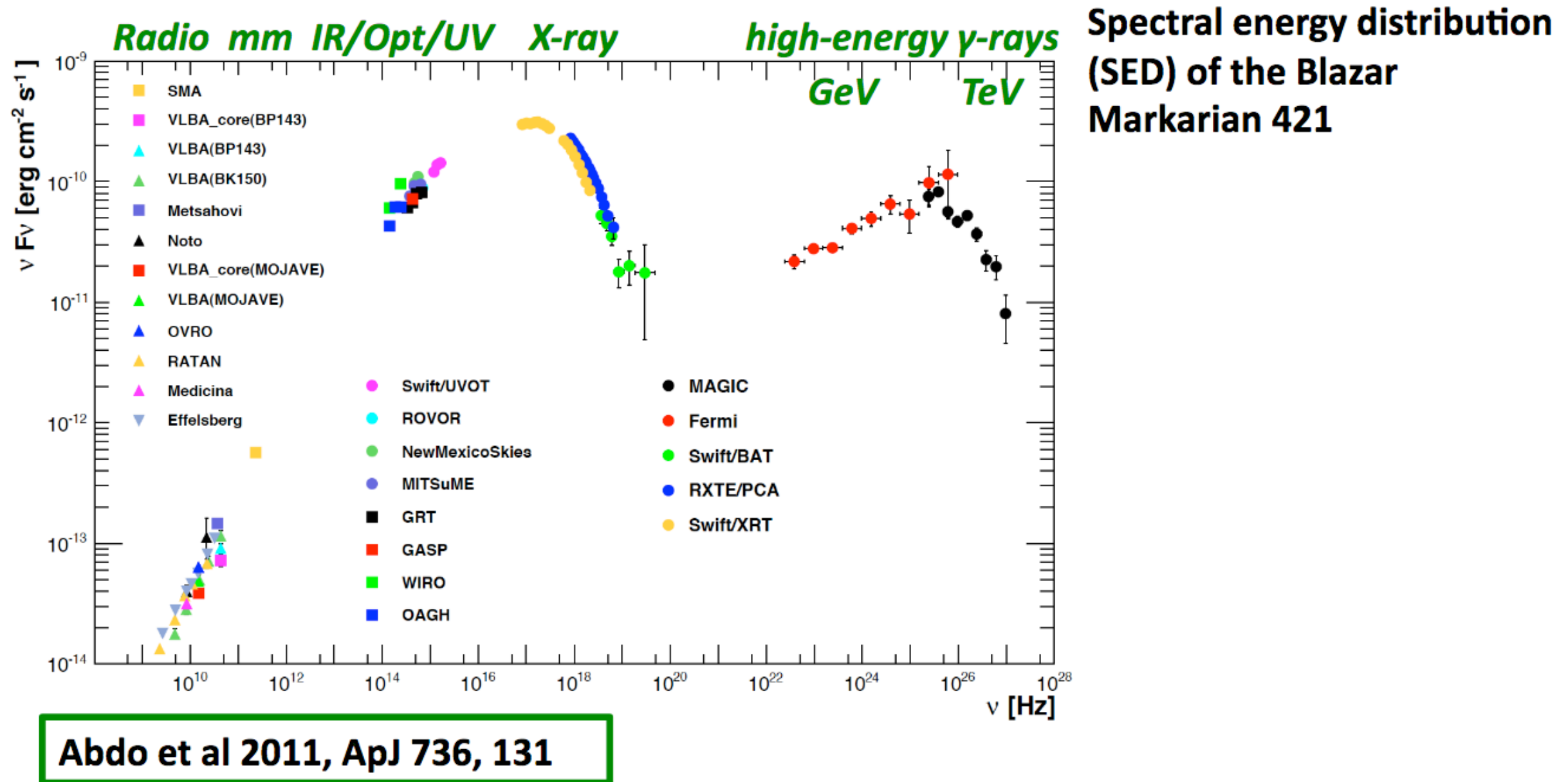
Synchrotron Self–Compton works in BL LAC

Consider a population of relativistic electrons in a magnetized region. They will produce synchrotron radiation, and therefore they will fill the region with photons. These synchrotron photons will have some probability to interact again with the electrons, by the Inverse Compton process. Since the electron “work twice” (first making synchrotron radiation, then scattering it at higher energies) this particular kind of process is called synchrotron self-Compton, or SSC for short.

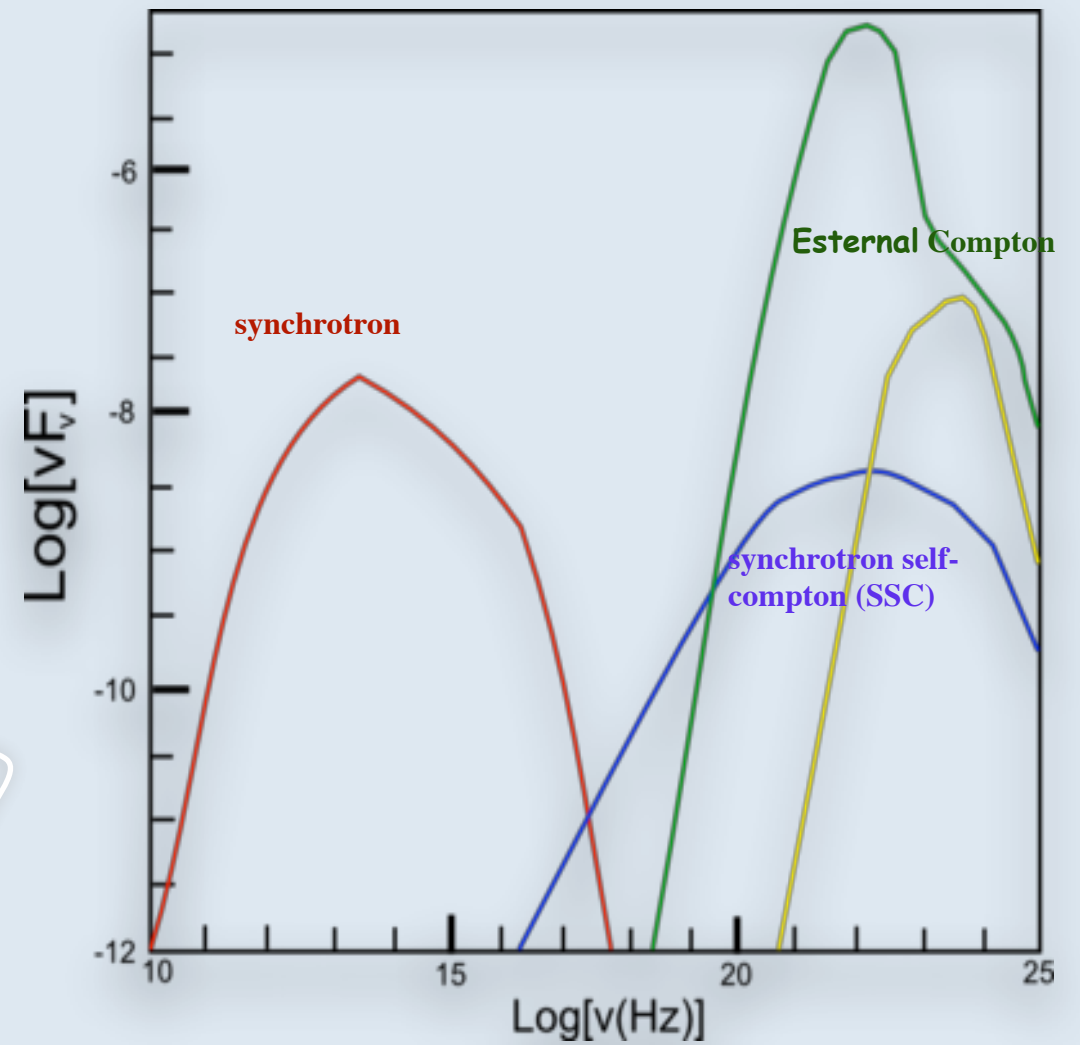
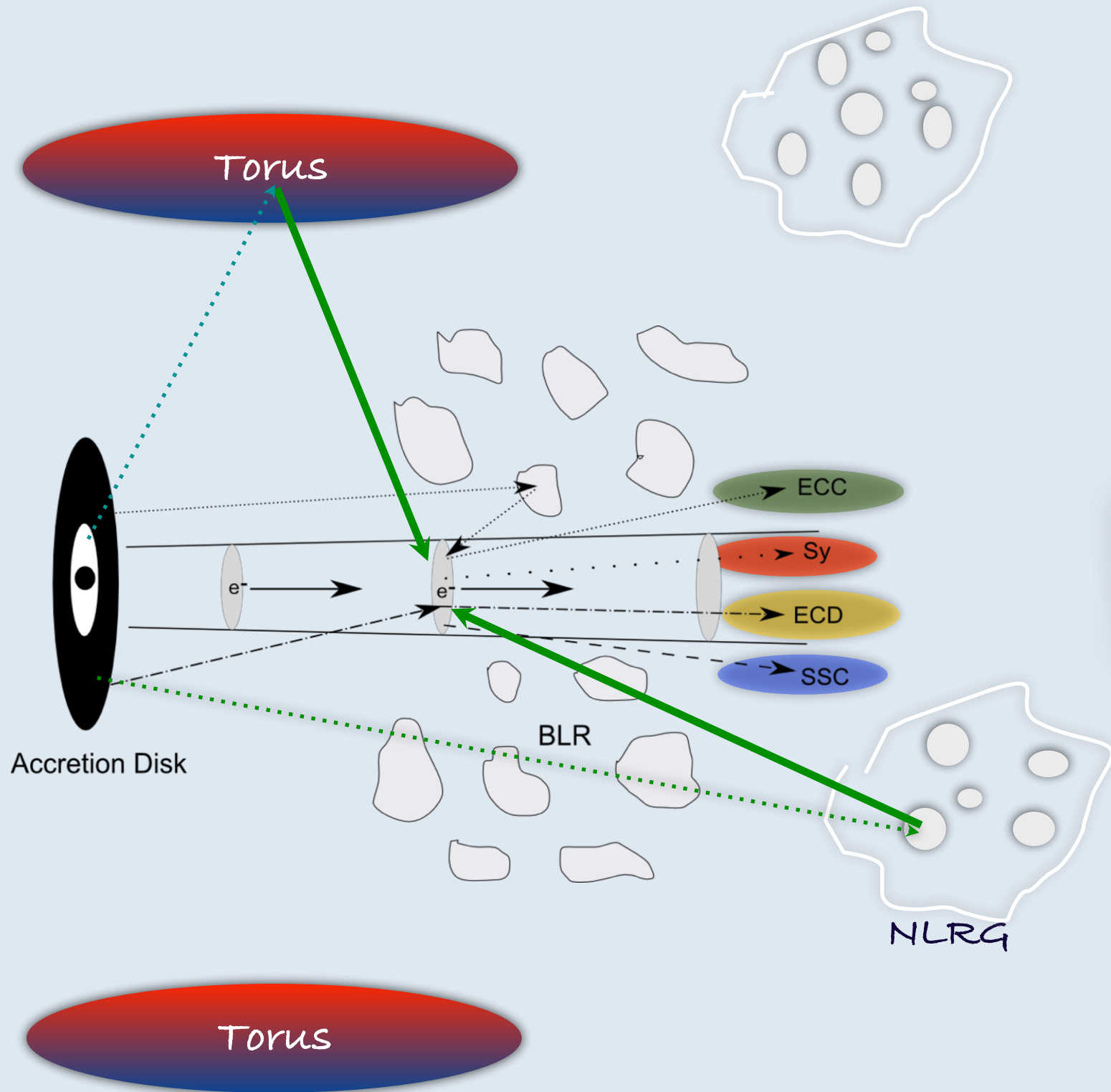
External Compton works in FSRQ

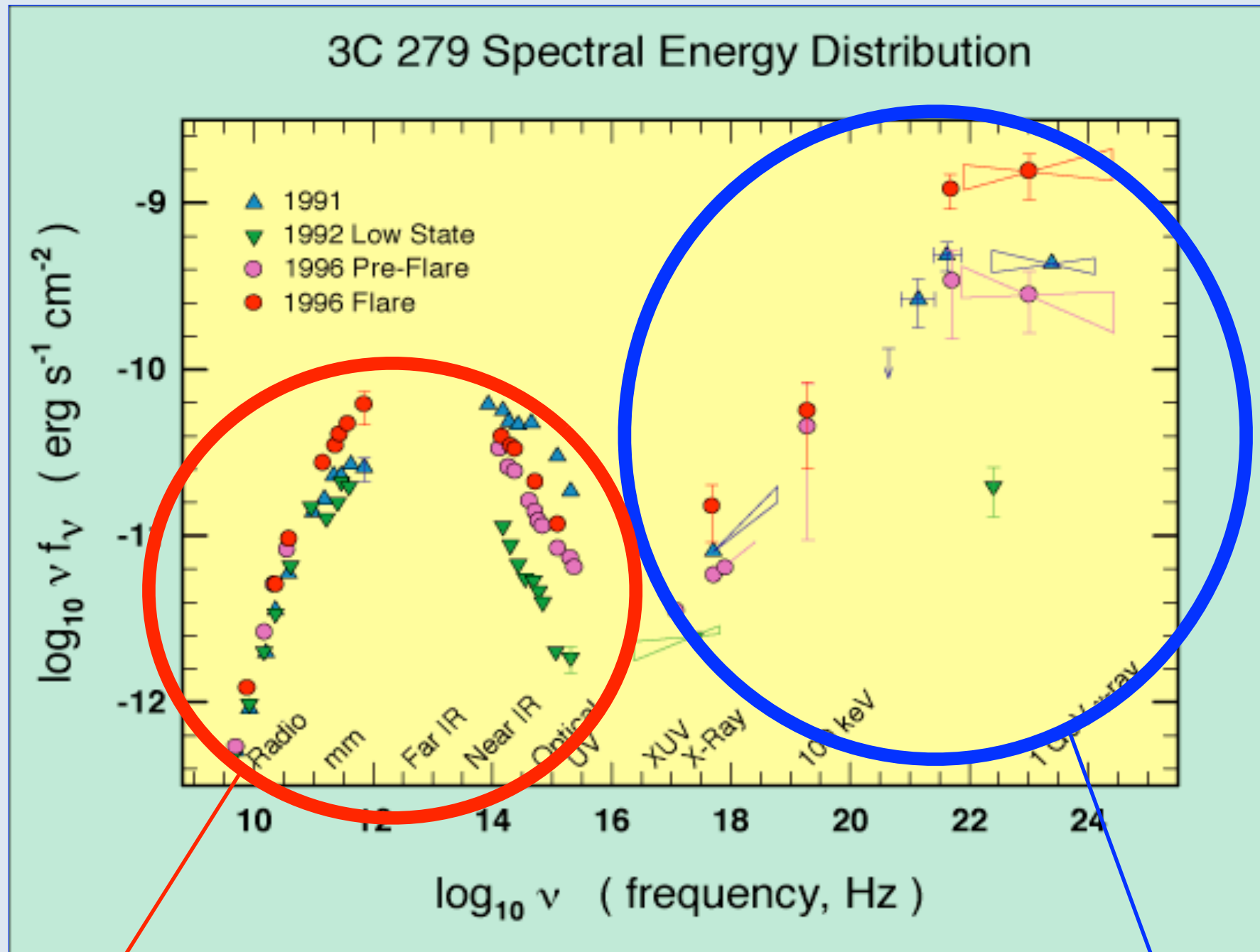
The population of relativistic electrons in a magnetized region can also interact with photons external to the jet produced in the accretion disk, in the broad/narrow line regions in the torus. This particular kind of process is called External Compton, or EC for short.

In the Self Synchrotron Model,
 $U(r)$ is due to synchrotron photons in the jet.



$U(r)$ is due to environment photons
from Accretion Flow, BLR, NLR, Torus





Synchrotron

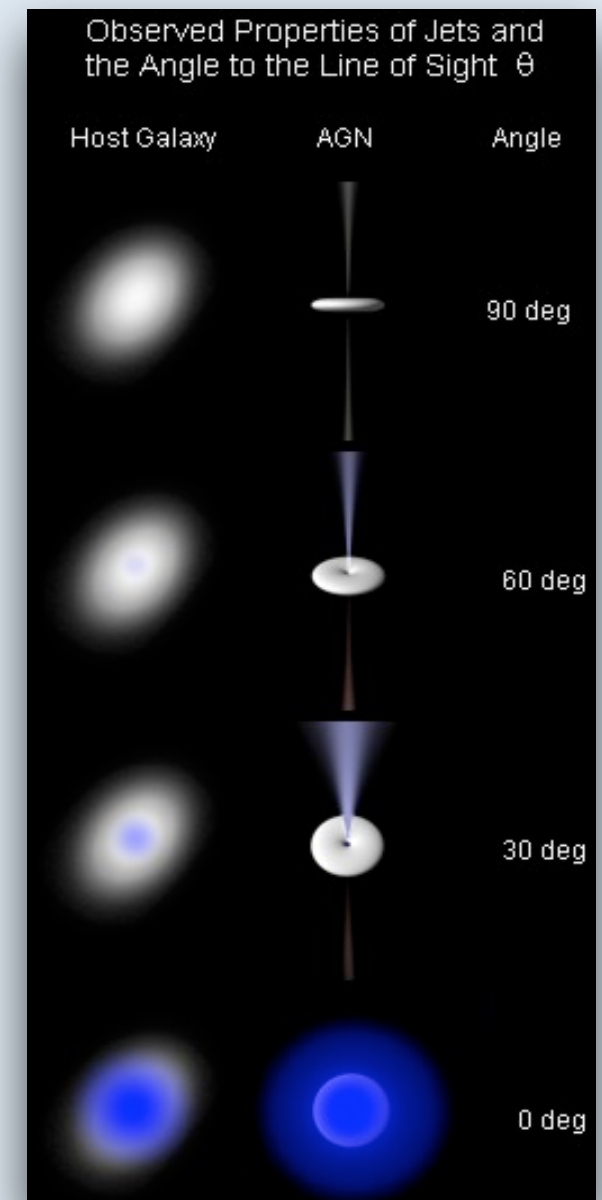
Inverse
Compton

While in LERG jet is always the dominant component, in HERG jet and disk emission are in competition

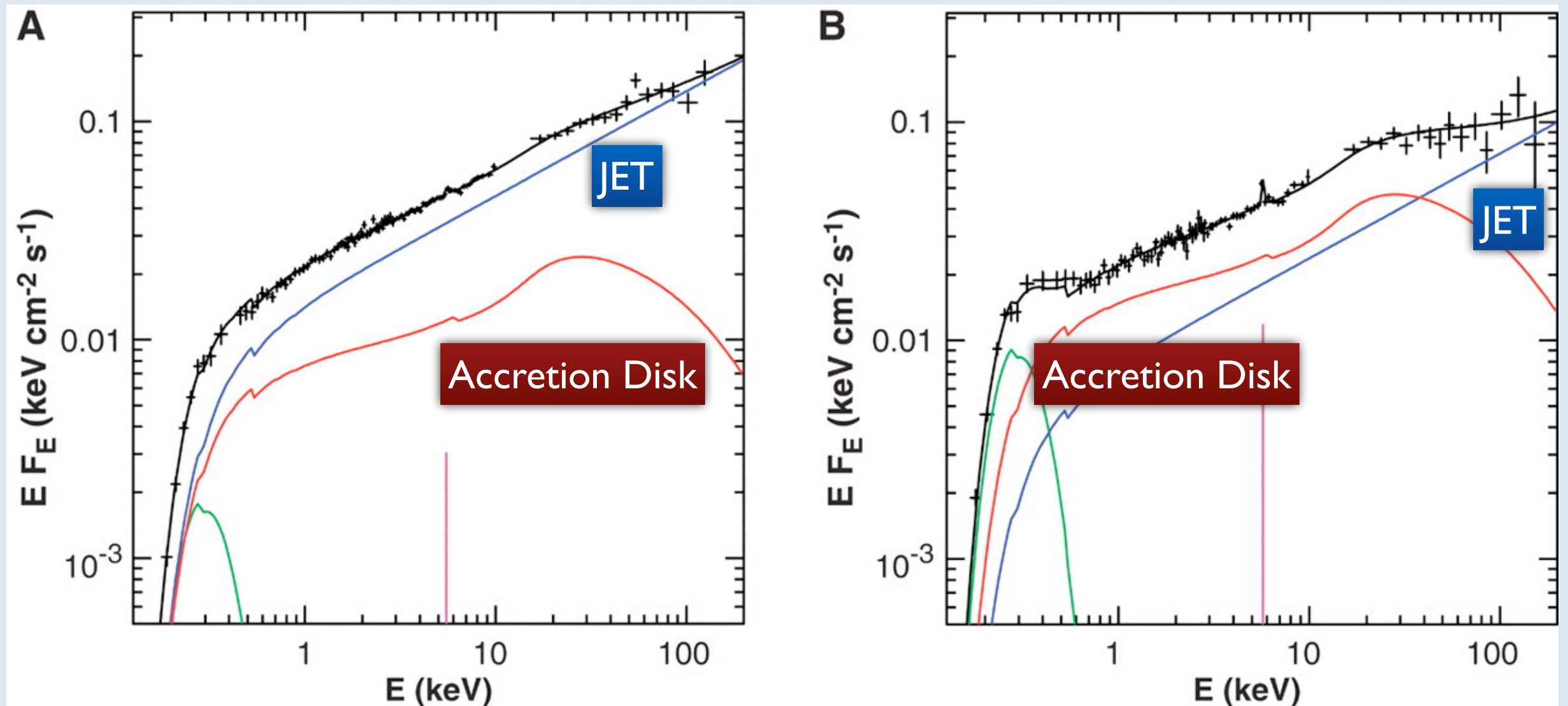
X-ray Spectra: Accretion Disk and pc-scale Jet emission are in competition in HERG spectra

Angle of sight = 0° ==> Jet radiation dominates

Angle of sight = 90° ==> Accretion disk dominates



An example: the case of 3C273. In this FSRQ at small inclination angle, the spectrum is generally a jet dominated continuum. However, when the jet is less bright, the accretion disk spectrum and the iron line can emerge from the continuum.

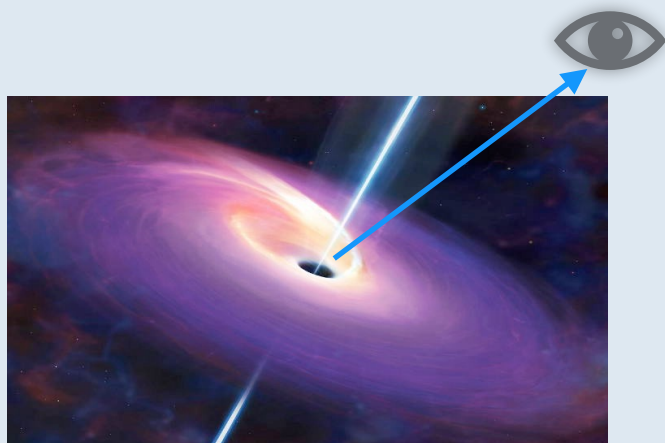
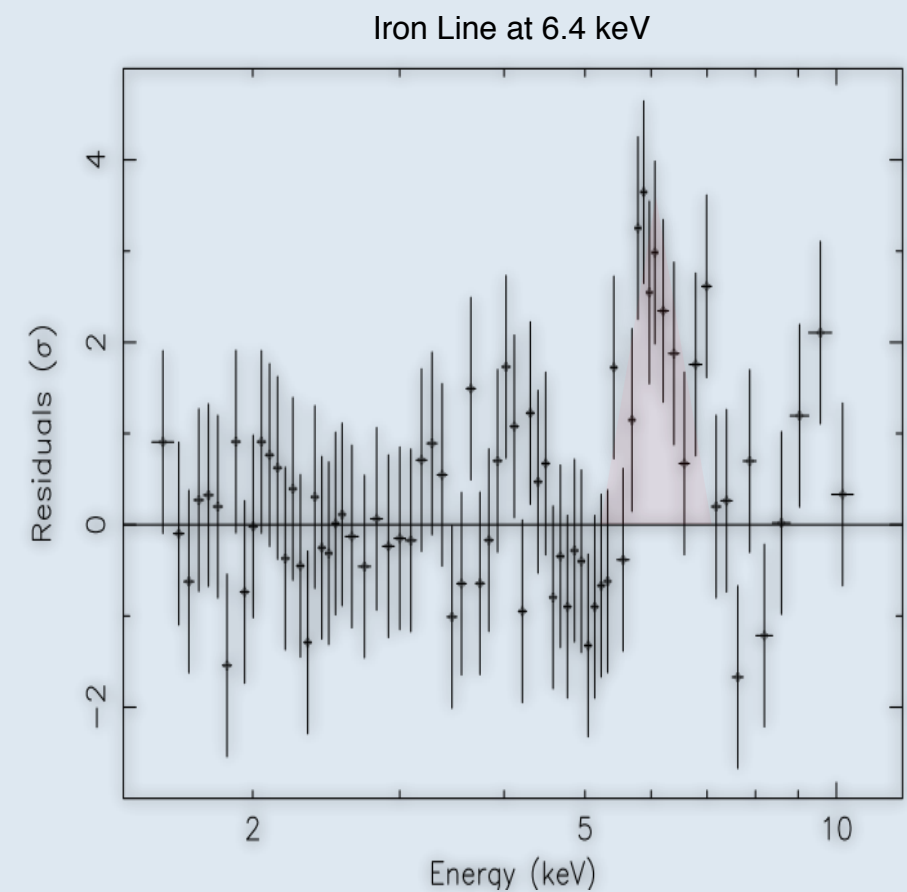
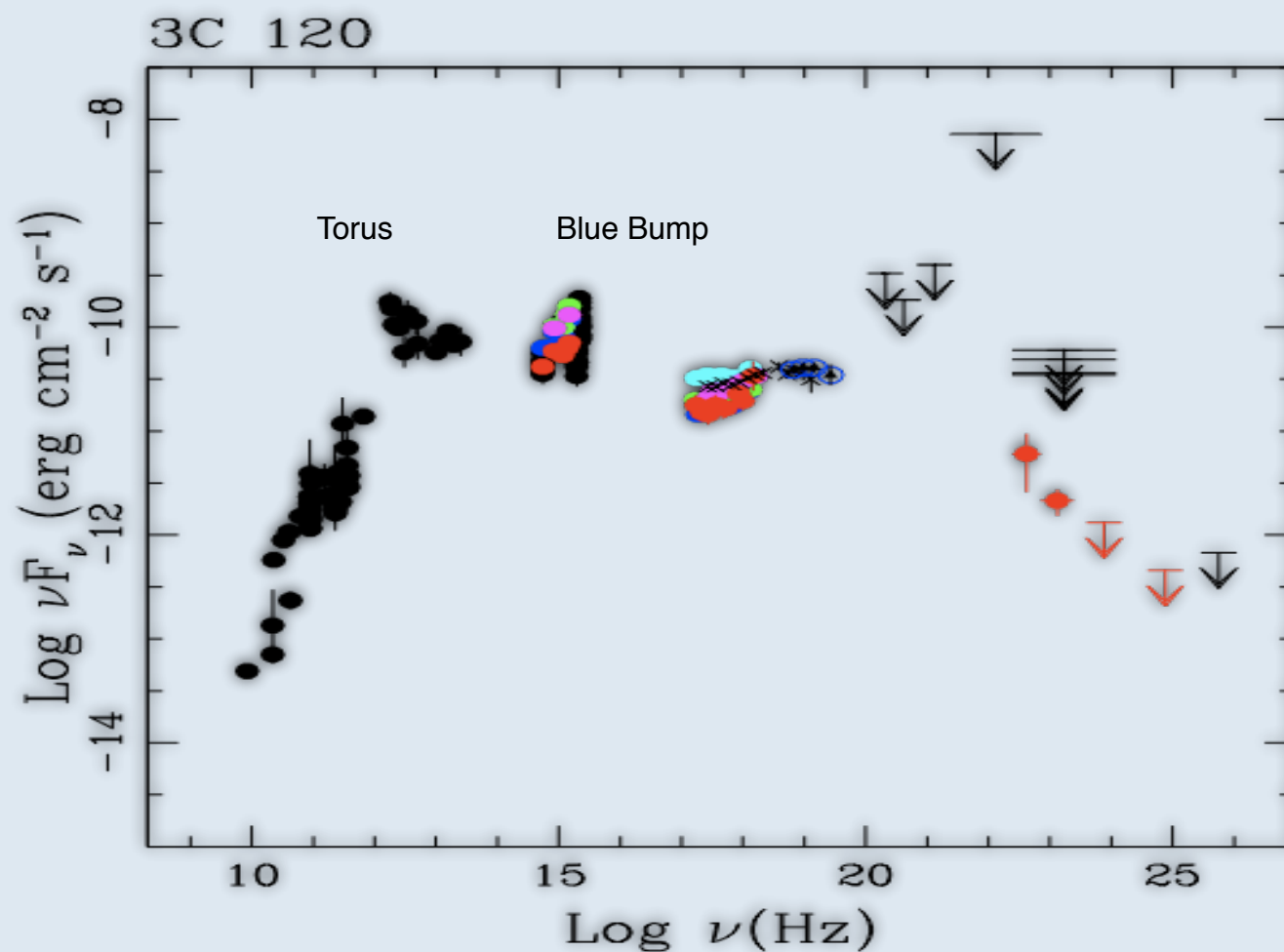


The observer is near the jet axis



In HERG the thermal components can be observed more easily

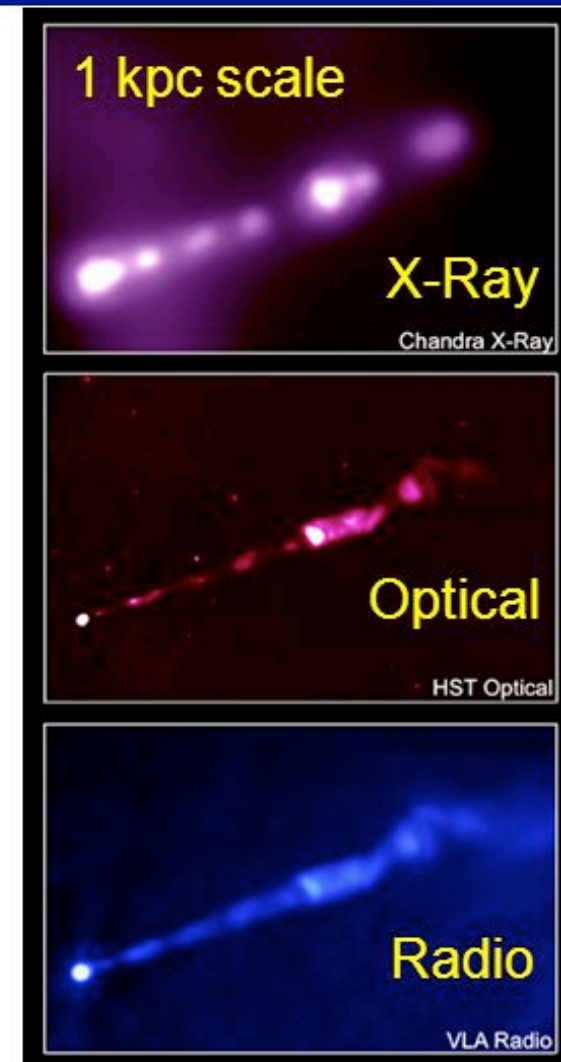
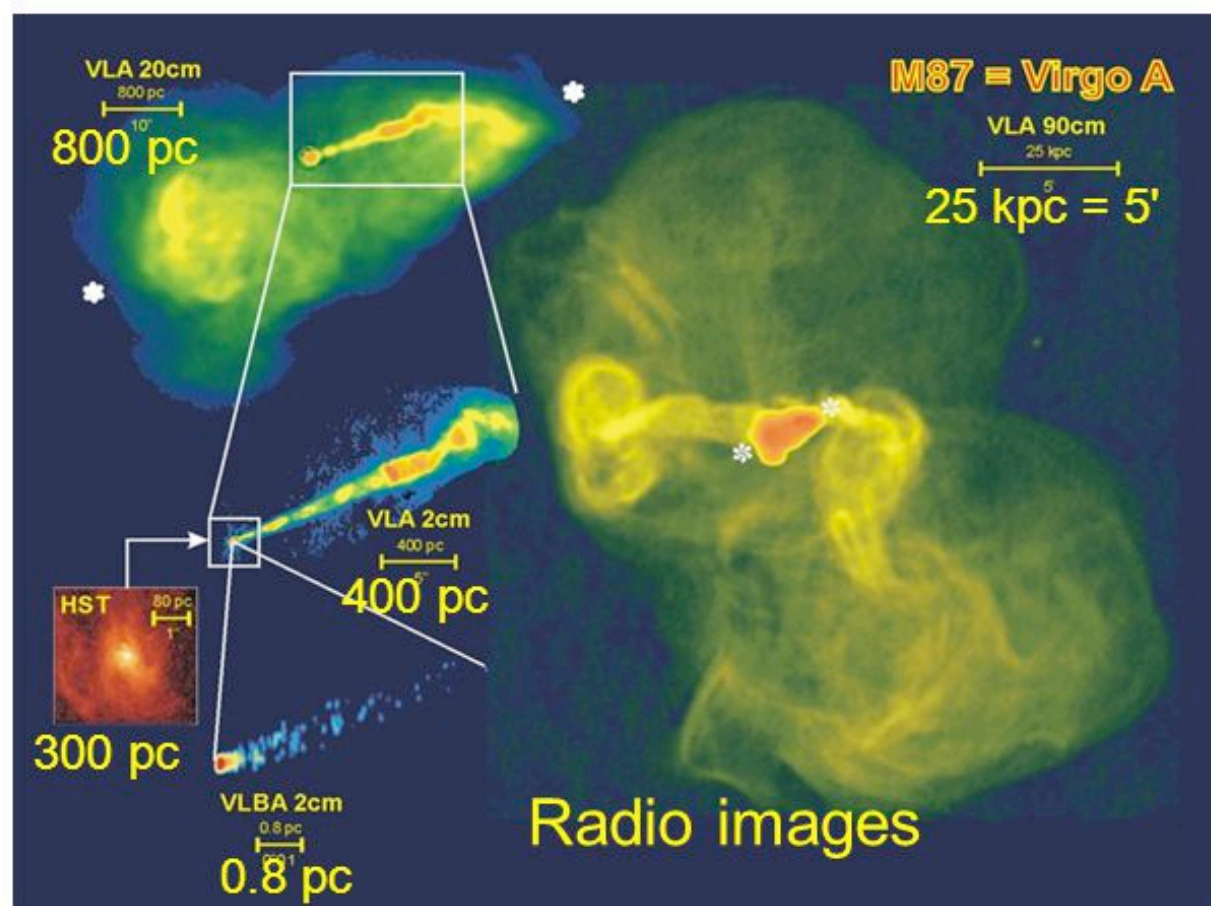
For example in the Broad Line Radio Galaxy 3C120, torus and blue bump are evident in the SED and the Fe iron line is detected in the X-ray spectrum.



In radio galaxies the jet pointed away from the observer favouring the observation of extended structures.
In blazars they are hidden by the jet luminosity amplification.

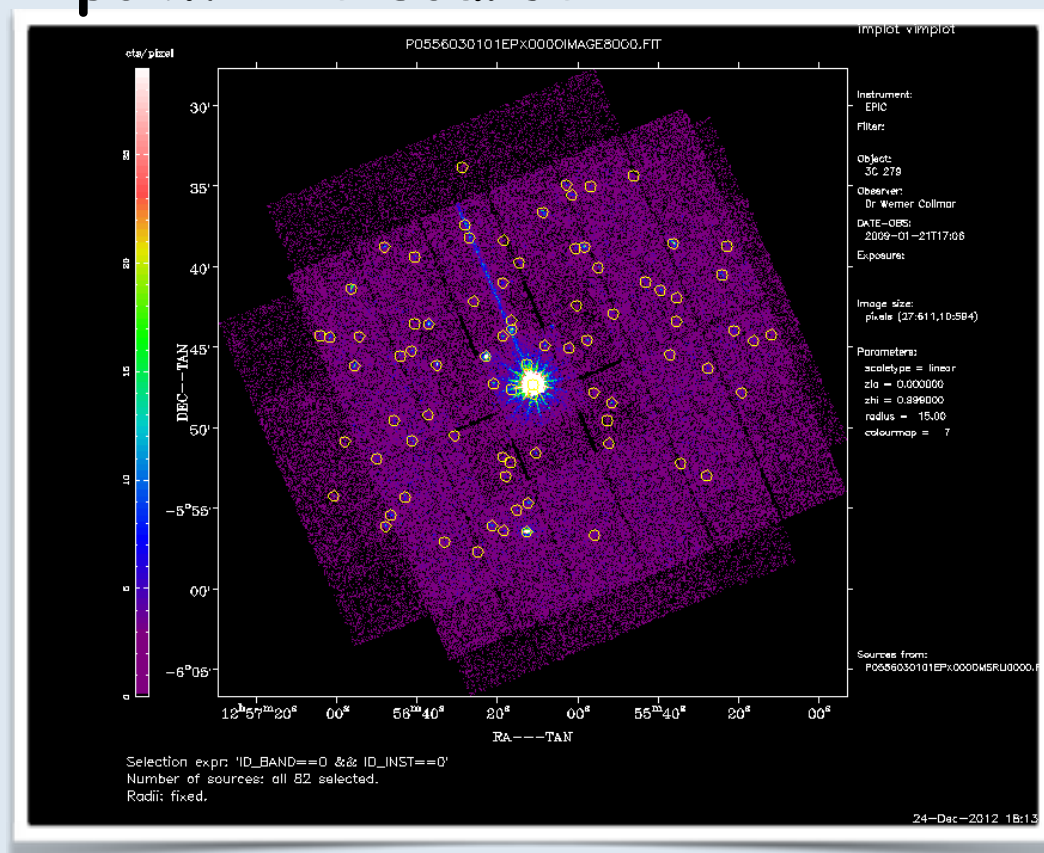
Extended structures can be studied

A dominant elliptical in the Virgo Cluster

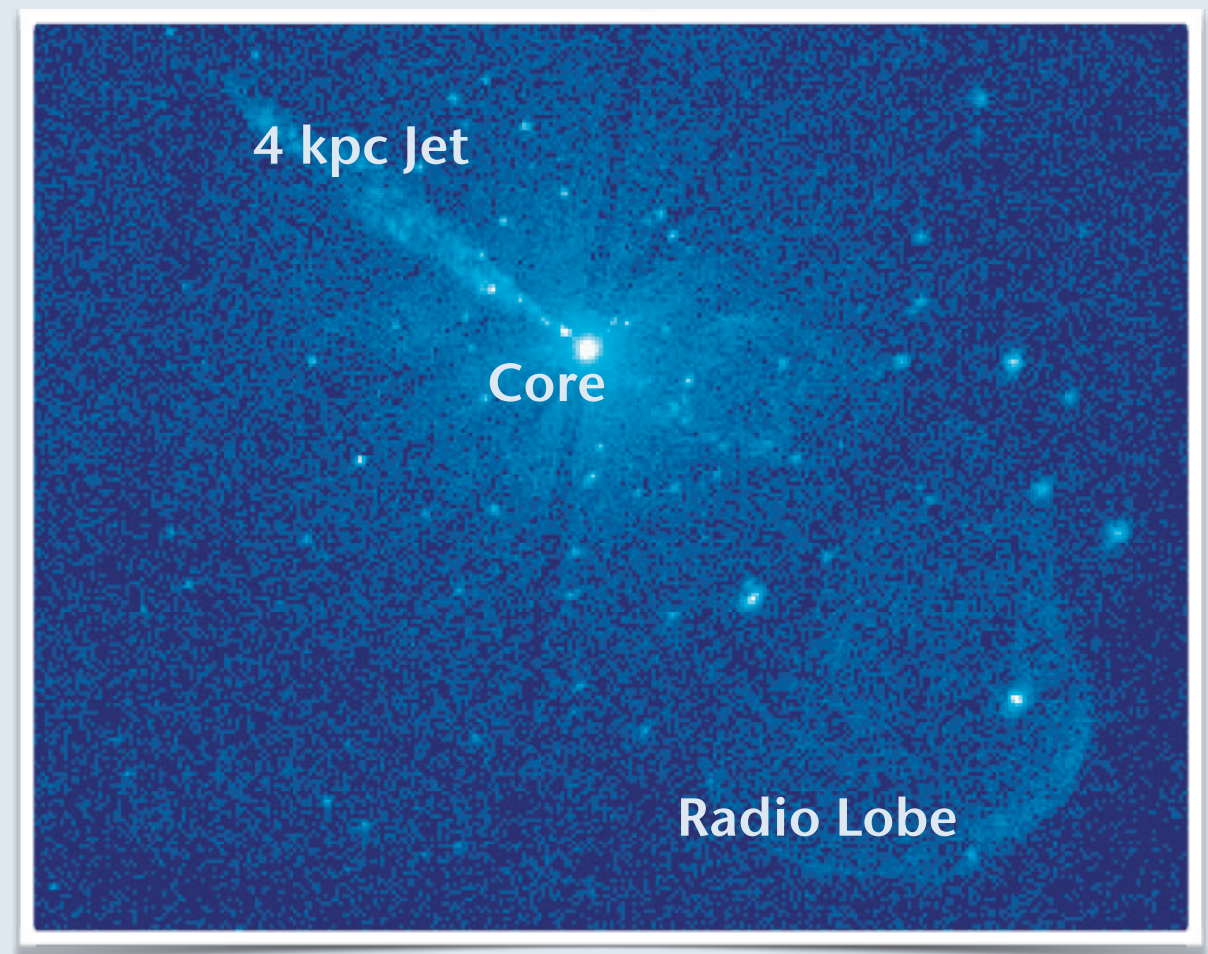


In the X-ray band

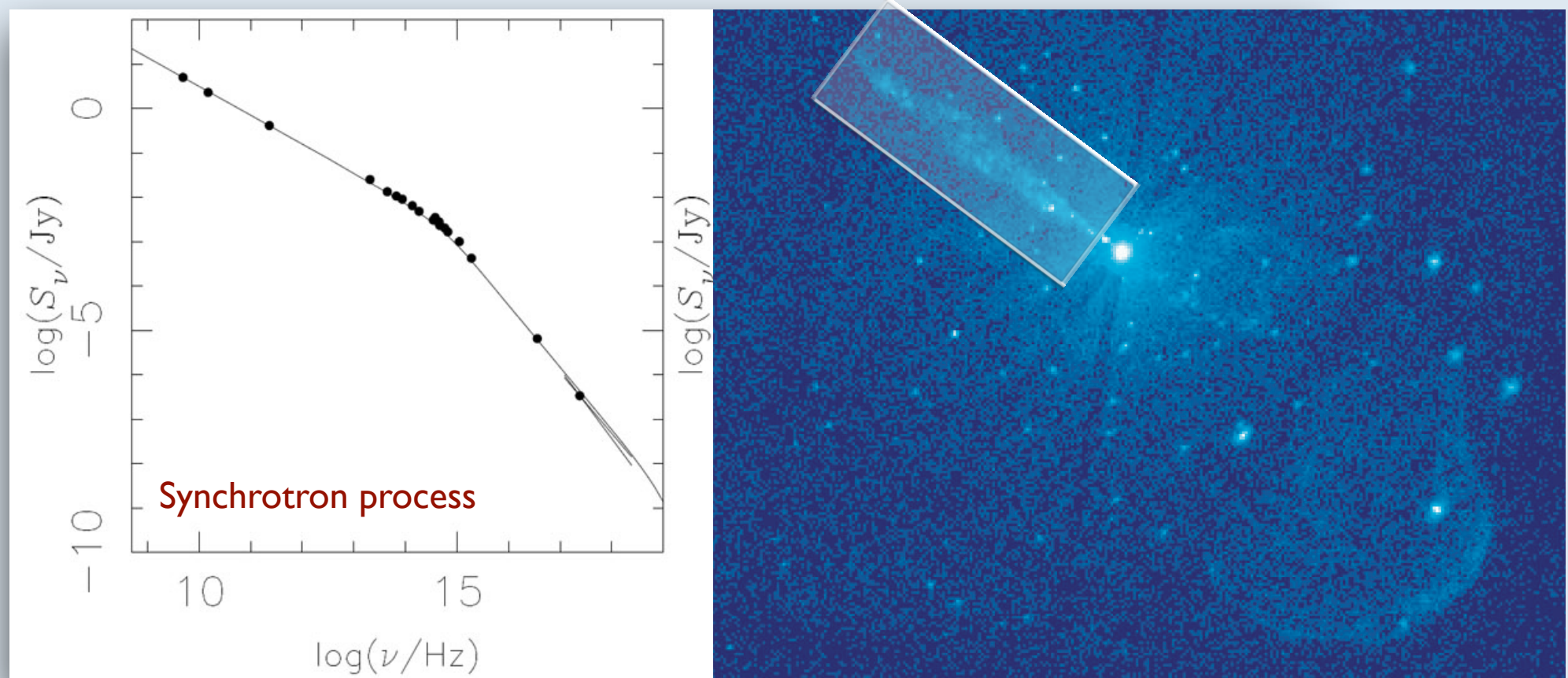
BLAZAR X-RAY IMAGE:
point like source



Radio Galaxy X-RAY IMAGE
resolves core, jet and lobe

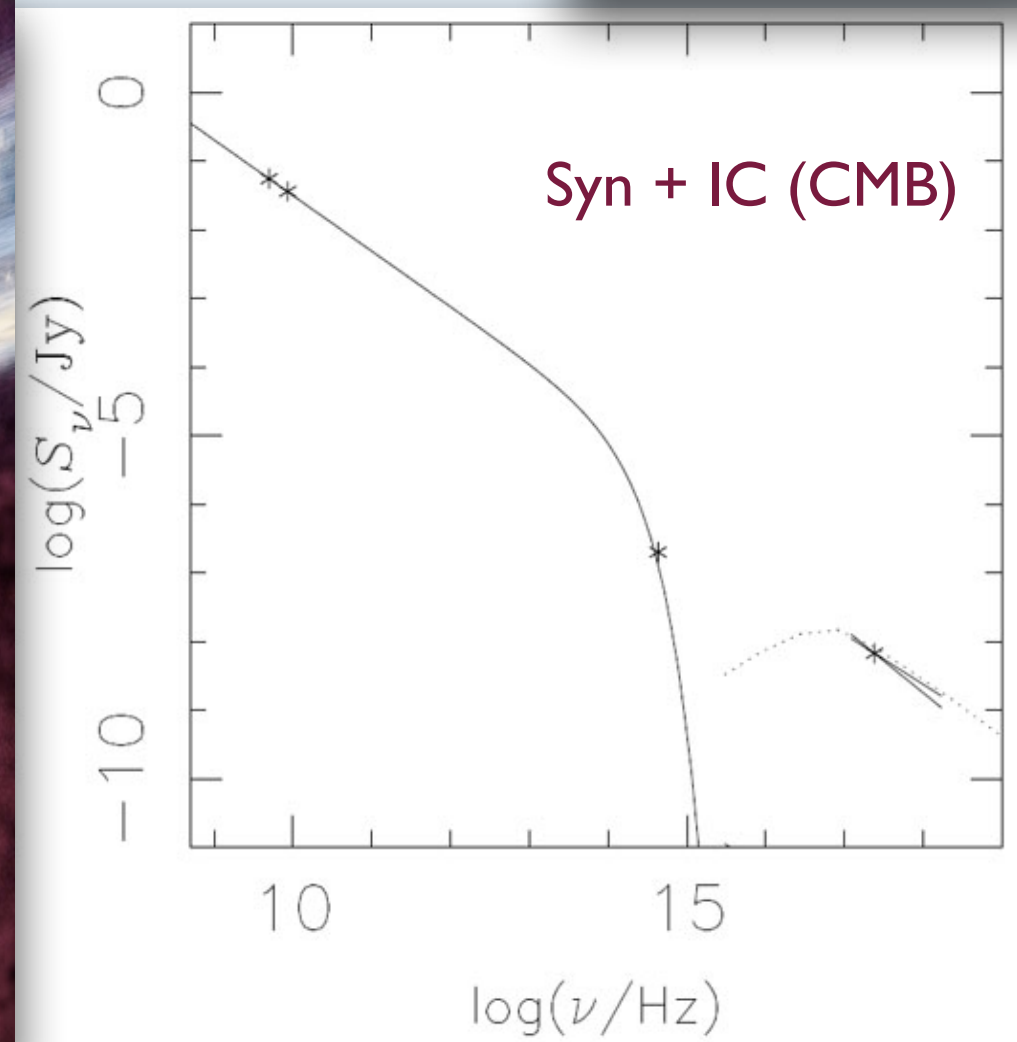
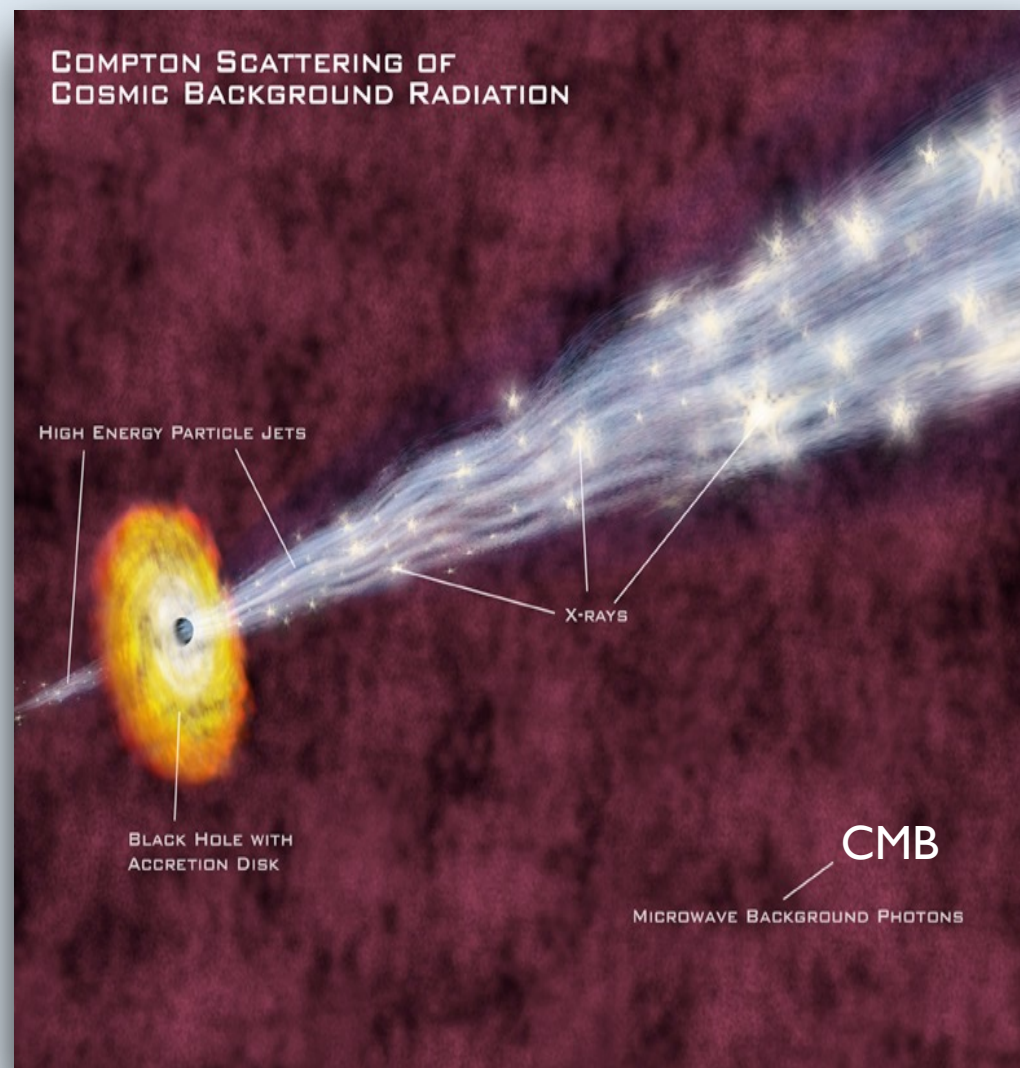


kpc-scale Jet

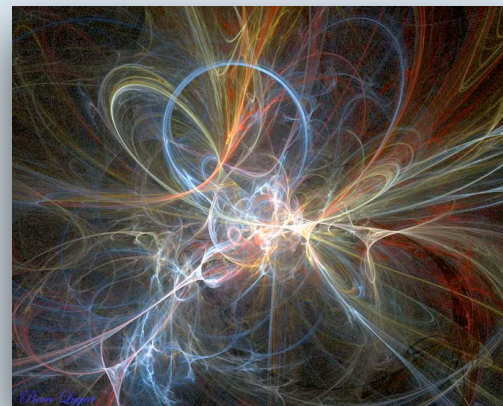


For low-luminosity (FRI) radio sources, there is strong support for the synchrotron process as the dominant emission mechanism for the X-rays, optical, and radio emissions

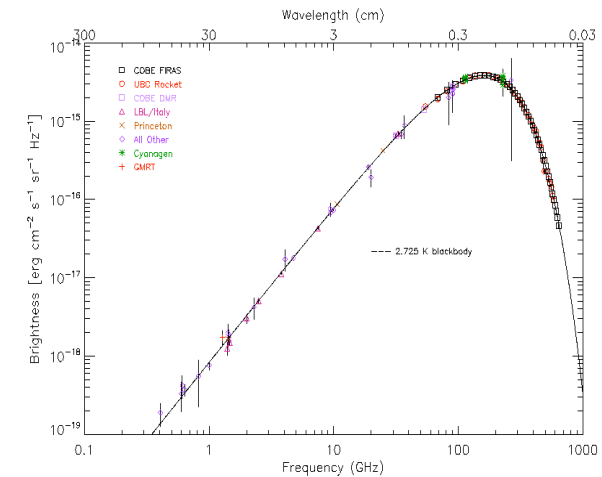
The most popular model postulates very fast jets with high bulk Lorentz factors Γ .



Lobes

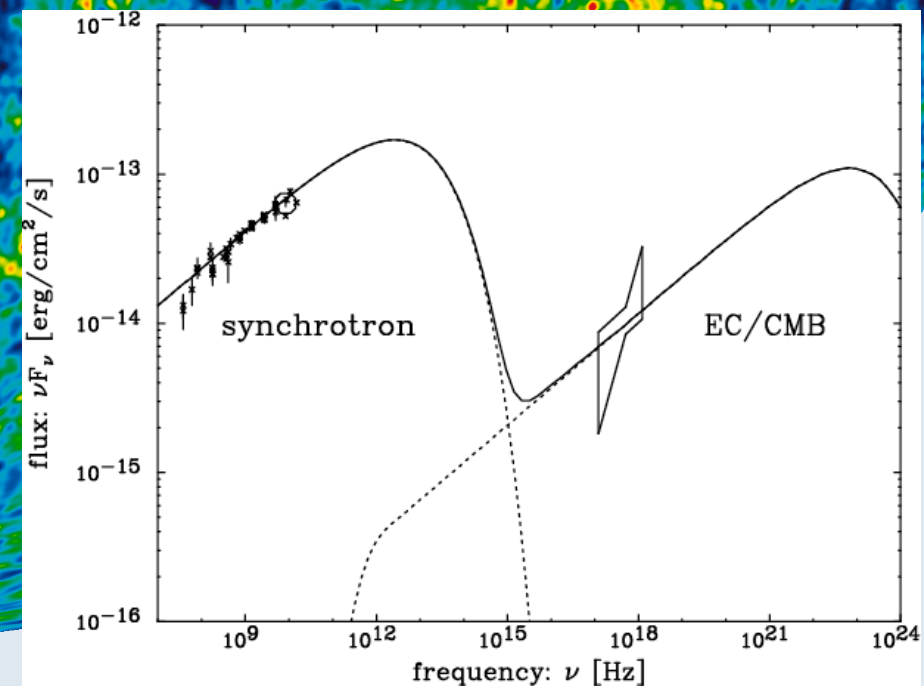
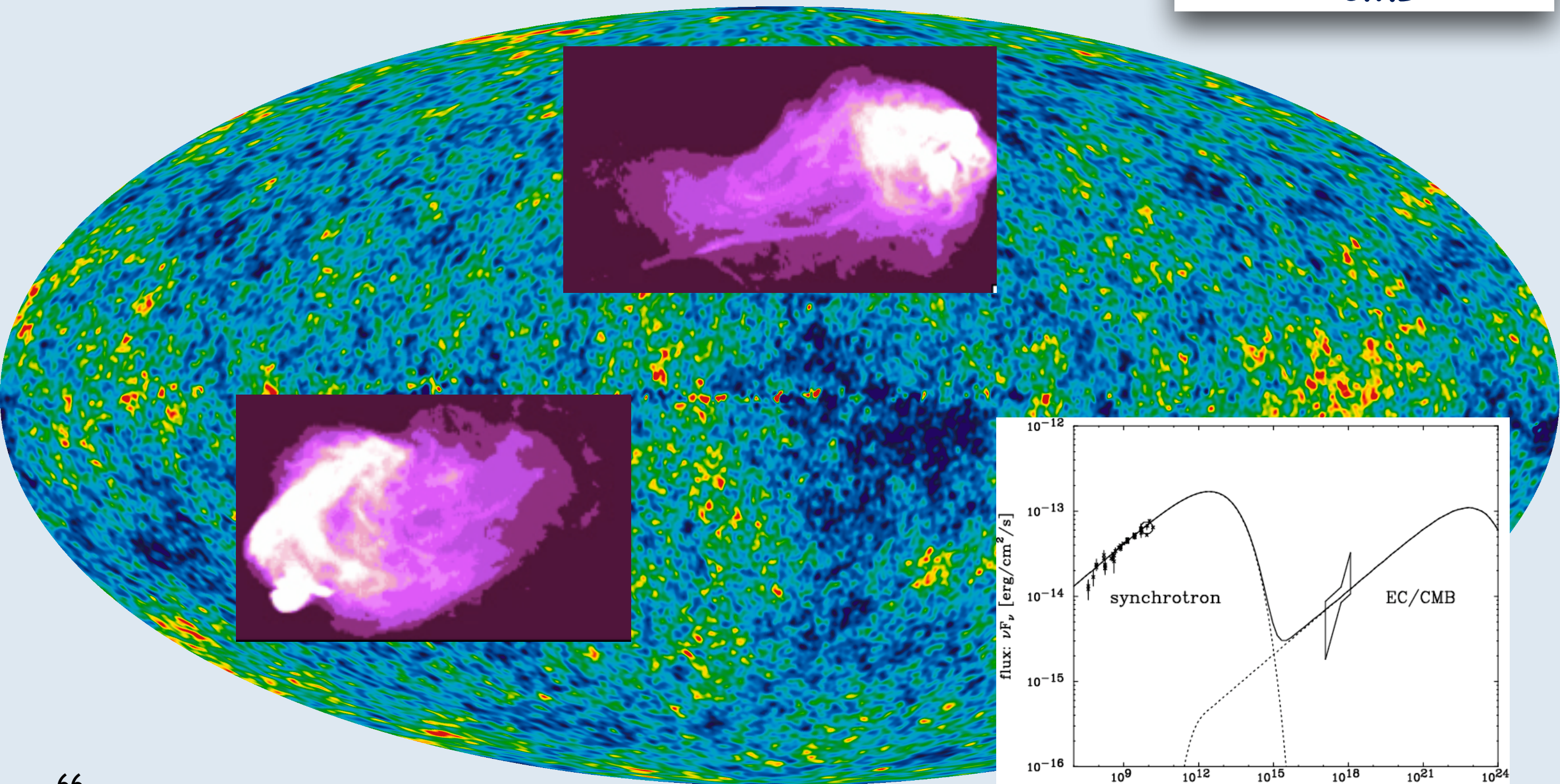


+

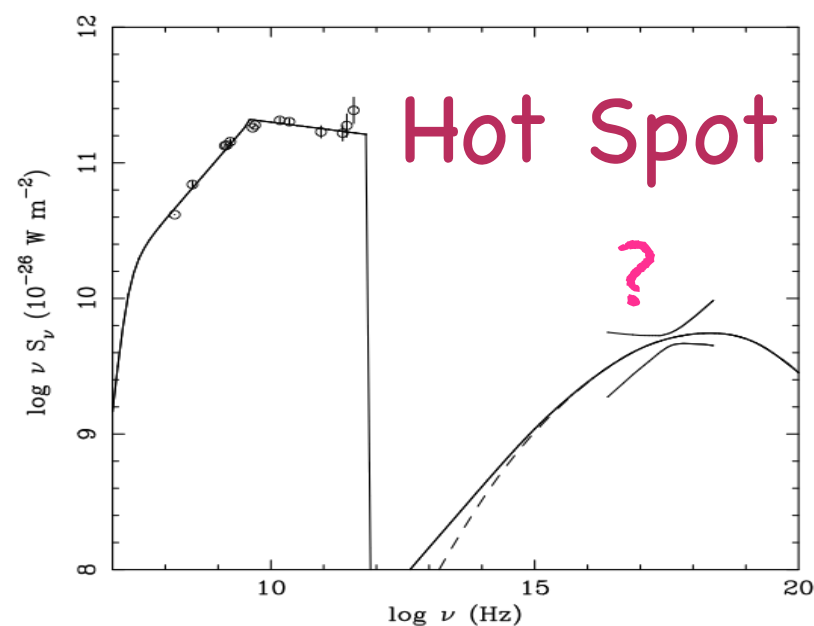
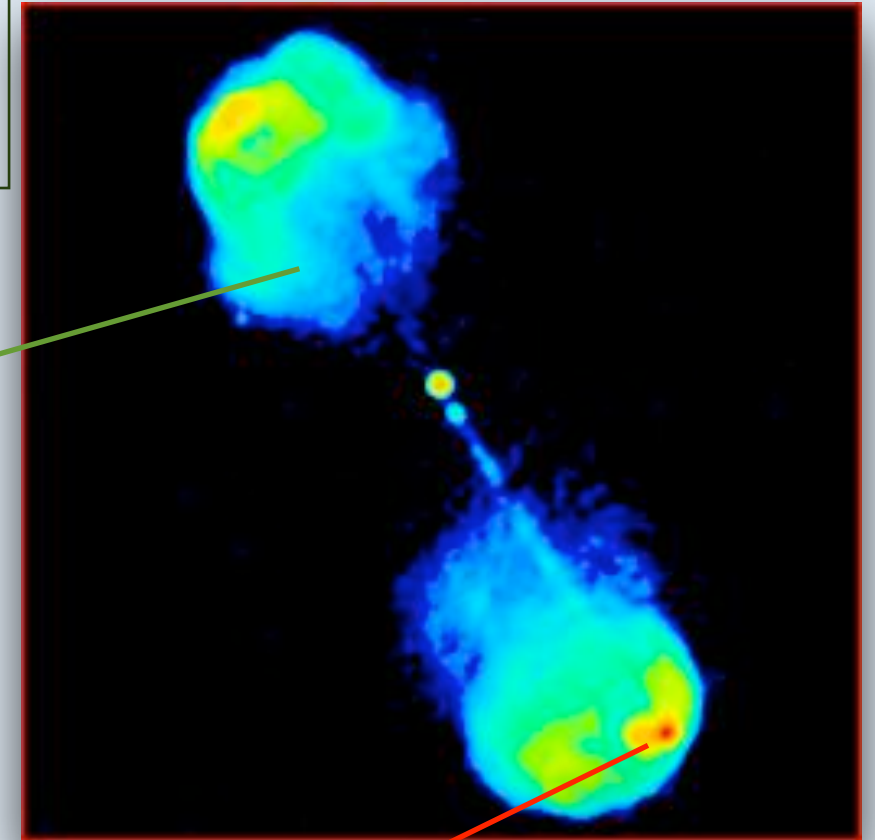
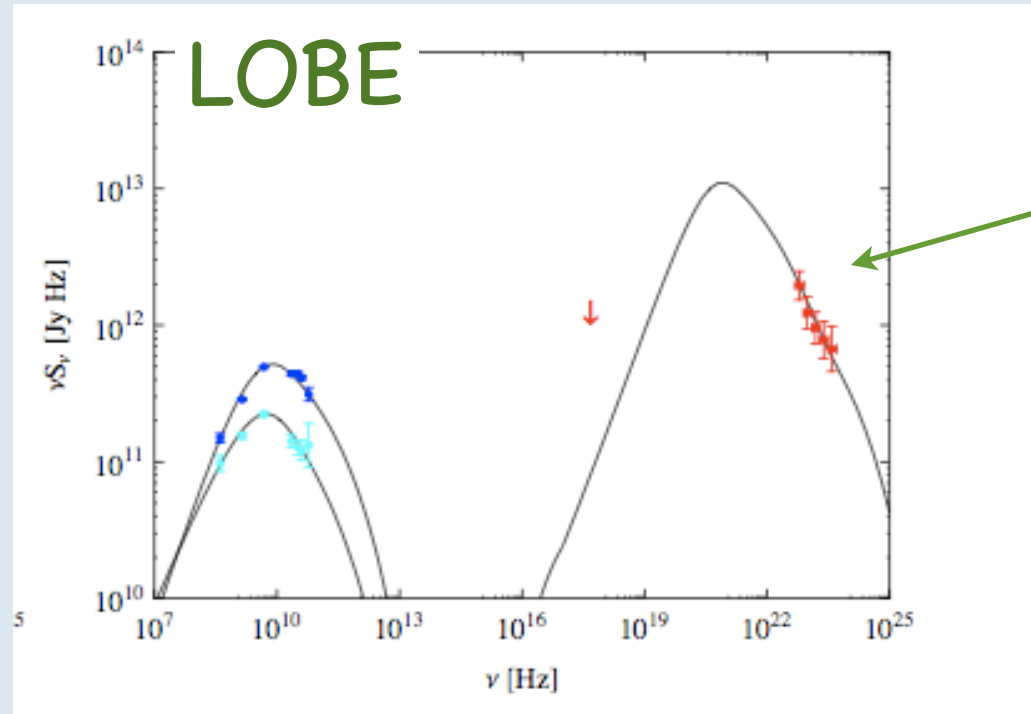


relativistic electrons

CMB



Radio Galaxies: hundreds of kpcs away from the core



We use new and archival Chandra data to investigate the X-ray emission from a large sample of compact hot spots of FR II radio galaxies and quasars from the 3C catalog. We find that only the most luminous hot spots tend to be in good agreement with the predictions of a synchrotron self-Compton model with equipartition magnetic fields. At low hot spot luminosities inverse Compton predictions are routinely exceeded by several orders of magnitude, but this is never seen in more luminous hot spots. We argue that an additional synchrotron component of the X-ray emission is present in low-luminosity hot spots